FACULTY OF ENGINEERING AND THE BUILT ENVIRONMENT

DEPARTMENT OF CIVIL ENGINEERING

REFINEMENT OF AIR-BORNE CHLORIDE EXPOSURE CLASSES FOR RC STRUCTURES IN THE CAPE PENINSULA

Submitted in partial fulfilment of the requirements for the degree of

Master of Science in Engineering M. Sc. (Eng.)

By

Olukayode O. Alao

Supervisor: Associate Professor Hans D. Beushausen

Co-supervisor: Professor Mark G. Alexander

Declaration

I Olukayode O. Alao declare that this dissertation is my own, unaided work. I have not plagiarized, nor tried to pass another authors work as my own. I have made every effort to ensure that where literature, discussions, collaboration, or contributions from other authors have been made, that it has been clearly acknowledged. This work has not been submitted previously at any other institution for any degree.

OLUKAYODE OLAWALE ALAO

March 2015

DEDICATION
TO
MY PARENTS

COL. & MRS WILLIAMS ALAO

Abstract

Innovative research pertaining to the use of concrete has made it the most commonly used material in the construction industry globally. Owing to their wide range of applications, reinforced concrete (RC) structures are subjected to a variety of exposure conditions including marine, industrial, and other severe environments. The atmosphere in marine environments is salt-laden, as a result of the presence of salts in seawater. The major components of these salts are chloride ions. It is well known that RC structures in marine environments are most susceptible to chloride-induced corrosion. The ingress of chloride ions into concrete breaks down the protective passive film on the steel and promotes corrosion of the embedded steel reinforcement.

In recent decades, concrete design Standards have attempted to classify the severity of RC exposure to chloride-induced corrosion in the marine environment. However, a shortcoming of the current marine exposure classifications in the South African (SANS 10100-2) and the Eurocode (EN 206-1:2013) is their generalist approach. RC structures exposed to airborne chlorides are identified as being within a distance of up to 30 km from the coastline in the current SANS design code (SANS 10100-2). The aim of this study was to carry out location-specific assessment in order to understand and/or validate the severity of RC exposure to airborne chloride attack in the marine environment of the Cape Peninsula in South Africa.

The assessment in this study is aimed at informing and modifying the design method for RC structures that are not in direct contact with seawater but are within the marine environment. The evaluation of the severity of the exposure environment will enable an informed design of concrete structures that satisfies their desired service life and durability performance.

In order to classify the severity of exposure, this study measured the concentration of airborne chlorides of select locations in the Cape Peninsula area, using the wet candle device. Five monitoring stations were exposed around the Cape Peninsula area at varying distances of 50 m, 150 m, 250 m, 2.7 km and 13.5 km from the coastline. Samples from the stations were collected twice every month over a period of 12 months and analysed for their chloride deposition rates.

A site-based study which involved the collection of concrete samples from existing structures at varying distances from the sea and investigating their chloride content was also carried out. In addition, data from previous forensic investigations (chloride profiles of structures) carried out from 1996 – 2013 were also collated and analysed. Both analyses were carried out in order to further validate if the distance of a RC from the coastline influenced the chloride deposition rate and surface chloride content of the structure. The local climate and weather conditions, with a focus on the dominating wind direction, wind speed, precipitation and relative humidity were also examined.

It was observed that the total concentration of airborne chlorides in the environment experienced a decrease which was linked to that of the locality's distance from the coastline. Indicatively, the total airborne chloride deposition rates that were measured over the 12-month period were about 10 times less at the 13.5 km monitoring station (11.8 mgCl/m^2.day), compared to the 50 m station (138.1 mgCl/m^2.day). Furthermore, the study found that the severity of exposure to airborne chloride attack of a RC structure is influenced by its prevailing microclimate (largely drawn from seasonal variations in weather conditions).

An assessment of the chloride profiles from existing structures and previous investigations indicated that at distances exceeding 14 km, the presence of airborne chlorides in the Cape Peninsula environment were minimal or totally absent. In addition, the influence of the orientation of structural components (sea-facing/ non-sea facing) such as piers and balustrades to their severity of exposure to airborne chlorides was found to be insignificant.

Finally, a classification scheme was proposed stating that RC structures at distances between 0-3 km are exposed to severe airborne chloride attack and structures at distances of 3-14 km are moderately exposed to airborne chloride attack. While structures that are at distances > 14 km have an insignificant exposure to airborne chloride attack.

Acknowledgements

The author wishes to acknowledge with gratitude the financial support over the period of this work (2013-2014) received from: The University of Cape Town, the erstwhile Cement and Concrete Institute (C&CI), The National Research Foundation (NRF), Sika (SA) Pty Ltd., PPC Ltd, AfriSam, The Tertiary Education Support Programme (TESP) of ESKOM, and the Water Research Commission (WRC).

The author would also like to appreciate the following people for their assistance during the period of this postgraduate degree study. You have all made this study possible.

- Associate Prof. Hans Dieter Beushausen, my thesis supervisor, for insight on research methods. Thank you for your continual support and motivation. Your door was always open for discussions and advice.

- Professor Mark Gavin Alexander, my thesis co-supervisor, for providing invaluable insight into the fundamentals and concepts of concrete durability. Thank you for your continual encouragement and knowledgeable guidance which you shared throughout my postgraduate studies.

- The Concrete Materials and Structural Integrity Research Unit (CoMSIRU) for their support throughout the postgraduate studies.

- The South African Weather Service (SAWS), Mr. Philip Ronne (AECOM), Mr. William Martin (SMEC), Mr. Stephen Roux (City of Cape Town) and Mr. Harry Viljoen (Provincial Government of the Western Cape) for assistance in data mining from previous forensic investigations and structural information.

- My friends with whom I have spent these past two years for your support and laughter. A special thanks to: Thuthukile Mbanjwa, Yorm Amesu, Emmanuel Okwori, Tosin Oladele, Tobi Fadiji and the Obz Crew. You have all made this journey worthwhile. My postgraduate degree studies would not have been the same without you.

- My siblings; Omotayo, Kolade and Kunle for your love and support throughout the studies.

"The greatest glory in living lies not in never falling, but in rising every time we fall." — Nelson Mandela (1918 - 2013)

Table of Contents

List of Figures

List of Tables

CHAPTER 1

1 Introduction

1.1 BACKGROUND TO THE STUDY

Concrete is one of the most extensively used human-made material. The annual global consumption of concrete in 2013 was estimated at 25 billion tons per year (Celik *et al*., 2014), which implied a 900 % increase in concrete consumption in comparison with that of 1950 (Klee, 2009). The reasons for concrete's significant use may be attributed to its numerous benefits which include its: versatility, affordability and its ability to be engineered to suit desired performance. Owing to the wide range of applications, reinforced concrete (RC) can be subjected to a variety of exposure conditions including marine, industrial or other severe environments. In most cases, concrete is inherently durable, performing well throughout its design life. However, in some cases it does not perform adequately due to poor design, poor construction, inadequate materials selection, environment exposure or a combination of these factors.

Consequently, the durability of RC structures is an important factor for consideration during design and construction. The durability of a RC structure is referred to as the ability of the structure to resist deterioration in its design environment during its design life (Alexander *et al*., 2009). Hence for durable RC structural design, it is important to understand the performance requirement of the structure at the design stage, its exposure environment and the major deterioration mechanisms to which it will be exposed (Fagerlund, 1985).

Although different deterioration mechanisms such as alkali silica reaction (ASR), freeze-thaw, sulphate or acid attack cause deterioration of RC structures, it is widely accepted that reinforcement corrosion is by far the most frequent deterioration mechanism (Mackechnie, 1995). The two main causes of steel bar corrosion in concrete are carbonation and ingress of chlorides into concrete (Martínez & Andrade, 2009). The focus of this study is on chloride-induced corrosion. Chlorides can be introduced into concrete not only through salt water ingress and airborne salts or deicing salts (typically used in winter maintenance of roads to keep them clear from snow and ice)

but also during the time of construction with their presence in mixing water, admixtures or aggregates (Mackechnie, 1995; Maio *et al.*, 2004).

The exposure of concrete structures in marine environments can be divided into two categories: direct and indirect. Directly exposed structures includes structures that are fully or partially submerged in seawater and structures in the splash and spray zone; indirectly exposed structures includes structures that do not come into direct contact with seawater. An example of the indirect category of exposure are structures that are some distance from the coastline – but they might be prone to airborne chloride attack.

The ingress of chloride ions into concrete can lead to the breakdown of the passive protective film on the steel reinforcement. This presents a risk of corrosion when the chloride threshold level is reached which causes a loss of rebar cross–sectional area and the subsequent spalling of the concrete cover (Figure 1.1).

Figure 1.1: Concrete spalling due to reinforcement corrosion on the Foreshore Bridge in Cape Town (*airborne chloride exposure, 300 m from the sea*)

The major source of airborne chlorides is marine aerosol, which is present in high proportions in coastal regions (marine environments). The chloride ions make up a significant part of the marine aerosol, and they are transported inland by the effects of environmental actions such as wind, precipitation, temperature and relative humidity (Meira *et al.*, 2007; Gao *et al.*, 2007). The deposition of airborne chloride particles is relative to their size and radius. A study on the transportation of aerosols inland has shown that the larger particles (which are >10μm in diameter) are typically deposited close to the shoreline (typically 400–600m), while finer particles (<10μm in diameter) travel further inland (Roberge, 2011).

The scope of this study in terms of location, is the marine environment of the Cape Peninsula in South Africa. A brief overview of the characteristics of the Cape Peninsula are provided in the next section.

1.2 REGIONAL CHARACTERISTICS OF THE CAPE PENINSULA

South Africa has a long coastline (stretching more than 3000 km, bordered by the Atlantic Ocean on the West and South West and by the Indian Ocean on the East and

South East) (Tinley, 1985). The focus in this research is on the Cape Peninsula area of South Africa. The Cape Peninsula is located in the Western Cape Province of South Africa (*Figure 1.2*).

Figure 1.2: Map of the Cape Peninsula (adapted from www.digitalmapstudio.com)

The Western Cape Province stretches about 400 km northwards along the Atlantic coast and about 500 km eastwards along the Indian Ocean coast which is an estimated 35% of the total South African coastline (Gribble, 2006; Ryan & Branch, 2012). Cities such as Cape Town (*Figures 1.2 and 1.3*) are situated on the coastline where in some regions there is the presence of airborne salts, which create an aggressive atmosphere for materials and products used in construction (Mehta, 1991). Such corrosive environments have caused significant damage to reinforced concrete structures such as buildings and bridges and reduced their expected service life.

Figure 1.3: Aerial view illustrating the marine environment of the Cape Town area (Reggie, 2009)

1.3 CURRENT EFFORTS IN ADDRESSING DURABILITY CONCERNS

The desired performance of a structure over its design life is a major factor in design for durability. Designing for durability needs to be part of an integrated and structured process that should follow the client's requirements for in-service performance, which takes into account service loads and environmental loads. Most relevant are the mechanisms and processes of deterioration to which different parts of a structure will be subjected.

Mackechnie (1995) collated and reported substantial information on the durability of RC structures in the Cape Peninsula in the 1990s. His research was on RC structures (such as bridges, tidal pools, breakwater structures and a jetty) between the ages of 3 – 75 years, which were exposed to various chloride-induced corrosion conditions from spray to tidal zones. The investigation was carried out in order to predict the durability performance of these structures relative to the chloride exposure severity to which they were exposed. However, very little research has been conducted to measure and evaluate the concentration of airborne chlorides vis-à-vis distance from the coast. Moreover, the study carried out by Mackechnie (1995) is about 20 years old and these structures would have undergone some rehabilitation/repair.

A shortcoming of the current marine exposure classifications in the SANS 10100-2 and EN 206-1 (EN 206-1:2000) is their generalist approach. These Standards are referred to as 'generalist' because they do not account for the fact that variations exist per location. Therefore, they might not be directly applicable in the adequate design of a RC structure to resist deterioration.

Table 1.1 provides the current framework for classification of marine exposure categories of RC in South Africa; a corresponding concrete quality is then prescribed with respect to the classified environmental severity. However, SANS 10100-2 refers to the Eurocode (EN 206-1) and British Standard (BS 8500) for guidance on how to deal with RC structures exposed to airborne salts (SANS 10100-2:2009). Also, from Table 1.1 it can be observed that the "very severe" classification indicates that structures which are 30 km from the sea are exposed to the effects of airborne chloride ingress. This motivates the need to carry out a location-specific study of the Cape Peninsula to characterize the severity of the marine environment.

Table 1.1: Marine exposure categories in SANS 10100-2 compared with EN 206-1 (SANS 10100-2:2009)

Marine Exposure category	Description of Exposure	Nearest matching exposure classes from EN 206-1
Moderate	• Surfaces protected by a waterproof cover or permanent formwork not likely to be subjected to weathering or corrosion • Enclosed surfaces • Structures or members permanently submerged	**XS 2** Permanently submerged
Severe	• All exposed surfaces • Surfaces on which condensation takes place • Surfaces in contact with soil • Surfaces permanently under running water • Surfaces protected by permanent formwork not likely to be subjected to weathering or corrosion	**XS 1** Exposed to airborne salt but not in direct contact with sea water
Very severe	• All exposed surfaces of structures **within 30km from the sea** • Surfaces in rivers polluted by industries • Cast in situ piles, wet cast against casings	**XS 1** Exposed to airborne salt but not in direct contact with sea water **XS 3** Tidal, splash and spray zones.
Extreme	• Surfaces in contact with sea water of industrially polluted water • Surfaces in contact with marshy conditions	**XS 3** Tidal, splash and spray zones.

In order to estimate the severity of the environmental loading in a specific location, the concentration of the airborne chloride must be studied. The presence of airborne chlorides in an environment is dependent on the concentration of the marine aerosol produced by the sea.

The production of airborne chlorides in the ocean depends on whitecap activity and general ocean wind velocity. Whitecaps are the white tips of an ocean/sea wave produced by the waves breaking against each other. Whitecap activity can be evaluated using whitecap coverage (Anguelova & Webster, 2006). This is a method used to evaluate quantitatively the breaking of waves in the ocean. From satellite captured images of whitecap, the whitecap coverage is obtained by evaluating the white part of the total area of the picture. When these droplets (spumes) are formed from the wave actions, they can be transported by the wind to locations inland.

Locations that are in regions of high south or north latitude (below or above the equator) experience higher wind speed than at the equator (Cole *et al*., 2003a). It can be expected that at the coastal regions of these locations, the airborne chloride concentrations measured would be higher compared to locations at the equator. However, besides the influence of meteorological factors, other factors such as land surface roughness (topography) due to forests and urban landscapes can cause a dramatic reduction in airborne chloride concentration in the air (Cole & Paterson, 2004; Cole *et al*., 2003a).

The consequences are that two locations with similar airborne chloride production can have significantly different chloride distribution, from the coast to inland, because of the varying weather and surface roughness conditions (Mustafa & Yusof, 1994). Therefore, it is probably inaccurate to assume airborne chloride concentration from other studies even if location and climate characteristics are similar.

1.4 MOTIVATION AND RESEARCH SIGNIFICANCE

For construction with concrete, most African countries largely revert to European or the United States (US) design codes although the prevailing climatic conditions in Africa differ greatly from their European and US counterparts. In order to implement durable concrete technologies, practical African design codes should be developed.

The causes of concrete deterioration have always been a subject of concern and much research has been carried out. Several factors have been identified to influence the severity of exposure to reinforcement corrosion in marine environments. As was previously shown in Table 1.1, the Standards do not give due consideration to the influence of climatic conditions on the severity of the deterioration mechanism(s). In marine environments, it is true to state that the presence of airborne chlorides and their concentration in the atmosphere are the most decisive factors when evaluating the severity of a RC structure's exposure to reinforcement corrosion (Trocónis de Rincón *et al.*, 2007). In addition, the diversity of microclimates per location in the Cape Peninsula needed a more accurate definition of their airborne chloride exposure severity. As a result, the motivation for this research was to determine the influence of climatic conditions such as wind speed and direction, temperature and relative humidity on the airborne chloride deposition rates of select locations in the Cape Peninsula. This would aid in informing and modifying the durability design for RC structures in the Cape Peninsula.

A large proportion of capital goes towards construction of reinforced concrete (RC) structures annually. These RC structures are subjected to continuous ageing once their construction are completed and depending on the severity of environment or the deterioration mechanisms to which they are exposed, the repair or rehabilitation of the RC structures may become imminent. Interest is increasing due to significant cost implications associated with the repair and maintenance of these concrete

infrastructure. Statistical data might not exist on the quantity of additional raw materials consumed during infrastructure repair, however, economically about R 11.8 billion (US$ 1.1 billion) is required annually in South Africa for the repair and maintenance of 8,246 bridges and culverts (SANRAL, 2013). In 2013, this expenditure on repair and maintenance was about 3.8 % of the South African gross domestic product (GDP) (StatsSA, 2014). The provision of RC structures with improved durability could significantly cut down on this annual expenditure.

1.5 RESEARCH OBJECTIVES AND KEY RESEARCH QUESTIONS

The main aim of the study according to the author, is to classify the severity of airborne chloride exposure of RC structures in the Cape Peninsula area. The RC structures considered are not in direct contact with sea water. In order to achieve the aim, the following objectives were established:

i. Measure the concentration of airborne chlorides in selected Cape Peninsula environments using the wet candle device.

ii. Analyse the influence of distance from the coast on airborne chloride loading experienced by RC structures, through collection of specimens for chloride content testing from RC structures close to the coast but with varying distances.

iii. Investigate the influence of environmental parameters such as wind speed, wind direction, rainfall and relative humidity on marine aerosol generation and emission in the Cape Peninsula.

iv. Aided with this information improve the environmental exposure classification guideline for the design of reinforced concrete structures in airborne chloride exposure environments in the Cape Peninsula.

Key research questions are:

i. What effect does the distance from the sea have on airborne chloride loading experienced by RC structures?

ii. How does the microclimate of a location influence transportation and deposition of airborne chlorides further from the coast?

iii. What is a practical and effective method of measuring environmental aerosols in locations at a distance from the coastline?

iv. How do other characteristics of the structure/structural component such as vertical/horizontal orientation influence the chloride deposition rates?

1.6 SCOPE AND LIMITATIONS OF STUDY

The scope of monitoring in this study is limited to locations in the Cape Peninsula marine environment of the Western Cape of South Africa. However, the data collated from previous forensic investigations (chloride profiles) are inclusive of RC structures in the Namib Desert of Namibia. This data is analysed separately because of the differences in the exposure environment and the climate of the Namib Desert compared to the Cape Peninsula. The wet-candle device was used to measure airborne chloride concentrations in the atmosphere. Due to time constraints only five stations were monitored around the Cape Peninsula and nine (9) existing RC structures examined. The measured airborne chloride concentrations and chloride contents of these existing structures were compared with other locations without consideration of differences in construction methods.

The calculation and comparison of surface chloride concentration for each RC structure was carried out by mass of binder (cement). The binder content for most RC structures in this study were estimated based on their tested core sample compressive strengths or from the mix design specified in their design documents. Finally, the selection of the locations monitored and sampled were dependent upon the safety of the equipment, reduced surface roughness (vegetation and buildings) and on the receipt of permission from the relevant authority to access the structures for core collection.

1.7 OUTLINE OF THESIS

This study comprises of five chapters, namely: Chapter 1, which provides a brief background and introduction to the scope and motivation behind the investigation.

Chapter 2, the relevant literature which encompasses the Cape Peninsula climate and the influences of weather and climate factors on the durability performance of RC structures are discussed and reviewed.

Chapter 3 discusses the materials and methods implemented in the experimental procedure. Chapter 4 discusses the results and any trends which emerge thereof. Finally Chapter 5 provides conclusions and recommendations with respect to the investigation.

CHAPTER 2

2 Literature review

2.1 INTRODUCTION

The practice of RC durability design has grown over several decades (Tuutti, 1982; Brown, 1991; Ballim *et al.*, 2009). However, there are still some issues that have not fully been addressed such as the influences of environmental factors on airborne chloride severity of a location. The improved understanding of the significance of environmental conditions on the exposure severity of RC structures would influence design methodologies and maintenance strategies for durable performance.

This chapter contains a literature review examining the Cape Peninsula climate and the importance of estimating service life and severity of exposure of RC structures to airborne chlorides. Discussions on the subject matters of concrete durability, corrosion of steel in concrete and the mechanisms of ingress of deleterious species into concrete in the marine exposure environment are also provided. In addition, it is important to have an understanding of the factors that affect the durability of RC structures (and mitigation measures) with regard to airborne chloride ingress in order to ensure an acceptable performance during the service life of these structures.

2.2 CAPE PENINSULA CLIMATE

All weather data used to describe the Cape Peninsula climate was collated from the South African Weather Service (SAWS), World Weather Online and Weather2 Limited (World Weather Online, 2012; Weather2 Ltd., 2012). The measurements were taken at the Molteno weather station in Oranjezicht and the Cape Town International Airport weather station.

The Cape Peninsula experiences a Mediterranean-type climate with wet-cool winters and dry summers (Cowling *et al.*, 1996). The winters are characterised by a daily high rainfall pattern while the summers are characterised by low to no rainfall. The winter period are characterised by north-westerly winds and the summer period are characterised by south-easterly winds. These winds are a result of a high pressure system formed over the Southern Atlantic Ocean, therefore these south-easterly winds

blow along the south western coastline and across the Cape Peninsula (Cowling *et al.*, 1996).

2.3 CAPE PENINSULA EXPOSURE ZONES

The Cape Peninsula is divided into exposure zones according to where existing air quality and weather monitoring stations are located (*Figure 2.1*). The climate of each zone is assessed and categorised into an exposure zone using the data obtained from these monitoring stations. When assessing the weather components of each exposure zone, only the average daily values are analysed, and not the extreme daily weather conditions. This is as a result of the type of data that is provided by the monitoring stations. In sections that follow, weather elements such as wind speed and direction, precipitation, temperature and relative humidity (RH) will be discussed.

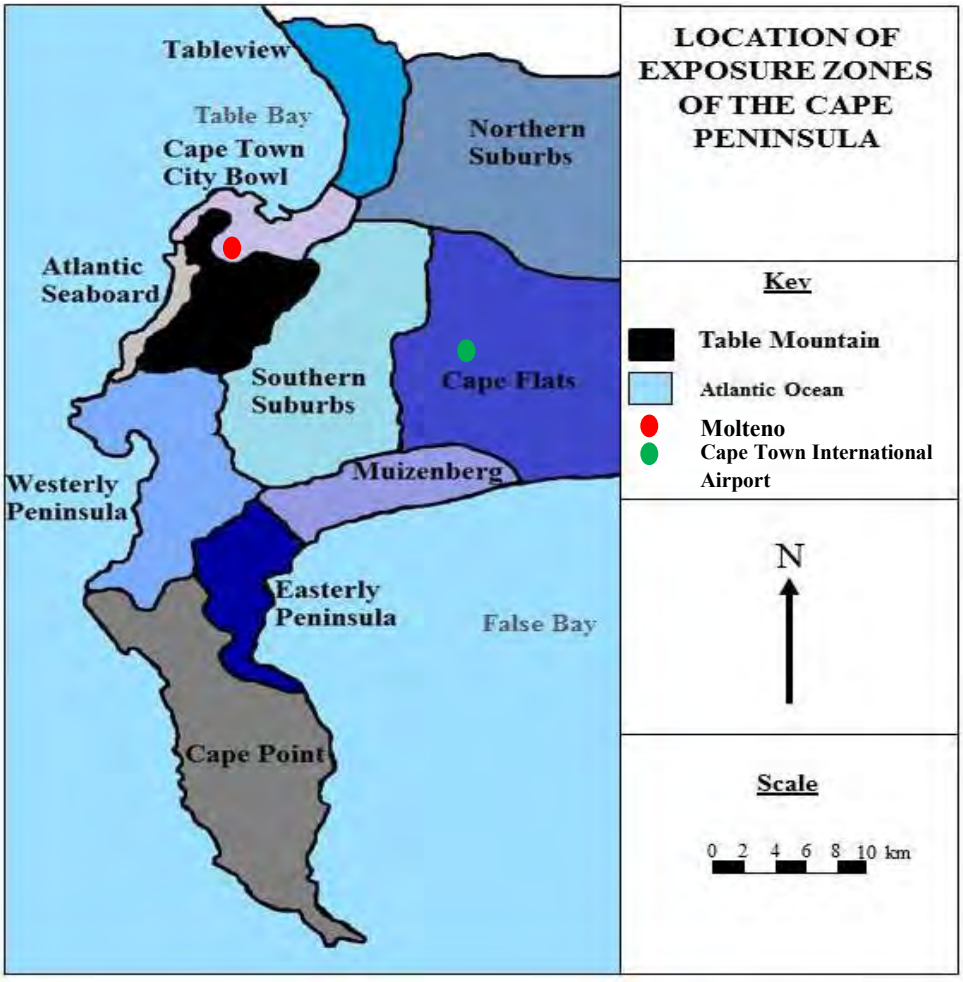

Figure 2.1: The Cape Peninsula divided into exposure zones (Ralfe, 2013)

2.3.1 Micro versus macro climates

Although, the general Cape Peninsula environment may be described as a marine environment, the exposure of RC structures to ingress of chlorides may vary

considerably depending on their location. Coastal locations on the Atlantic Seaboard, Cape Point, Westerly Peninsula and Cape Town City Bowl (

Figure 2.1), which are relatively more seaward would have more severe exposures. Thus, it is important to distinguish between the macro and micro effects of the prevailing climate.

2.3.2 Average wind speed and direction

In winter, the predominant direction of the wind in the Cape Peninsula is north-westerly. It also has an average speed classified as a strong breeze according to the Beaufort wind scale. The summer experiences a strong southerly and south-easterly wind than the winter winds (Cowling *et al*., 1996). Figures 2.2 and 2.3 illustrate the predominant seasonal wind directions in the Cape Peninsula *(Note: the arrows in the diagrams are not quantitative but an indication of wind direction)*.

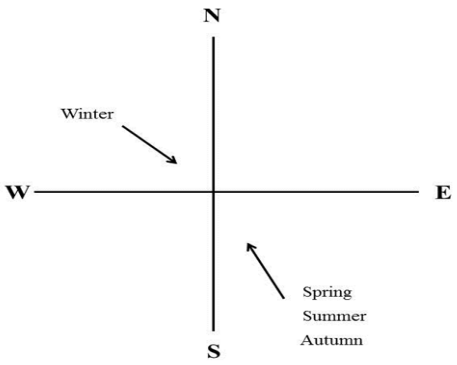

Figure 2.2: Predominant seasonal wind direction at Northern Suburbs (Paarden Eiland and Montague gardens and Bellville) (König & Kaufmann, 2012)

The average weekly wind speed at Cape Town in winter is 19 km/h and 23 km/h in summer, Muizenberg is 27 km/h in summer and 18 km/h in winter and for the Cape Point in winter is 30 km/h and 40 km/h in summer (Cowling *et al*., 1996). But gale-force winds may blow for a consecutive number of days during summer in the south-easterly, usually referred to as the "Cape Doctor" (Deacon, 2004; Britannica Online, 2014).

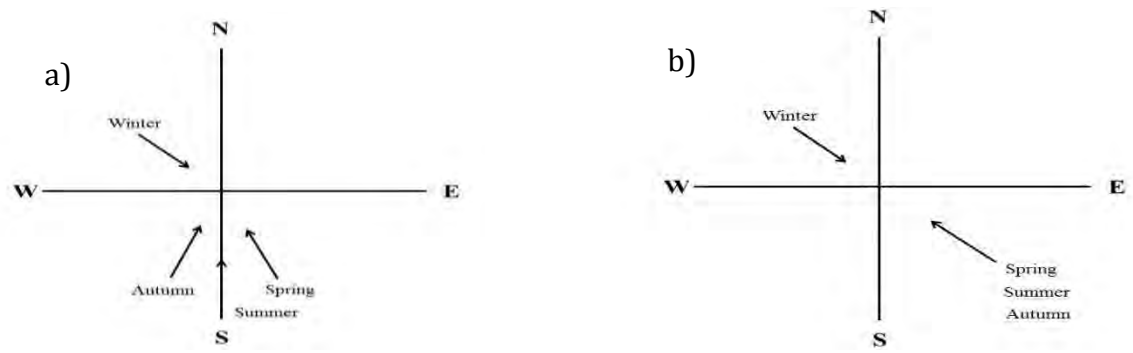

Figure 2.3: a) Seasonal Wind direction at Muizenberg, b) Predominant wind direction at Atlantic Seaboard (Granger Bay) (König & Kaufmann, 2012)

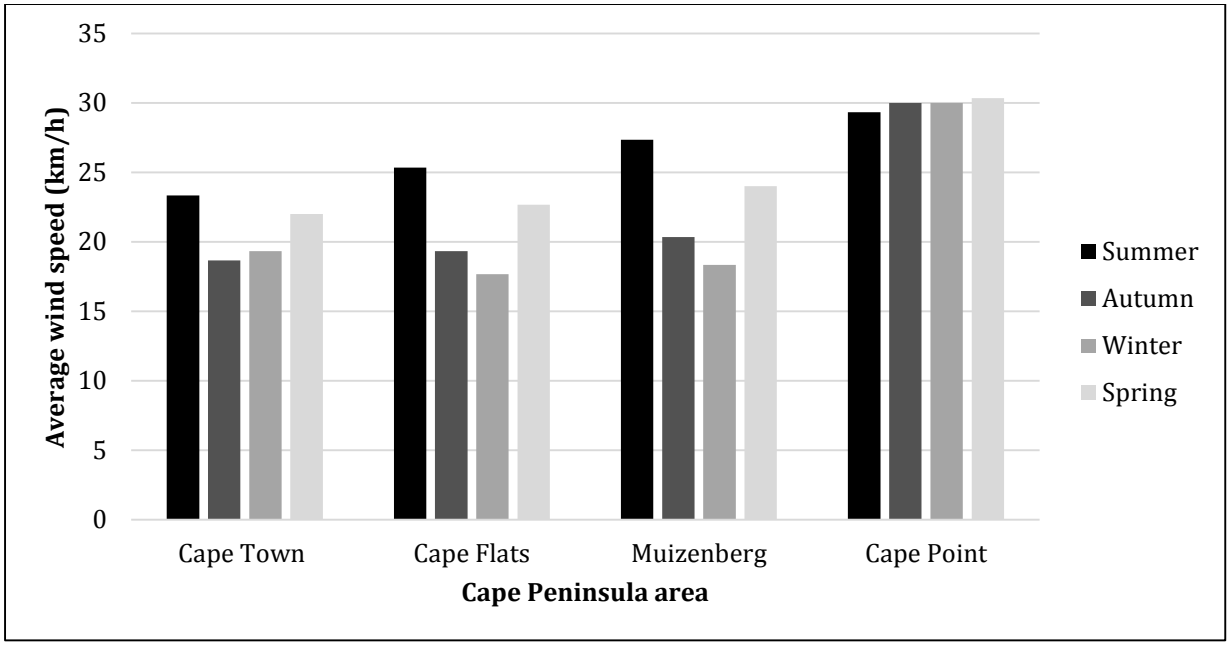

Figure 2.4: The average wind speed during winter and summer at Cape Point and Cape Flats in the Cape Peninsula (adapted from König & Kaufmann, 2012)

In the Cape Flats, the wind speed is quite consistent at 20 km/h as depicted in Figure 2.4. During the high wind speed periods experienced in certain areas in the Cape Peninsula in summer, the generation of airborne chlorides will be expected to be high because larger waves develop on the sea. Whilst for the Cape Point location, the similarities in wind speed infers that all seasons should have similar airborne chloride generation rates. These larger waves break to form white foams which are rich in salt. But factors that could influence the distance which the airborne chloride travels include surface roughness (such as vegetation) and urban infrastructure (such as orientation and height of structures).

Certain areas of the Cape Peninsula, such as the certain areas of the Southern Suburbs, are considered relatively windless (wind speeds that are < 5 km/h) (Cowling *et al.*, 1996) as shown in Figure 2.5 as a result of being blocked off by mountains.

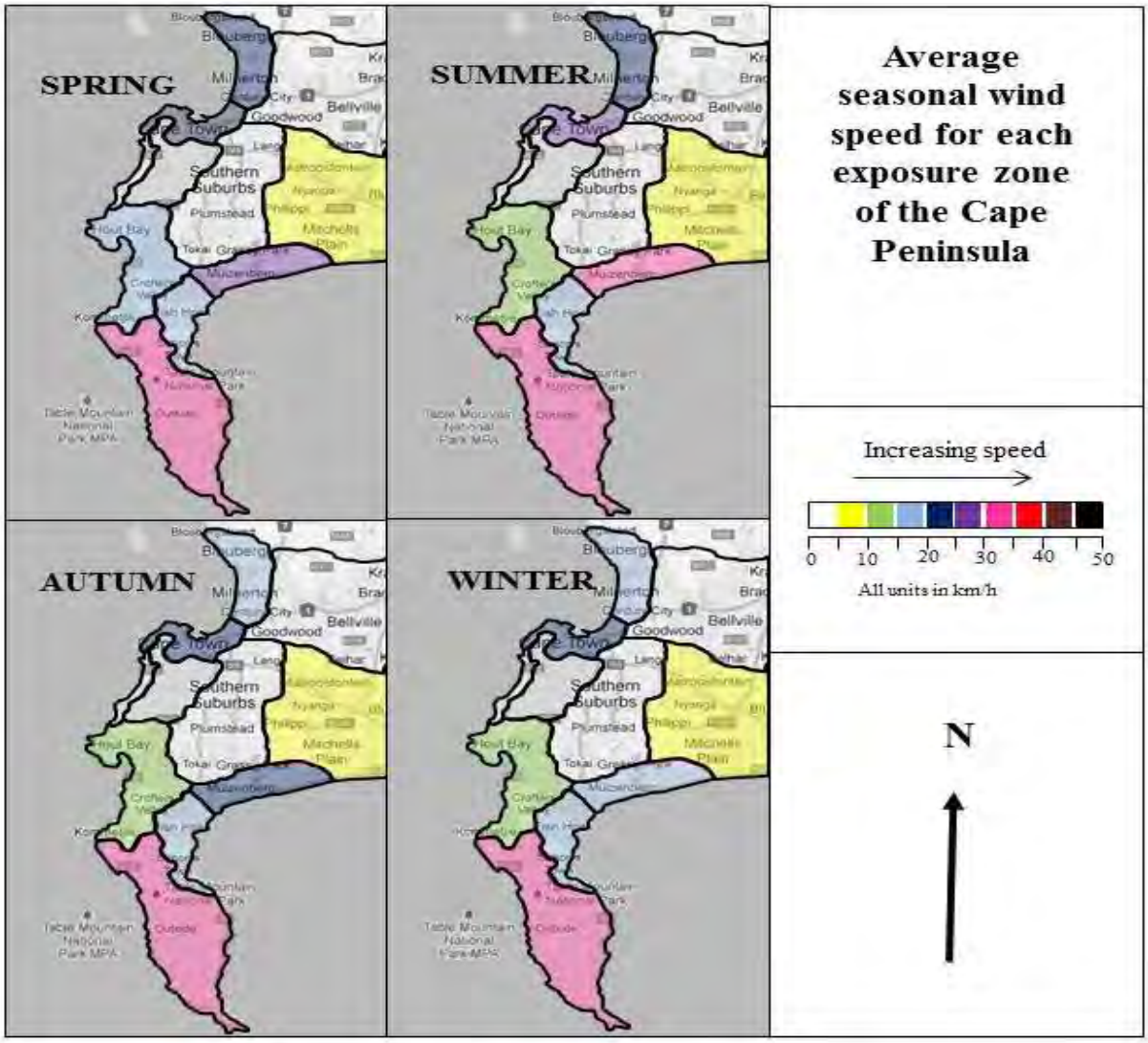

Figure 2.5: Average seasonal wind speed for each exposure zone throughout the year (Ralfe, 2013)

2.3.3 **Precipitation (rainfall)**

Figure 2.6 indicates there is variability in the annual average precipitation for different locations in the Cape Peninsula. Therefore it is necessary to compare the average annual rain days data collected at different monitoring stations (Molteno & Airport) as illustrated in Figure 2.7. Also, from Figure 2.7 it is shown that in summer, the number of rainy days are low, but relatively winter has more rainy days (Cowling *et al.*, 1996). It can be observed that the season with the lowest amount of precipitation is the summer (January).

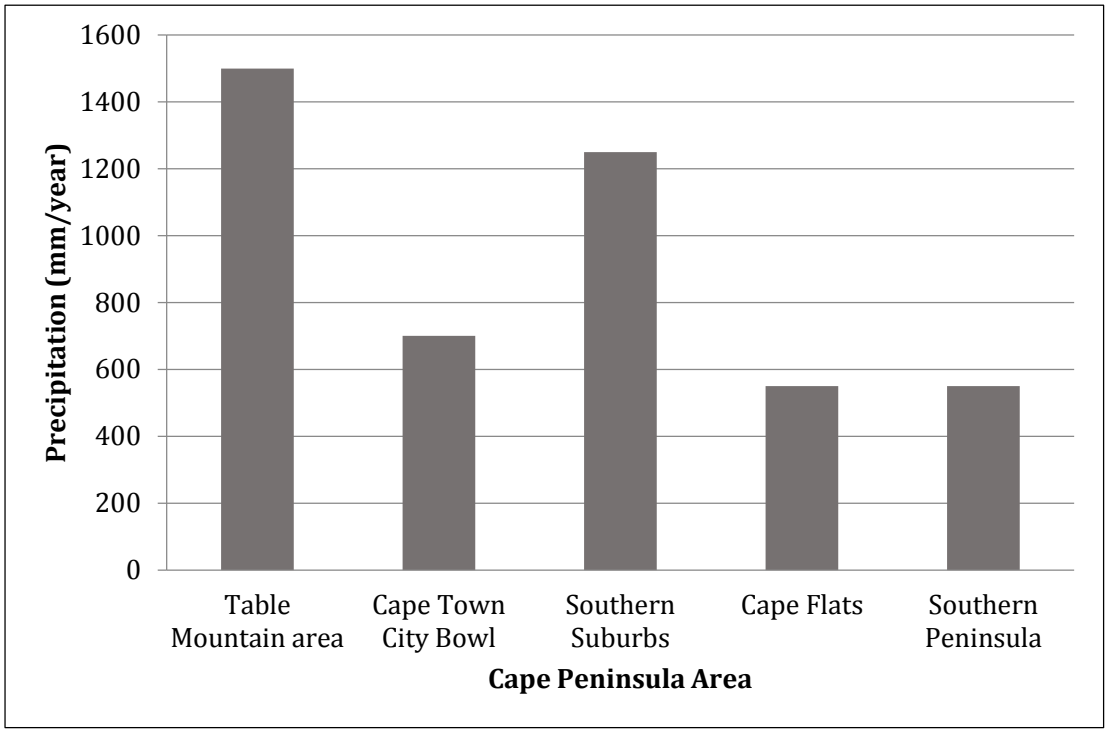

Figure 2.6: The average annual precipitation for particular locations in the Cape Peninsula (Cowling *et al.*, 1996).

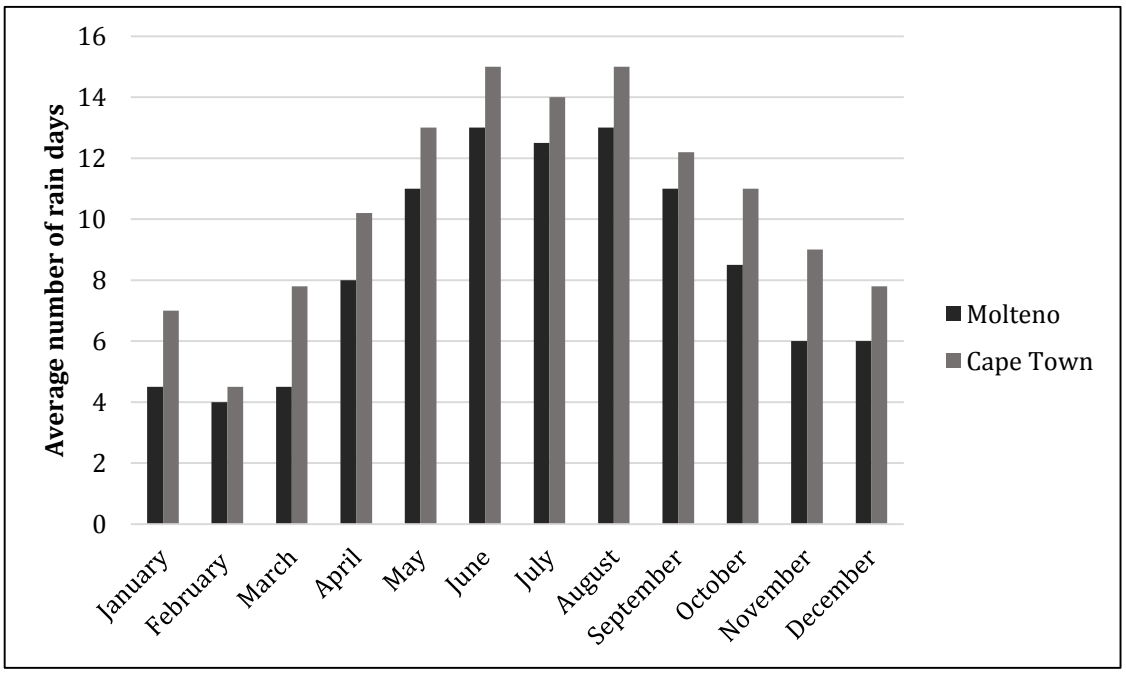

Figure 2.7: A comparison of the average number of rain days between Molteno and Cape Town International Airport (South African Weather Service, 2005).

A broad view of the rainfall pattern for the Cape Peninsula indicates a moderately-high number of rainfall days during winter and a low number of rainfall days at the beginning and end of the year.

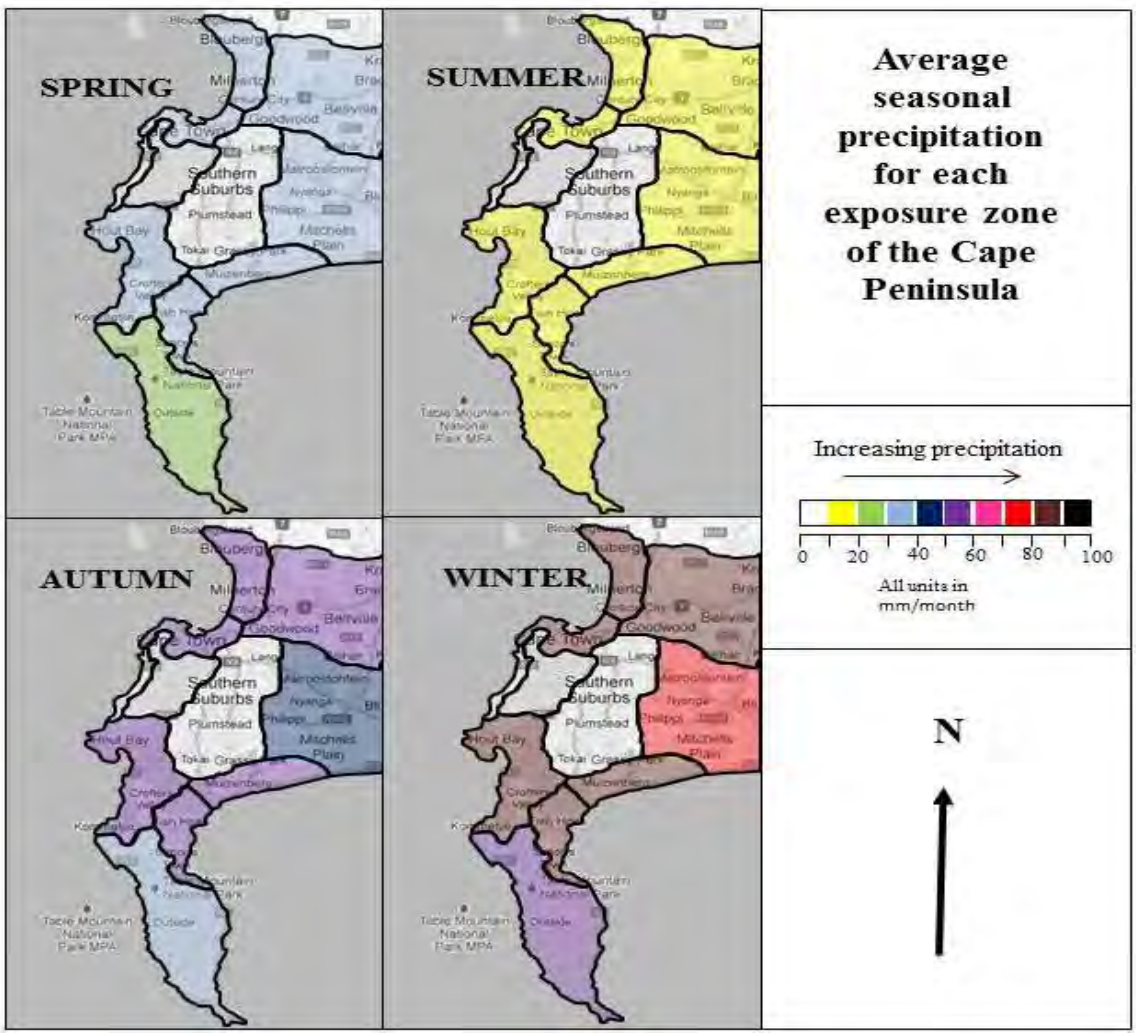

Figure 2.8: Average seasonal precipitation for each exposure zone (Ralfe, 2013)

(Note: Southern Suburbs has higher rainfall in winter than indicated in the image plot)

From Figure 2.8, it can be observed that there is high variability in the seasonal precipitation in the Cape Peninsula. In autumn and winter, average monthly precipitation ranges between 30 – 90 mm/month (with an exception of Newlands in the Southern Suburbs having about 200 mm/month). In spring, the average monthly precipitation is roughly between 5 – 40 mm/month in the Cape Peninsula, but in summer the lowest average monthly precipitation is recorded which is between 0 – 10 mm/month.

2.3.4 **Temperature**

The average annual temperature in the Cape Peninsula lies within the range of 20 – 30˚C. Figure 2.9 shows the average monthly temperature variations. In summer, autumn and spring the temperature roughly ranges between 20 - 30˚C. However, in winter there is a considerable drop in temperature to between 13 – 19˚C.

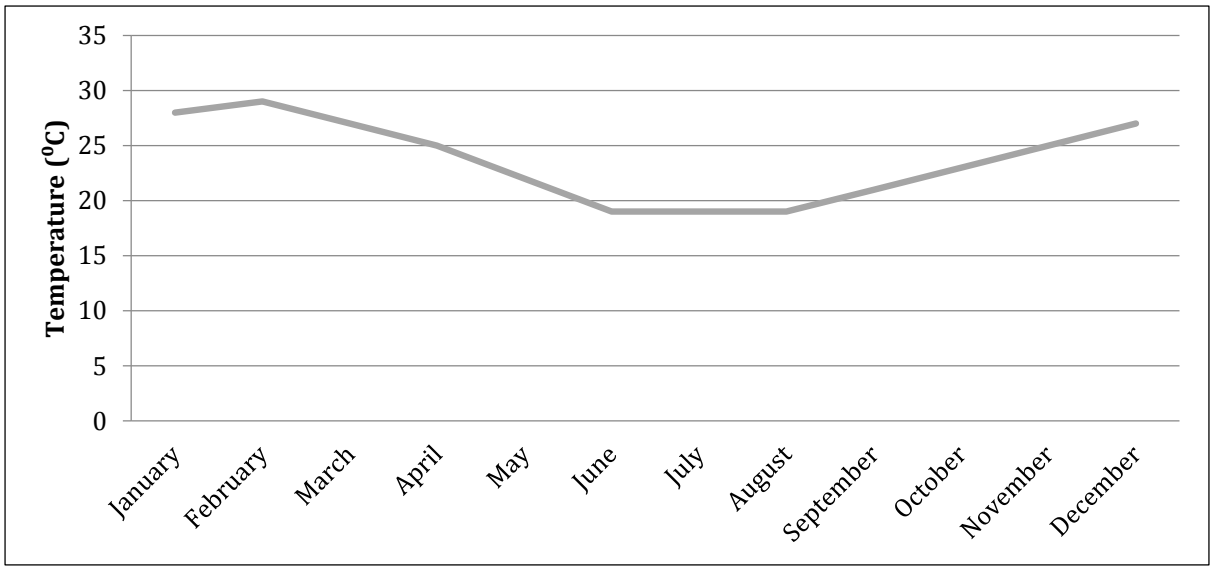

Figure 2.9: Average monthly temperature in the Cape Peninsula area (World Weather Online, 2012)

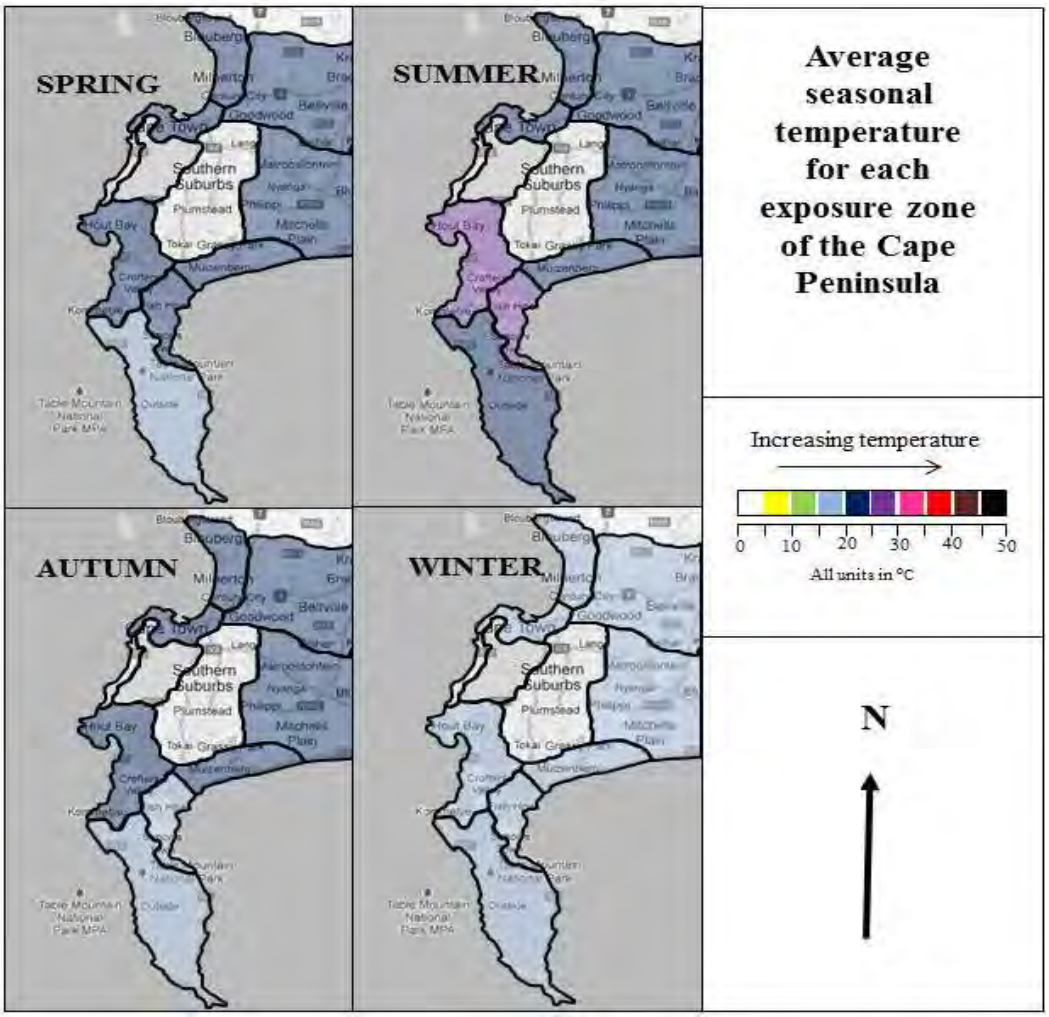

Figure 2.10: Average temperature for each exposure zone throughout the year (Ralfe, 2013)

(Note: Southern Suburbs has similar temperature ranges as the surrounding in the plot locations in all seasons except for winter)

Figure 2.10 depicts the range of average daily temperature for the Cape Peninsula over the four seasons. The maximum average daily temperature in summer is about 30˚C. The exposure locations that experience this maximum average temperature in summer are the Westerly Peninsula and Muizenberg (*see exposure Map in Figure 2.1*).

2.3.5 **Relative humidity (RH)**

Relative humidity (RH) is defined as the ratio of the ambient vapour pressure (P) to saturation vapour pressure (P_s) at the ambient temperature as is expressed as a percentage as indicated in the equation 2-1:

$$\mathrm{RH} = \frac{\mathrm{P}}{P_s} \times 100\ \% \qquad (2\text{-}1)$$

Where P_s is saturation vapour pressure when evaporation and condensation rates are in a state of dynamic equilibrium and P is the ambient vapour pressure. Although RH is defined in terms of pressure, it is in fact determined by measuring the temperature and moisture content of the environment (Matthew *et al.*, 2006). It is measured using the wet-and-dry-bulb hygrometer.

RH of a location is dependent on the moisture content of the atmosphere and this is influenced by precipitation and temperature. The more saturated the air with moisture the higher the RH. During spring and summer seasons, the Cape Peninsula experiences a low RH. The RH is the highest during autumn and winter, when there is a higher precipitation (Cowling *et al.*, 1996) as shown in the figures 2.11 and 2.12.

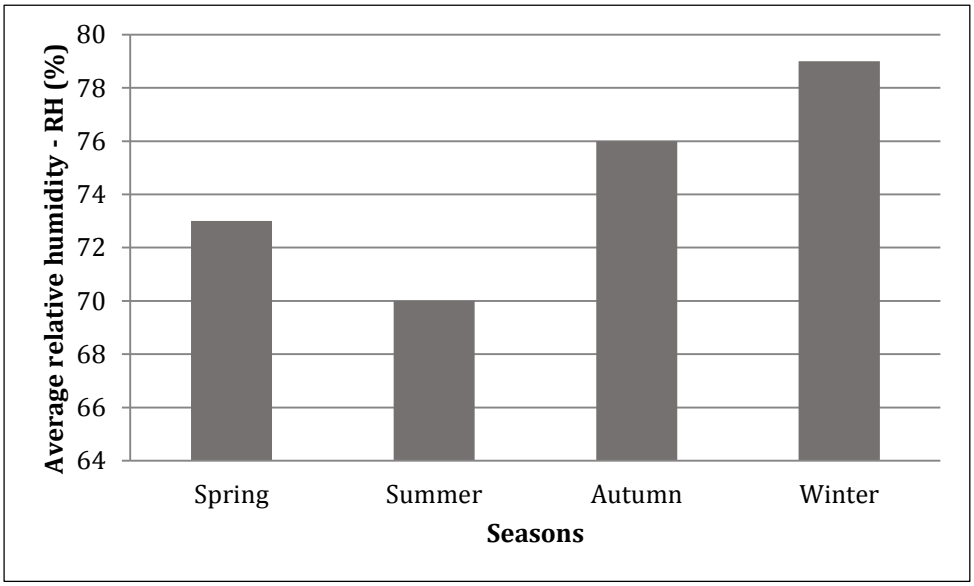

Figure 2.11: Average seasonal relative humidity in the Cape Peninsula (Ralfe, 2013)

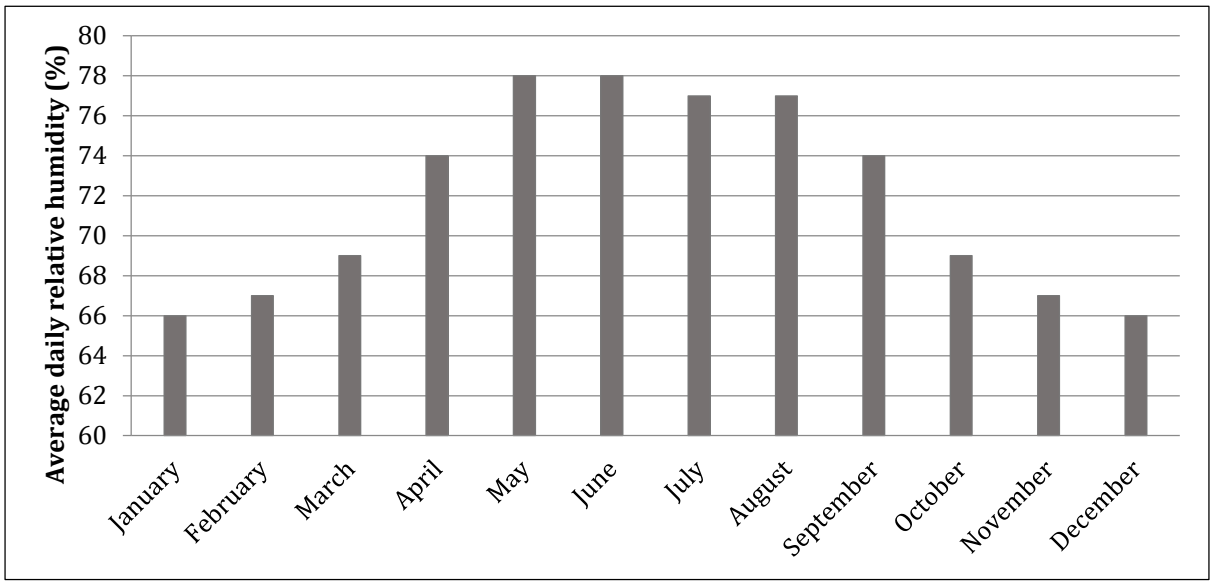

Figure 2.12: Average monthly relative humidity measured at the Cape Town International Airport station (Weather2 Ltd., 2012)

The average RH for the Cape Town area in the Cape Peninsula is 78 % (Alexander & Beushausen, 2009). This is relatively high and implies there is always a substantial availability of moisture in the atmosphere.

2.3.6 Interrelationship of weather elements

The plot in Figure 2.13 depicts the interrelationship of the weather elements. It can be observed that the average sea temperature ranges between 15 – 19˚C measured at the Atlantic Seaboard and False Bay (depicted by light green curve).

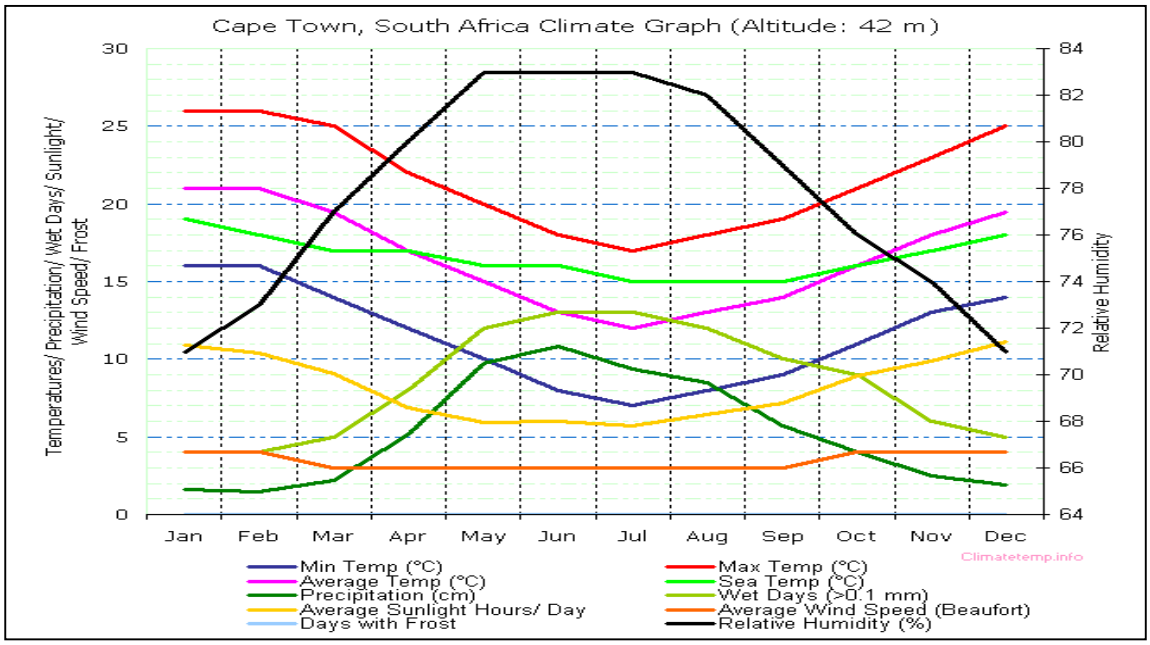

Figure 2.13: Climatic characteristics of Cape Town in one year (Climatemps.com, 2008)

The minimum atmospheric temperature curve ranges from 8 – 16°C and the maximum temperature ranges between 16 – 26°C. The wind speed ranges from 30 – 40 km/h, precipitation is between 20 – 110 mm/month and RH ranges from 71 – 83 % .The RH and precipitation peak in the months of June – August.

There is a noticeable decrease in temperature and wind speed over the middle of the year (winter) but a corresponding increase in precipitation during the same season. However, it can be noted that the Cape Peninsula is generally windy with occasional gale force in summer and relatively humid all year round. There also exists an inverse relationship between temperature and RH, since as temperature decreases in winter, RH increases. There is a direct relationship between RH and precipitation as they both increase in winter, and then decrease towards the beginning of summer

2.4 EFFECT OF CLIMATE ON CONCRETE

With respect to the interactions of RC structures in the Cape Peninsula to their environment, it can be expected that concrete structures will remain saturated for a long period of time due to the high number of rain days during winter. Whereas during summer, the number of rain days are fewer and therefore the time that concrete structures will be saturated will be less. Therefore it can be expected that during the cooler months, winter, chloride ingress will most likely be accelerated than in summer. However, the rate of corrosion in the structure will be dependent on the concentration of chloride ions at the level of the reinforcement.

2.5 CONCRETE DURABILITY

It is important that to understand the fundamentals of the durability of concrete and how it affects its performance during its service life. In this section, a brief background on the issue of concrete's durability and service life is covered. Also discussed briefly are benefits gained from the construction of durable structures and finally, factors affecting the durability of concrete are also examined.

The durability of a RC structure is closely related to the structure's performance during its service life (Narasimhan & Chew, 2009). Service life is the period of time after a structure's construction during which the designed serviceability limits or properties have exceeded the minimum acceptable values (EN 1990:2002). The Building Research Establishment (BRE) states that design service life should be defined as "*…the assessment of a structure, both as a complete building and individual components, which predicts its potential lifetime based on levels of design, workmanship, maintenance and the environment*" (Kelly, 2007). In addition, Khatri & Sirivivatnanon (2004) give a simplistic definition of service life with the main focus on chloride-induced corrosion *"…as the period of initiation or the time required for the chloride concentration at the reinforcement to reach the critical chloride level"*. Fagerlund (1985) also defines service

life of any material as the time over which it fulfils its functional requirements. However, a more appropriate definition for the service life of a structure should include the time to deterioration of the constituent materials of the structure which affects its functionality and cost of repairs. All these are decisive factors in determining the service life duration for a structure.

Overall, numerous factors influence the service life and durability of a structure, one of these is the variation in material characteristics. Invariably in any structure or building, there is bound to be variation in the quality of concrete due to variation in water/binder (w/b) ratio, site construction practice, variation in extent of curing or the variation in the hydration of cement due to changes in temperature. Another factor is the deviation in the thickness of the cover on the steel provided by the concrete or some of sections of the cover could be damaged. Variation in the service environment is another considered factor in service life. The structure could either be in the tidal zone, the splash zone, continuously immersed in the seawater or be exposed to airborne chloride.

2.5.1 Factors affecting durability of RC structures in the marine environment

Durability of materials and structures is dependent on the resistance of the material to the ingress of aggressive substances and prevailing environmental conditions at the exposed surfaces of the structure. The performance based design approach is based on predicting the future deterioration rates of a RC structure. In order to design a durable structure using the above design method, certain information is needed (Fagerlund, 1985):

1. The structure's performance requirements
2. Its prevailing environmental conditions – microclimate of environment
3. The major deterioration mechanism(s)
4. A method of predicting the rate of deterioration

This study looks critically at the prevailing environmental conditions of the exposure locations. It also predicts the interaction between the environment and the RC structures. Salinity in marine atmospheres accelerates reinforcement corrosion and varies, ranging from extremely high values close to coast to low values as distance increases. The concentration of marine aerosol in the atmosphere determines the severity of exposure of a RC in its service environment. The severity of exposure in an airborne chloride environment is affected by multiple factors such as altitude, distance from the sea, land orography, land topography, direction and velocity of prevailing winds.

2.5.1.1 Material characteristics

The physical and chemical properties of the materials that compose the concrete would have an effect on its resistance to deterioration. Therefore the type of concrete used to

protect reinforcement has a major effect on durability. Higher grade concretes are usually prescribed by design codes but the resistance of the concrete is also dependent on binder type and water to binder ratio. Importance should be placed on binders that interact with the chloride, deplete chloride concentration and reduce concrete pore space. Binders that have higher chloride binding ability such as fly ash (FA), ground granulated blast-furnace slag (GGBS) and condensed silica fume (CSF) reduce the permeability of concrete (Yildirim *et al.*, 2011), compared to using pure Portland cement (PC). GGBS and FA have similar chemical composition as PC but GGBS has a lower calcium oxide (CaO) content ranging between 32 – 37 %, FA has 4 – 7 % and CSF 0.3 – 0.6 %, whereas PC has 63 – 69 % (Grieve, 2009) (*Table* 2.1). The ratio of CaO/ SiO_2 (silicon dioxide) content determines the ability to form hydration products. The figure below illustrates qualitatively the major chemical composition of PC in relation to supplementary cementitious materials (SCMs) and their hydration products.

Table 2.1: Chemical composition of South African PC and SCMs (Grieve, 2009)

	CaO	**SiO_2**	**Al_2O_3**	**MgO**	**Fe_2O_3**	**Na_2O + 0.658 K_2O**	**TiO_2**	**K_2O**
PC	63-69	19-24	4-7	0.5-0.6	1-6	0.2-0.5 (0.7*)	-	-
GGBS	32-37	34-40	11-16	10-13	0.3-0.6[a]	-	0.7-1.4	0.8-1.3
FA	4-7	48-55	28-34	1-2	2-4	1-2	-	-
CSF	0.3-0.6	92-96	1-1.5	0.6-0.8	1-1.6	-	-	1.2-2.0

a – Iron Oxide (FeO)

* current alkali content of commercial PC - CEM II/ A-L 52.5N

PC is the major component in concrete that gives it the binding ability with the aggregates and the high alkali content in the pore solution (pH of 12-13) (Papadakis *et al.*, 1990). One of the products of PC hydration process is calcium-silica-hydrate (CSH) which forms a stable bond in an alkaline medium, hence it is important that this alkalinity is maintained. The CSH will breakdown to calcium hydroxide (CaOH) which raises the alkalinity if the pH reduces in the pore solution due to alkali consumption/combination with deleterious species such as chloride ions or carbon dioxide.

Fly ash (also known as pulverized fuel ash, PFA) is a by-product of the combustion of coal powder in thermoelectric power plants. It is composed of fine-spherical particles (dimensions from 1-100 μm) that are collected from exhaust gases with electrostatic precipitators or mechanical filters (Bertolini *et al,.* 2013).

In South Africa, two slag types are commercially available, ground granulated blast-furnace slag (GGBS) and ground granulated corex slag (GGCS). Slag is used to substitute PC in concrete from about 30% - >50%, depending on the performance (in terms of equivalent strength or durability) needed from the concrete (Lothenbach et al. 2011). Ground granulated Corex slag (GGCS) is produced locally in the Western Cape and hence

available. GGBS and GGCS are both by-products of iron refining processes, but GGCS is a by-product using the Corex method at the Saldanha plant in the Western Cape. GGCS also has as high chloride binding capabilities as GGBS (Ballim *et al*., 2009). Also, GGCS when used in concrete production produces earlier-age concrete strength compared to GGBS which only starts to form hydration products after about 3 days (Alexander & Beushausen 2009).

Condensed Silica fume (CSF) is a waste product of manufacturing alloys of silicon. It consists of an extremely fine powder of amorphous silica. The partial replacement of CSF with Portland cement may lead to a very low porosity of the cement paste, increasing the strength and lowering the permeability. However, since it consumes the hydroxyl ion content (OH^-) of cement, it reduces the pH of the pore solution (Baroghel-Bouny *et al.*, 2011). It is usually added in the proportion of 5-10 % and it is combined with the use of a superplasticizer in order to maintain adequate workability of the fresh concrete (Bertolini *et al*., 2013).

The use of SCMs to partially replace plain PC is common because of the associated benefits with their use, which generally relates to improved economic and durability performance and sustainability properties (Naik, 2008; Otieno *et al.*, 2014). SCMs have been observed to improve resistance to chloride penetration, extend time to corrosion initiation and decrease corrosion rate in both cracked and uncracked concretes (Uysal *et al.*, 2012; Safehian & Ramezanianpour, 2013; Otieno *et al.*, 2014).

2.5.1.2 **Construction site practice**

This is a very important factor affecting the durability of cast-in-place structures more than precast structures. In construction of precast RC structures, usually better quality control measures are more easily adopted compared to cast in-situ structures. Provision of admixtures, cement extenders and concrete of high compressive strength does not solve corrosion problems, if adequate quality control is not ensured on site. Substandard site practice will also cause structures to be susceptible to penetration of carbon dioxide and deposited chlorides. Unsuitable site practices include but are not limited to; lack of curing, low or variations in concrete cover, inadequate compaction of in-situ concrete, use of contaminated mixing water, non-uniform cover depth and inaccurate batching of mixes.

Costa & Appleton (2002) reported that an adequately designed concrete mix may still have a high deterioration rate primarily as a result of poor workmanship on site. Case studies of different concrete structures such as docks, wharves and bridges located in the estuary of River Sado, on the west coast of Portugal affirmed this inference. One of the case studies examined during their investigations was a bridge with measured characteristic compressive strength of 50 MPa and w/b ratio of 0.32. However, poorly made construction joints and honeycombing defects were often observed on the construction site, also with quite high variation in cover depths. Locations where corrosion products were visible in the RC structures had cover depths of less than 20

mm (Costa & Appleton, 2002). Suitable case studies discussing the durability effect of concrete cover depth on service life are examined in chapters 4 and 5.

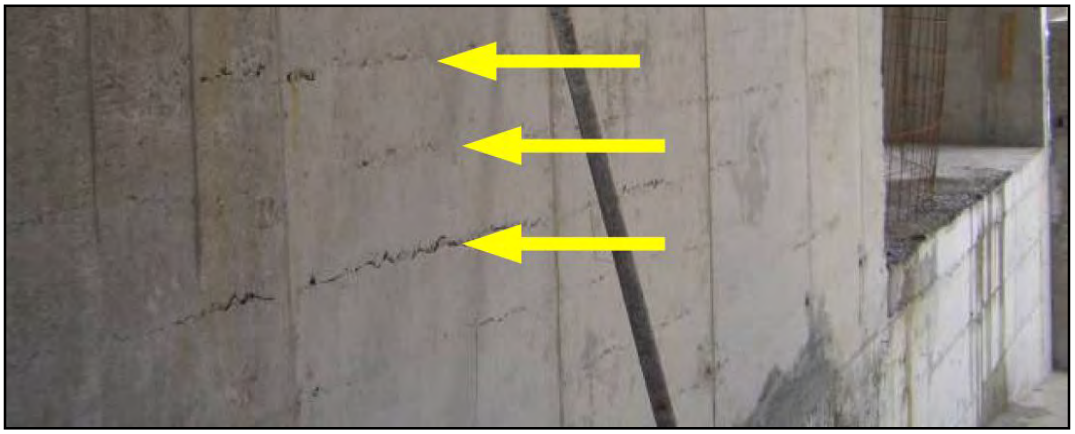

Figure 2.14: Poorly constructed joints at a site in Cape Town

An example of poorly constructed cold joints can be seen in Figure 2.14 taken from a construction site. Joints not properly constructed, lean concrete mixtures and localized poor concrete compaction can serve as openings where deleterious materials ingress into the concrete. Poor execution quality during construction can reduce the expected performance of a good durability design.

2.5.1.3 **Concrete cover depth**

Cover depth is one of the factors that can be controlled during design and execution of a structure. The concrete must provide protection for reinforcement from the ingress of deleterious species. The potential durability of a structure is greatly increased if it provides adequate cover to reinforcement and if this is maintained during in-situ placement.

A sensitivity analysis with respect to life cycle cost carried out by Narasimhan & Chew (2009) indicated that steel cover depth seemed to be most influential factor for longer service life. In addition, it should be noted that high strength concrete does not imply reduction in cover depth, as cracks and voids may reduce resistance of the structure to ingress of chlorides. Design codes indicate that cover between 50 – 75 mm in marine region is sufficient (BS 8500-1: 2002). On the other hand, if cover depths are greater than 100 mm, it could lead to increased crack width formation (Pillai & Devadas, 2003).

2.5.1.4 **Service environment**

Ultimately, the rate of deterioration of any material is dependent on the environment to which it is exposed. The service environment is a major factor to be considered when designing RC structures. It is important as durability of concrete structures is location-specific – in a particular location a structure can be durable, but in different climatic conditions the rate of deterioration for the same structure changes. RC structures located along the coastline, which are exposed to airborne chlorides generated from the sea, are prone to a greater degree of corrosion than most inland structures

(Anwar Hossain *et al.,* 2009; Meira *et al.,* 2010; Hossain & Easa, 2011). For this reason, it is essential to assess the severity of exposure at each specific site whether inland or in a coastal region by determining the microclimatic conditions, whether coastal or inland (Wilmot, 2006).

The transfer and subsequent deposition of chloride ions from the sea to inland locations may vary to a large extent depending on the location of structure, prevailing climate of the environment and the degree of exposure to chlorides. Location of a structure refers to the nearness or orientation of the structure to the sea. Song et al. (2008) analysed the transport inland and ingress of airborne chlorides into concrete, by placing different concrete specimens in three different latitudes: in the UK, Japan and Venezuela. It was found that concrete structures exposed to a tropical (equator) environment showed more susceptibility to chloride attack (Safehian & Ramezanianpour, 2013; Song *et al.*, 2008; Bertolini *et al.*, 2013). This was attributed to the high level of relative humidity, temperature and chloride concentration experienced in the tropics. High relative humidity and temperature experienced in the tropics usually causes an increase in the rate of evaporation and moisture retained in the atmosphere. This causes a drop in sea level, therefore, the salinity of the sea water is higher in the tropics. Consequently, the aerosols generated in the tropics have a higher saline content.

The most important factors to consider in the service environment's interaction with chloride corrosion is chloride ions and moisture, carried inland by rain, dew, condensation, or high relative humidity (RH) and global or local winds. In the absence of these chloride ions and moisture, the corrosion of embedded reinforcement will be stifled.

Precipitation

Precipitation may have a beneficial effect in washing away corrosive agents that have settled on exposed surfaces. This effect is could be particularly beneficial in marine environments. However, if the rain collects in cracks on surface of concrete, it may accelerate corrosion by supplying continued wetness. Roberge (2011) indicated that dew and condensation are undesirable from a corrosion viewpoint if not accompanied by frequent rain washing which dilutes or eliminates contamination. A film of dew, saturated with sea salt or acid sulphates, and airborne chloride provides an aggressive solution for the propagation of corrosion.

Furthermore, winds coming down off a mountain may also carry chlorides from the sea. The proximity of a mountain to the ocean gives rise to orographic precipitation. Orographic precipitation occurs when air masses are forced up the side of elevated land formations, such as mountains, by ocean wind. The upward movement of the rising air hits the side of the mountain resulting in its cooling and eventually cloud formation and precipitation. Figure 2.15 illustrates that in an orographic precipitation regime it is possible to transport airborne chlorides (through vapour) from the ocean to the far side of the mountain. This could also imply that RC structures that are situated behind

mountains with proximity to the sea should still be considered as possibly being exposed to a marine environment.

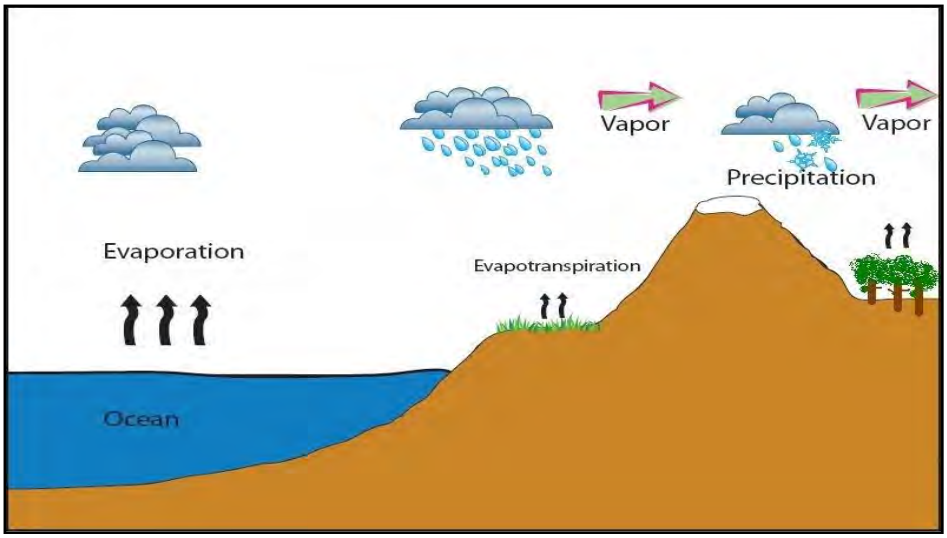

Figure 2.15: Orographic Precipitation model (Science Education Resource Centre-SERC, 2012)

On the other hand, a high amount of precipitation leading to saturation of concrete pores could be beneficial to RC structures with low permeation or high permeation. If the moisture cannot penetrate to the steel then the rate corrosion slows down or is non-existent. However, if the structure is fully submerged, it is fully saturated and the supply of oxygen is reduced and reinforcement corrosion is stifled.

Wind

Ocean air is rich in marine aerosols resulting from the evaporation of drops of sea water, mechanically transported by the wind (Woodcock & Blanchard, 1980). Certain marine wind directions contribute to the entrapment and transportation inland of airborne chlorides from the sea; these are referred to as saline winds (Morcillo *et al.*, 2000). The study by Morcillo et al., 2000 also indicated that there was a critical velocity (approximately 3 ms^{-1}) for these saline winds where there was a noticeable surge in coastal atmospheric salinity in the air.

During winter, a north-westerly wind is experienced across the Cape Peninsula. The summer period on the other hand, experiences strong southerly and south-easterly winds over a longer period of time in comparison with winter winds (Cowling *et al*., 1996). Certain areas of the Cape, such as parts of the Southern Suburbs, are considered relatively windless (Cowling *et al*., 1996). The wind speed experienced around the Cape Peninsula is relatively high due to the exposure of the Peninsula to the ocean winds, which transport sea spray on-shore and cause higher concentrations of chlorides in the atmospheres of the exposure zones that are bordered by the sea.

The seasonal differences in prevailing wind directions and speeds implies seasonal differences of RC exposure to airborne chloride deposition. During the high wind speed

periods in summer, the generation of airborne chlorides will be expected to be high because larger waves develop on the sea. These larger waves break to form white foam which is rich in salt. But factors that could influence the distance which the airborne chloride travels include surface roughness such as the presence of vegetation and urban infrastructure.

Temperature

Temperature also plays an important role in corrosion severity of an environment (Bertolini *et al.,* 2013). There is an expected doubling in corrosion activity for every 10˚C increase in temperature (Roberge, 2011). An increase in temperature was noted to serve as a catalyst for increasing the rate of chloride attack experienced by steel reinforcement embedded in concrete (Lindvall, 2007; Alhozaimy *et al*., 2012). Temperature also influences the relative humidity and affects the atmospheric residence time for airborne sea salts. The residence time of an airborne chloride particle in the atmosphere is the period of time between its generation from the breaking of an ocean wave to its deposition onto a surface. Higher temperature in a moisture-laden atmosphere would increase the formation of vapour which serve as carriers of salts.

For embedded reinforcement, the moisture at the steel surface depends on the moisture present in the pores of the concrete. The steel is then prone to corroding in the presence of this moisture and also the presence of oxygen (Morinaga, 1990).

Relative humidity (RH)

Marine environments typically have higher RH, as well as aerosols high in salt concentrations (Roberge, 2011). A study carried out in an environment with high RH indicated that higher airborne chloride concentrations were measured inland (Meira *et al,.* 2010), as a result of the moisture present in the atmosphere giving the aerosol particles longer residence time. Also for corrosion initiation, the critical humidity level is a variable that depends on the nature of the corroding material (Roberge, 2011). It has been found that critical RH for exposed steel to corrode is 60% (Roberge, 2011), this also holds for steel embedded in uncracked concrete but could range from ≥ 80% (Tuutti, 1982; Fagerlund, 1985). At a RH of less than 45%, corrosion processes are completely mitigated (Morinaga, 1990).

In some cases, it has been suggested that at RH of 85-100 % corrosion initiation time decreases and hence rate of deterioration is slowed down (Tuutti, 1982; El Hassan *et al.*, 2010). This can be attributed to the blocking of pores at high RH and temperature – the conversion of moisture to vapour can result in discontinuity of concrete pores (Alhozaimy *et al.*, 2012). Humidity is more important in the first stage of corrosion which is the diffusion of chloride ions through the concrete cover (Tuutti, 1982), while the temperature is influential in accelerating the rate of steel corrosion (Tuutti, 1982; El Hassan *et al.,* 2010).

2.5.2 Transport mechanisms of chloride ions into concrete

Chloride ingress in concrete occurs through a combination of mechanisms. These include permeation, diffusion, capillary absorption, migration and convection. Another mechanism of transport which will not be discussed further is wick action – it is the movement of water and ions in a concrete element from a saturated to a drying surface (Kessy *et al.*, 2013). The pore structure, environmental conditions and degree of saturation of a concrete structure strongly influence the rate of chloride ingress into concrete and the interaction between species (Hilsdorf *et al.*, 1995).

In addition, the moisture state of concrete and the prevailing environmental conditions determine the rate at which chloride penetrates concrete. In saturated concrete, chloride transport occurs by diffusion through the pore solution. However, for concrete with surfaces exposed to the atmosphere (unsaturated or partially saturated concrete) the ingress of chlorides is predominantly controlled by capillary absorption through the pores and diffusion of chloride ions through pore solution (Basheer, 2001; Song *et al.*, 2008; Kessy *et al.*, 2013). The chemical interactions between ions in the pore solution and the pore walls affect the movement of chloride ions through concrete.

Cement has a chloride binding capacity which occurs as a result of the interaction between the porous matrix and chloride ions which results in the effective removal of ions from the pore solution. All cements bind a proportion of the chloride present but blended cements have a higher chloride binding capacity *(*Yildirim *et al.,* 2011*;* Meira *et al.,* 2007). This binding action slows down the rate at which the threshold value of chloride in concrete is reached. Thus, it lengthens the time taken for the initiation of reinforcement corrosion.

While there are many factors associated with the constituents of the concrete, the binder type and admixtures used in its production and its pore solution composition influence its chloride binding ability. The pore structure is mainly influenced by w/b ratios. Concrete with lower w/b ratios are less porous than concrete with higher w/b ratios. In concrete with higher w/b ratio, the unused water in the hydration process forms capillary pores when the moisture dries out.

2.5.2.1 **Permeation**

Historically, permeability was used as the criterion to characterize the penetrability of concrete regardless of other transport mechanisms (Page *et al.*, 1981; Dhir & Byars, 1993; CCAA, 2009). Penetrability is broadly defined as the degree to which a material allows the movement of gases, liquids, or ionic species through its pores. It embraces the concepts of permeation, sorption, diffusion and migration and is measurable in terms of the transport parameters (Alexander & Mindess 2005)

There are situations when permeability is relevant such as in permanently submerged concrete where water is forced through concrete by hydraulic pressure. When concrete

structures are not in contact with water under pressure, such as a bridge exposed to the environment, permeability is generally not the most important mechanism (Bamforth *et al*., 1997).

Permeability relates to the movement of a liquid under hydrostatic pressure (head of water). Broadly, permeability can be defined as that property of a medium which characterizes the ease with which a fluid will pass through it under the action of a pressure differential. The permeability of concrete depends on its porosity as well as the size, distribution, shape, tortuosity and continuity of capillary pores. Therefore it depends on all factors that influence the pore structure of concrete i.e. water to cement ratio, type of cement, cement replacement materials and the progress of hydration (Dhir & Byars, 1993; Kessy *et al.*, 2013)

Darcy's law has been generalized to apply to any fluid flowing in any direction through a porous material, so long as the conditions of flow are viscous as shown in Equation 2-2 (Bertolini *et al,.* 2013)

$$\frac{\mathrm{dq}}{\mathrm{dt}} = \frac{\mathrm{K}\,.\Delta\mathrm{P}.\mathrm{A}}{L\,.\,\mu} \qquad (2\text{-}2)$$

Where $\frac{\mathrm{dq}}{\mathrm{dt}}$ is flow velocity, K is referred to as the intrinsic permeability of the porous medium, ΔP is the pressure loss over the flow path length of L (thickness of the specimen), A is the surface of the cross-section, μ is the viscosity of the fluid.

Intrinsic permeability is the most rational concept of permeability. Intrinsic permeability has dimensions of area and depends purely on the characteristics of the porous medium as mentioned earlier. It is independent of the fluid characteristics which govern the flow, i.e. viscosity μ expressing the shear resistance of the fluid. For gases, the compressibility must be considered as well and the pressure difference is related to the mean pressure.

2.5.2.2 **Capillary absorption**

The movement of liquids in unsaturated porous concrete due to surface tension acting in capillaries is referred to as capillary absorption (Soshiroda & Voraputhaporn, 1999). A linear relationship has been observed between the square root of time and the total volume or mass of liquid absorbed or the depth of penetration. Absorption in concrete is not only controlled by the pore structure, but also by its moisture content (Basheer, 2001).

The absorption of water into concrete is considered to have two basic parameters.

1. The mass of water which is required to saturate the concrete (the effective porosity);
2. The rate of penetration of the capillary rise (the sorptivity).

Since the filling of capillary channels, voids and the advancing of water occur almost simultaneously during absorption, a combined effect only can be measured, which will give a capillary effect. Rate of sorptivity in concrete can be estimated by the Equations 2-3 and 2-4, according to Soshiroda & Voraputhaporn, (1999).

$$S = \frac{\Delta M}{\sqrt{t}}\left[\frac{1}{A.Z}\right] \tag{2-3}$$

$$Z = \frac{M_{sat} - M_0}{A.L} \tag{2-4}$$

where, S is sorptivity , Z is effective porosity, A is the cross sectional area of the specimen M_{sat} is mass of specimen at saturation and M_0 is dry mass of specimen and $\frac{\Delta M}{\sqrt{t}}$ is the slope of straight line produced when mass of water absorbed is plotted against the square root of time.

2.5.2.3 **Diffusion**

Diffusion is the process by which particles, ions, liquids etc. are transported from one part of a system to another due to concentration gradient. The rate of diffusion is defined by the diffusion coefficient of the medium either in gaseous, ionic and molecular forms (Anwar Hossain *et al.,* 2009; Arito, 2012). The movement occurs as a result of random molecular motions, which take place over small distances. The progress of diffusion is much faster in gases than in liquids with respect to time.

The diffusion equation can be expressed by Fick's second law of diffusion applied to chloride penetration in the marine environment as shown by the expression in equation 2-5. Crank-Nicholson's closed-form solution is used to solve for a unidirectional diffusion by the expression in Equation 2-6 (Crank & Nicholson, 1947).

$$\frac{\partial C}{\partial t} = D\frac{\partial^2 C}{\partial x^2} \tag{2-5}$$

$$C(x,t) = C_s\left[1 - erf\left(\frac{x}{2\sqrt{Dt}}\right)\right] \tag{2-6}$$

Where $C(x,t)$ is the chloride concentration at a depth x and time t and D is the diffusion coefficient, C_s is the surface chloride concentration and erf is a mathematical error function. Since diffusion is not the only one of transport mechanism acting concurrently the diffusion coefficient D is referred to as apparent diffusion D_{ac} (Bamforth *et al*., 1997; Costa & Appleton 1999).

Table 2.2 gives a summary of the dominating transport mechanisms for ingress of deleterious species into RC structures which are exposed to the direct and indirect marine environment classification.

Table 2.2: Predominant chloride transport mechanism for various exposures (CCAA, 2009)

Exposure	Example of structures	Predominant chloride transport mechanism
Submerged	RC structures below low tide.	Diffusion.
	Basement exterior walls or transport tunnel liners below low tide. Liquid containing structures	Permeation, diffusion and possibly Wick action.
Tidal	RC structures in the tidal zone.	Capillary absorption and diffusion.
Splash and spray	RC structures about high tide in the open sea	Capillary absorption and diffusion.
Coastal	Inland RC structures in marine environment or structures above high tide	Capillary absorption (in moist concrete) and subsequent diffusion.

Most researchers agree that the ingress of chloride ions into concrete is due to a combination of transportation mechanisms. However, diffusion is suggested to be the dominant mechanism for structures exposed to airborne chloride attack (Muthulingam & Rao, 2014). In this study, the transport mechanism for ingress of chlorides into dry or non-saturated concrete has been attributed exclusively to ionic diffusion. Even though this assumption is an oversimplification of the true situation, but it will aid in simulating ingress pattern.

Apparent chloride diffusion coefficient

The apparent diffusion coefficient (D_{ac}) is the "global" diffusion coefficient involved in Fick's law which relates to the combined effect of pure diffusion and chloride binding. It is used as input data in empirical models of chloride ingress. D_{ac} reflects the influence of all possible transport mechanisms acting on the concrete that have contributed to establishing the chloride profile (Glass & Buenfeld, 2000; Baroghel-Bouny *et al.*, 2011). D_{ac} can be calculated by applying Fick's 2nd law to a chloride profile, and then applying a non-linear regression analysis, which yields best-fit value for D_{ac} and surface chloride concentration (C_s). It can also be calculated from chloride profiles of cores taken from structures.

The effective chloride diffusion coefficient D_{ec} is the "pure" transport property involved in Fick's 1st law or in the Nernst-Planck equation, i.e. it describes the pure diffusion process without the effects of chloride binding. D_{ec} is obtained from steady-state diffusion tests according to Fick's 1st law, or from non-steady state diffusion tests according to Fick's 2nd law. In the latter case, the D_{ec} is determined from a knowledge of the binding capacity and the total chloride profile of the concrete (Page et al., 1981; Stanish et al., 2000; CCAA, 2009).

D_{ac} is different from D_{ec} because it both reflects the influence of all the possible transport mechanisms acting on the concrete that have contributed to establishing the chloride profile, and because it does not yield an instantaneous measure of the present resistance to chloride penetration. Instead, it reflects the 'time-averaged' performance of the concrete over the period between first exposure of the structure and the time when the chloride profile was determined.

2.5.3 Compressive strength and cement content

Both concrete strength and transport characteristics can be correlated to the pore structure of the concrete (Powers, 1958). Concrete with low porosity usually has higher strength and should have a higher resistance to the penetration of aggressive ions. But, sometimes this is not the case, as it is hard to find a relationship between strength and durability (Ballim & Alexander, 1990). This is because concrete strength can be enhanced without simultaneously reducing its penetrability with new material technologies.

The capillary porosity of concrete is highly sensitive to water-binder ratio (w/b) (Hilsdorf, 1995). The connectivity of the pores depends on the amount of original mixing–water filled space and the degree to which it has been filled with hydration products. Capillary pores are those voids remaining that were originally water-filled. At different ages of the concrete, as a function of w/b and curing condition, the interconnectivity of capillary pores will be reduced (CCAA, 2009).

2.6 CORROSION OF STEEL IN CONCRETE

Production of metals from their ores involves large amounts of energy. Apart from gold and platinum, all other metals are thermodynamically unstable when exposed to atmospheric conditions. In order to return to its naturally existing state, a metal undergoes the process of corrosion. Corrosion can be defined as the deterioration of a material by reaction with its environment.

In hardened concrete, capillary and gel pores containing moisture serve as routes for chloride ion transport. The porosity of the concrete matrix depends on the type of binder/cement used, mix proportions, and concrete production quality. In airborne chloride environments, chloride ions are deposited onto concrete surfaces and consequently penetrate the concrete, reaching the steel reinforcement. But for steel to corrode it must have access to both moisture and oxygen in sufficient quantities to enable the initiation of corrosion.

Concrete usually provides a high degree of protection from corrosion for embedded steel reinforcement. This is as a result of the high alkalinity (pH) of 12–13 of the pore solution, which is from its calcium hydroxide (CaOH) and metal alkali (sodium oxide Na_2O and potassium oxide K_2O) contents. Calcium hydroxide is a by-product of the

hydration of the calcium silicates in the cement. The alkalinity favours the formation of a thin passive film of ferric oxide. This film protects the surface of the steel from corrosion. This protective layer is stable throughout the service life of the RC structure, provided there is no attack on it by deleterious species.

The protective layer can however be destroyed, inter alia, by chloride ingress or carbonation. For chloride-induced corrosion, when a certain chloride threshold content (critical value) is attained at the level of the steel reinforcement, the passive layer is destroyed. The chloride ions act as a catalyst by speeding the corrosion process but are not consumed in the chemical reactions. There are different views about the critical value of chloride for corrosion to be initiated but the generally accepted range is 0.4 to 2.5% by mass of binder (Meira *et al.*, 2014; Papakonstantinou & Shinozuka, 2013).

The process of carbonation involves the diffusion of atmospheric carbon dioxide (CO_2) through the pores of the concrete. It dissolves in moisture to form carbonic acid (HCO_3) which reacts with the alkaline pore solution and forms calcium carbonate ($CaCO_3$). This process consumes the calcium hydroxide (CaOH) in the pore solution and consequently reduces the pH of the solution causing depassivation. Depassivation is the lowering of pH of the pore solution which destroys the passive coating film that protects the steel reinforcement. At this low pH of about 7.5-8.3, the passive layer is destroyed and this may increase the porosity of the concrete and open up the reinforcing steel to action of deleterious materials (Papadakis *et al.*, 1990; Huet *et al.*, 2005; Chang & Chen, 2006).

A schematic of chloride-induced corrosion in uncracked concrete is shown in Figure 2.16. Corrosion is an electrochemical process which means that for it to occur, the anode-cathode must be connected in such a way that electron flow is permitted.

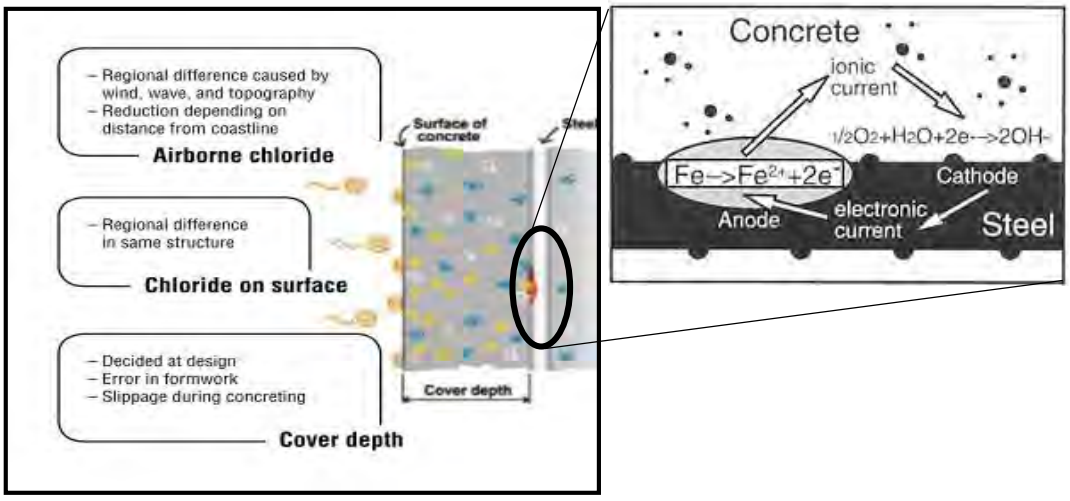

Figure 2.16: Corrosion mechanisms in uncracked concrete with anodic and cathodic reactions (Tanaka *et al.*, 2006)

Concrete serves as the electrolytic medium. Anodic reactions involves the dissolution of the steel by an oxidation process, while the cathodic reaction is characterised by the reduction of water and oxygen by the electrons supplied from the anode to form hydroxyl ions.

The expansion of the corrosion products of the reinforcement causes cracking and spalling of the surrounding concrete. However, it is difficult to detect the existence of early products of corrosion in uncracked concrete through visual assessment methods and when noticed, major repairs may no longer be effective.

2.6.1 Corrosion initiation and propagation

A schematic representation of corrosion model suggested by Tuutti is given in Figure 2.17. According to Tuutti's model (Tuutti, 1982), the service life of RC structures can be divided into an initiation stage and a propagation stage. The period marked as "initiation" defines the length of time it takes for deposited chlorides to penetrate from the surface through the cover concrete and accumulate at the level of the steel in sufficient concentration (chloride threshold level) to break down the passive protective layer on the steel surface and thereby cause active corrosion (Otieno, 2008).

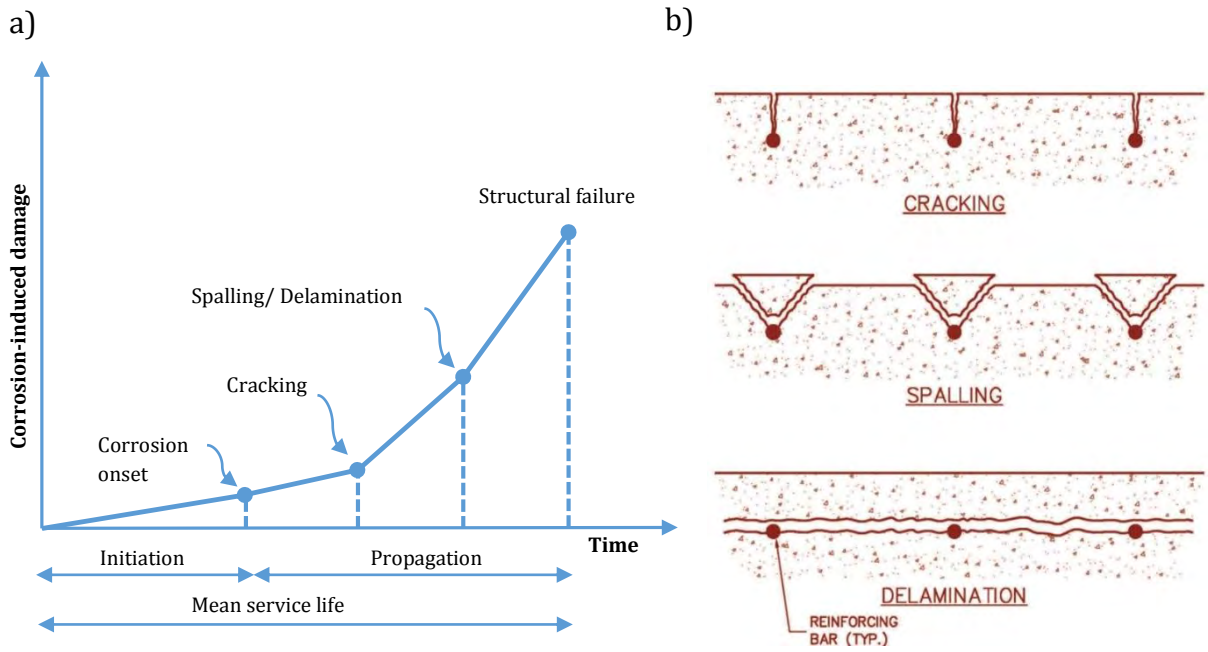

Figure 2.17: a) Corrosion process model by Tuutti (Tuutti, 1982), b) Effects of steel corrosion on concrete integrity (Banville, 2008)

The propagation stage involves continuous accumulation of chlorides at the level of the steel where chloride threshold level is sustained with a corresponding active corrosion rate, until an unacceptable level of damage has occurred (Arito, 2012). The length of the propagation period depends on the definition of unacceptable corrosion damage (Otieno, 2008) which might be cracking, spalling or structural failure. Spalling or cracking failures are attributed to the volume increase of the oxides of iron formed from the corrosion processes. These iron oxide products are usually between 2-6 times the volume of the uncorroded steel (Papakonstantinou & Shinozuka, 2013).

2.6.2 Chloride threshold level

The presence of chloride ions above a certain threshold value in concrete structures at the level of steel causes depassivation (Medeiros *et al.,* 2013). An accepted global common value of the chloride threshold level for reinforcing steel has not been developed (El Hassan et al., 2010). More so, the impact of the variance in acceptable threshold levels has not yet been identified.

In the US, chloride threshold value is commonly recognized as 0.7 % by mass of cement (Tanaka *et al*., 2006). In Japan, the acceptable value is from 1.2-2.5 % (JSCE, 2010). In New Zealand, it is 0.5 % for prestressed concrete, 0.8% for RC in contact with moisture and chlorides and 1.6 % for RC structures exposed to a dry environment (CCANZ, 2005). The British design code limits the chloride content to less than 0.4 % for RC structures and 0.1 % for prestressed concrete structures (BS 8500-1: 2002) and is the most conservative of all standards. These differences in chloride threshold value may be as a result of various testing conditions, a lack of precise definitions for corrosion level, and a non-standard definition of the threshold level.

However, the conventional and conservative limit of 0.4 % by mass of binder for the chloride threshold level for corrosion initiation and propagation given by most authors is usually selected (Daigle *et al.*, 2004).

2.6.3 Influence of steel properties on corrosion rate

The ability to engineer the properties of steel has made it the most widely used metal. Its tendency to corrode readily means that corrosion inhibition in steel is of great economic importance. The critical chloride threshold level at which steel begins to corrode is also influenced by material characteristics such as steel composition and surface condition. Research indicates that embedded reinforcement with higher carbon contents is more prone to corrosion. This is explained by the retarding effect on the formation and performance of the passive film by mill scale (Cascudo & Helene, 2000). Mill scale is the formation of flaky surface on hot rolled steel. It is composed of iron oxides mostly ferric and is bluish black in colour; it also does provide protection for steel from corrosion but it is easily broken down relative to the passive protective layer (Cascudo & Helene, 2000).

Secondly, the presence of ribs on reinforcement surface is another factor that could influence chloride threshold levels for corrosion (Meira *et al.*, 2014). The ribs can cause entrapment of air bubbles or aid in the generation of internal exudation (Meira *et al.*, 2014).

In addition, the diameter of steel prescribed during design can also affect service life of a structure by prolonging the time to corrosion initiation (Muthulingam & Rao, 2014). It was found using a model based on long-term studies, that the corrosion rate in a RC structure was influenced directly by the chloride content, w/b ratio, reinforcement

diameter and inversely proportional to the cover depth (Morinaga, 1990). Using a reliability model, El Hassan et al. (2010) also found that if a smaller diameter steel bar is prescribed instead of a larger one, the probability of failure due to cross-sectional loss of area is reduced in the larger diameter reinforcement. This is as long as similar crack openings and corrosion rate conditions are satisfied. Therefore, when designing an engineer should select a rebar with larger diameter that satisfies the steel area required (El Hassan *et al.*, 2010). Nevertheless, this might not be an economical solution, using larger diameter steel bars can be problematic for cracking control and the strategy may only viable if both reinforcement sizes are exposed to the same corrosion rates.

2.7 MARINE ENVIRONMENTS

Marine environments are locations which are predominated by the presence of seawater and marine aerosol. Seawater has a typical salt content of 3.5%, with chemical ion composition of Na^{+}, Mg^{2+}, Cl^{-} and $(SO_4)^{2-}$ (Mehta, 1991). It also has at its surface or dissolved in it, certain gases that influence its chemical and electrochemical properties such as oxygen (O_2) (Mehta, 1991). Long-term monitoring of concrete structures indicates that one of the major deterioration mechanism of RC structures in the marine environment is chloride-induced corrosion (Maldonado *et al.*, 2006; Thomas & Matthews, 2004; Costa & Appleton, 2002).

An aerosol is a dynamic system; in that the concentration, particle size distribution and chemical composition evolve due to coagulation, evaporation, condensation, dispersion, deposition, and chemical reactions (Tang & Guo, 2011). Aerosols naturally exist in the atmosphere, deriving from various sources such as volcanoes, dust storms, fires, living vegetation and sea spray (Tang & Guo, 2011). But more specifically, marine aerosol is generated from sea spray. Airborne chloride ions, which are also referred to as marine aerosols, in the marine environment exist in the form of dissolved crystals of salts generated from seawater (Moreda-Piñeiro *et al.*, 2014) and transported by wind action (Monahan *et al.*, 1986).

2.7.1 Airborne chloride generation & transportation in the marine environment

The concentration of the airborne chlorides differs by location. As discussed earlier, intrinsic factors such as wind speed, temperature, precipitation, RH govern the production and transportation of airborne chlorides.

The ocean is one of the major sources of natural aerosols. On the global scale, the total mass of natural aerosols is much higher than that of anthropogenic aerosols (Winter & Chýlek, 1997). Sea salt is the strongest natural source of aerosol compared to anthropogenic sources, with a production rate of about 1000 – 10,000 megatonnes (Mt)

per year accounting for 33-57% of total annual aerosol production (Woodcock & Blanchard, 1980; Winter & Chýlek, 1997).

Marine aerosol particles are carriers of chemical species of chlorides, bromides, iodine and sulphur ions (Gong *et al.*, 1997). These marine aerosols are generated from a process referred to as whitecap activity (Monahan *et al.*, 1986). Whitecaps are formed by the breaking of sea waves. Numerous models that simulate whitecap activity have been developed by researchers over the years and are further discussed in the section method for estimating airborne chloride concentration (Lovett, 1978; Monahan *et al,.* 1986).

2.7.1.1 **Whitecap activity from wave action**

Surface winds are the propagators of sea wave breaking (Gong *et al.*, 1997). Through friction the wind energy is converted to wave energy (Mehta, 1991). Breaking waves create whitecaps and sea-spray droplets that consist of a large number of air bubbles, which are essential for the production of marine aerosols (Fairall *et al.*, 1983). Whitecaps are the tip of the sea waves which are usually white (*Figure 2.18*). The generation of whitecaps has been attributed to a series of processes, but the most promiment mechanism is assumed to be bursting of air entrained bubbles due to effects of surface wind (Monahan *et al.*, 1986).

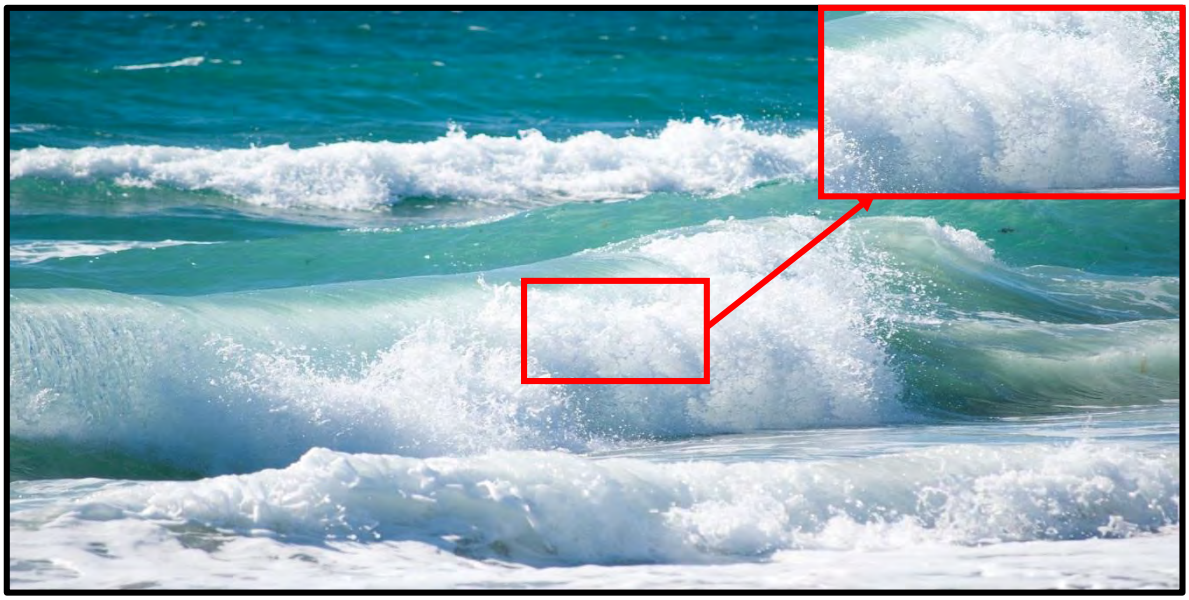

Figure 2.18: Breaking of sea waves (***zoomed image*** - *illustrates whitecaps*)

An illustration of whitecap formation postulated by Monahan et al., (1986). is shown in Figure 2.19. There are 3 components that make up whitecaps, the larger particles which travel at a slower speed of greater than 14.4 km/h are referred to as film droplets and jet drops. The relatively lighter particles called spumes travel at a faster speed of >36 km/h and tend to travel longer distances.

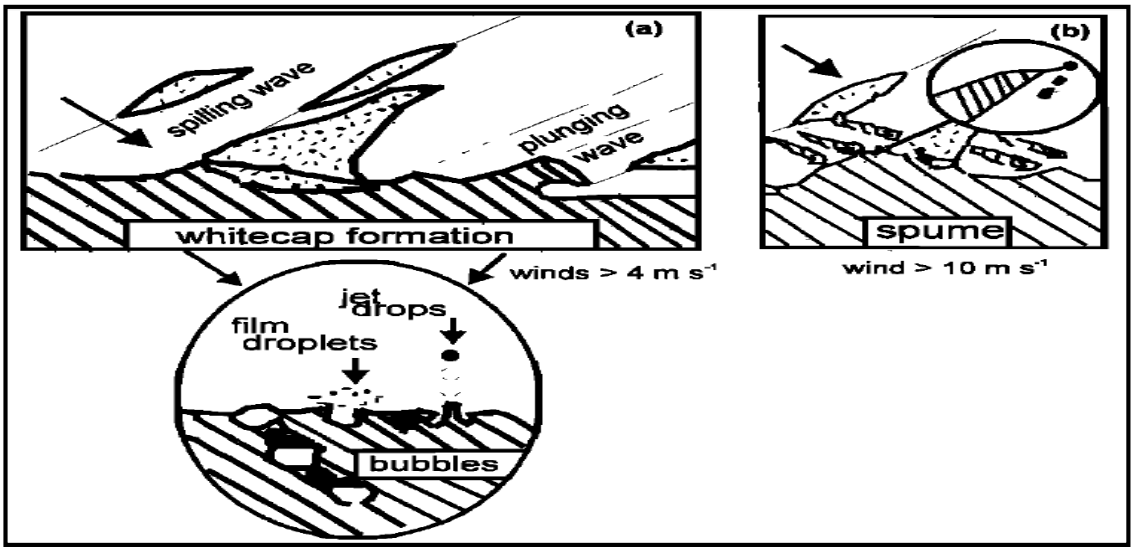

Figure 2.19: Mechanism of marine aerosol from whitecap activity (a) indirect production by bubbles and (b) direct production of spumes (Monahan *et al.*, 1986)

2.7.1.2 **Ocean wind speed effects on airborne chloride generation**

Airborne chloride production is attributed to both surf waves (generated at the shoreline and modelled as a function of local winds) and oceans (dependent on the whitecap activity) (Cole *et al.*, 2004). These two methods of airborne chloride production involve bursting of bubbles from the generated whitecaps and breaking off of spume drops from the crests of whitecaps by wind. Taking into consideration the production from surf waves, which is largely dependent on local winds, an estimate of the airborne chloride concentration S (μg/m^3) in the air above the surf zone can be quantified by (McKay, 1994):

$$\ln S = 0.23U_2 + 3.05 \qquad (2\text{-}7)$$

Where, U_2 is the wind speed at 2 m above sea level in m/s.

2.7.1.3 **Ocean wind speed effects on airborne chloride transportation**

The ocean wind speed is an important factor in transportation of airborne chloride. Previous experiments to estimate airborne chloride concentration of a location indicated that the higher the ocean wind speed measured, the higher the amount chloride ions transported to inland sites (Lovett 1978; Meira *et al.,* 2007a). A series of mathematical models used to predict airborne chloride concentration inlands by researchers also indicated that wind speed and direction are important factors when considering its generation and transportation (Cole *et al,.* 2003; Gong *et al.,* 1997; Jones *et al.,* 2010).

Low wind speed implies low bulk deposition rate of chlorides and vice versa (Harkel, 1997). Therefore, a number of models postulated by researchers have only considered wind speed as the major parameter in airborne chloride formation. On the

contrary, Cole et al., (2003a) analysed the sources of atmospheric salinity providing a holistic mathematical model that incorporated more environmental parameters (such as relative humidity, ocean whitecap activity, rainfall, global wind patterns, and local winds) in estimating concentration of airborne salt in marine atmosphere. The multiple parameters used in the model makes it adaptable to any location. The term 'airborne salt' refers to both salts of chlorides and bromides (Finlayson-Pitts & Hemminger, 2000).

Lovett (1978) related the effect of wind speed (and other meteorological parameters) on airborne salt concentration in the North Atlantic Ocean. Total airborne salt concentrations were measured by air sampling through membrane filters at varying vertical heights of 5, 10, and 15 m on weather ships. A relationship was found that total airborne salt concentration could be represented as a function of wind speed by the Equation 2-8:

$$ln\,\Theta = 0.16U + 1.45 \qquad (2\text{-}8)$$

Where Θ = airborne salt concentration in $\mu g m^{-3}$ and U = wind speed in ms^{-1}

Lovett (1978) also noted that airborne salt concentrations were not only a function of ocean wind speed but they also had residence time in the atmosphere. This implied that when ocean wind speed reduced, there was no corresponding immediate drop in airborne salt concentration. A limitation to the study was in measuring airborne salt concentration on moving ships as this did not ensure accurate height measurements.

2.7.2 Deposition of marine aerosol particles

The presence of marine aerosol particles in the atmosphere is dependent on climatic factors that govern their generation, transportation and deposition. The concentrations of aerosols depends upon a multitude of factors including location, time of day or year, atmospheric conditions, presence of local sources, altitude and wind velocity. Production of aerosols can be by emission into the atmosphere, this production method is referred to as primary aerosol production (Roberge, 2011). It can also be produced through physical and chemical processes within the atmosphere referred to as secondary aerosol production (Roberge, 2011). Primary aerosol are majorly generated from sea spray of which airborne chlorides dominates its composition. The secondary aerosols are usually produced by condensation of atmospheric gases, or by cooling of vapour (gas to particle conversion) (Roberge, 2011).

Aerosols that are present in the atmosphere can be altered, removed or destroyed. They cannot stay in the atmosphere indefinitely, and average lifetimes are of the order of a few days to a week (Roberge, 2011). Aerosol residence time in the atmosphere depends on its size and location. Studies on the migration of aerosols inland from a marine region have shown that typically the majority of the aerosol particles are deposited

close to the shoreline (Meira *et al.,* 2007) and consist of large particles (>10µm diameter), which have a short residence time and are controlled primarily by gravitational forces (Khatri & Sirivivatnanon, 2004; Roberge, 2011).

There are exceptions to the aforementioned scenario; some locations about 30 km from the coast still have RC structures showing major damage from chloride-induced corrosion. This might be as a result of the movement of dew from the coastline inlands and also from the formation of fog which promotes movement of water vapour. The aerosols that form during fog formation have larger masses and are subjected to the influences of wind resistance, gravity, droplet dry-out, and possibilities of deposition on a solid surface, as they progress inland. An example of such a phenomenon was found in the Namib Desert, Namibia and will be examined in the case study section.

2.7.3 Measurement of airborne chloride concentration and simulating its interaction with concrete

Chlorides ions are present as droplets and particles in marine aerosol from ocean or sea activity; they are then deposited as the aerosol move inland. Gravitational forces affect larger particles to settle closer to the coast and the smaller particles are transferred further inland (Gustafsson & Franzén, 1996). The larger particles of marine aerosol (diameter >10 µm) remain for a short time in the atmosphere; the larger the size of the particle, the shorter its residence time. On the other hand, particles of a diameter <10 µm may travel hundreds of kilometres in the air without being deposited (Morcillo *et al.,* 2000).

Various methods exist for measuring the presence of airborne chloride in the atmosphere. The wet candle device is one of these methods but it only gives information on the chloride ions deposition rate (Meira *et al.*, 2010; Hossain & Easa, 2011). Other methods involve examining the corrosive effects of airborne chloride on exposed metals, through analysis of the exposed metal's loss of mass. This method can also be used to classify environmental severity (Muster & Cole, 2005; HDGASA, 2005; Cole *et al.*, 2004; Strekalov & Panchenko, 1994). Also, mathematical models that estimate the amount of airborne chloride generated and transported from the sea have been formulated. These models for airborne chloride atmospheric concentration estimation are discussed in Sections 2.10.1, 2.10.2 and 2.12.6. The inland transfer of these chloride ions is then carried out using computational fluid dynamics (CFD) and geographic information system (GIS) information (Cole *et al.,* 2004; Cole *et al.,* 2003).

2.7.4 **Wet candle device**

The wet candle device (an ASTM standard) method of measurement is relatively simple, but has the drawback that it also collects particles of dry salt that might not be deposited. This technique uses a wet wick (bandage or gauze wrapped around test tube with loose ends) of a known diameter and surface area to measure aerosol deposition. The wick is maintained wet using a reservoir of water or 40% glycol or distilled (or deionized) water solution. Aerosol particles are trapped by the wet wick and retained. At intervals which need to be chosen carefully, quantitative determination of the chloride collected by the wick is made.

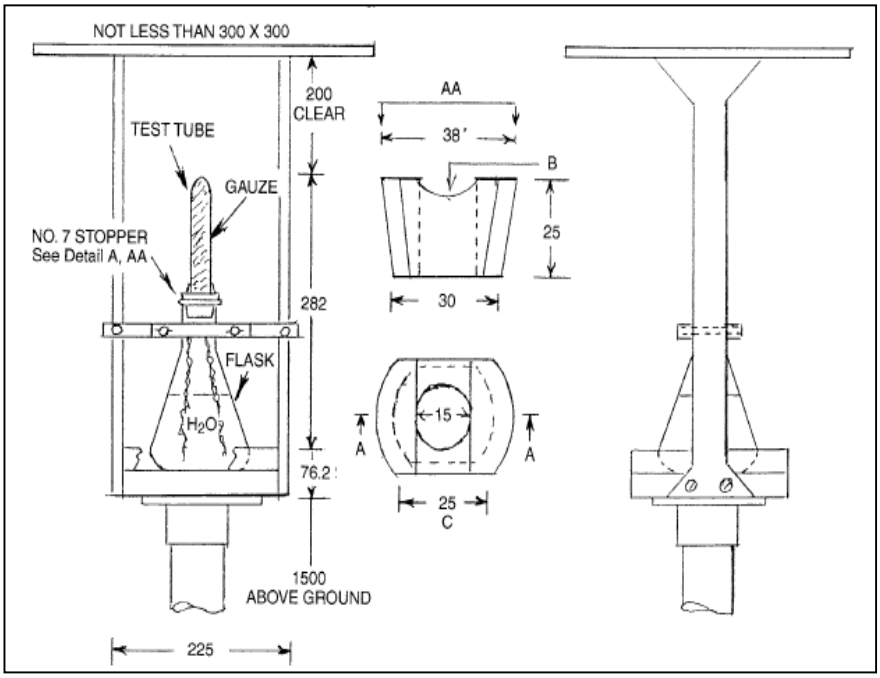

Figure 2.20: Wet candle device apparatus (dimension in mm) (ASTM G-140-02:2008)

2.7.4.1 **Case studies using wet candle technique**

Meira et al., (2002) carried out a study the concentration of airborne chlorides in Joao Pessoa, which is located in the north-eastern coast of Brazil. The airborne chloride concentrations were estimated using the wet candle device, using specifications in ASTM G-140 (ASTM G-140-02:2008). Figure 2.20 illustrates the fabrication technique and dimensions for the wet candle according to the ASTM standard (ASTM G-140-02:2008). The method of use is further discussed in the method's section (Section 3.2).

In the Joao Pessoa study, the device was exposed at various locations for a duration of 46 months. In addition to characterise the environment, it was important to collect weather data during the period of monitoring. Joao Pessoa, Brazil has a typical tropical climate with local temperatures ranging from 20^0C – 30^0C and RH ranged between 60 – 80 % (Meira *et al.*, 2003). It was noted that a higher RH was recorded during

periods of prolonged rainfall and the daily wind speed measured averaged between 4 – 15 km/h with prevailing wind direction S–SE–E.

It was found that airborne chloride concentration decreased with increasing distance from the sea (Meira *et al.*, 2010). Hossain *et al.*, 2009 and Harkel, 1997 also came to similar conclusions. Evidence for this was found by comparing the amounts of chlorides deposited on the wet candle apparatus at distances of 50 m, 100 m, 200 m, 500 m and 1100 m from the sea as shown in Figure 2.21.

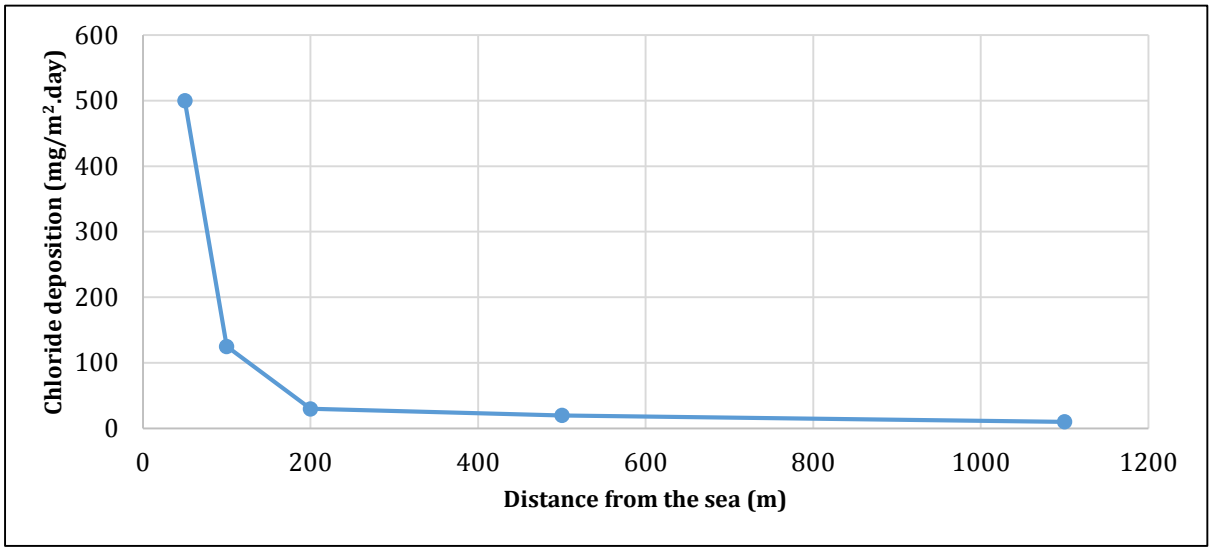

Figure 2.21: Chloride deposition on the wet candle device at varying distances at Joao Pessoa, Brazil (adapted from Meira *et al.,* 2010)

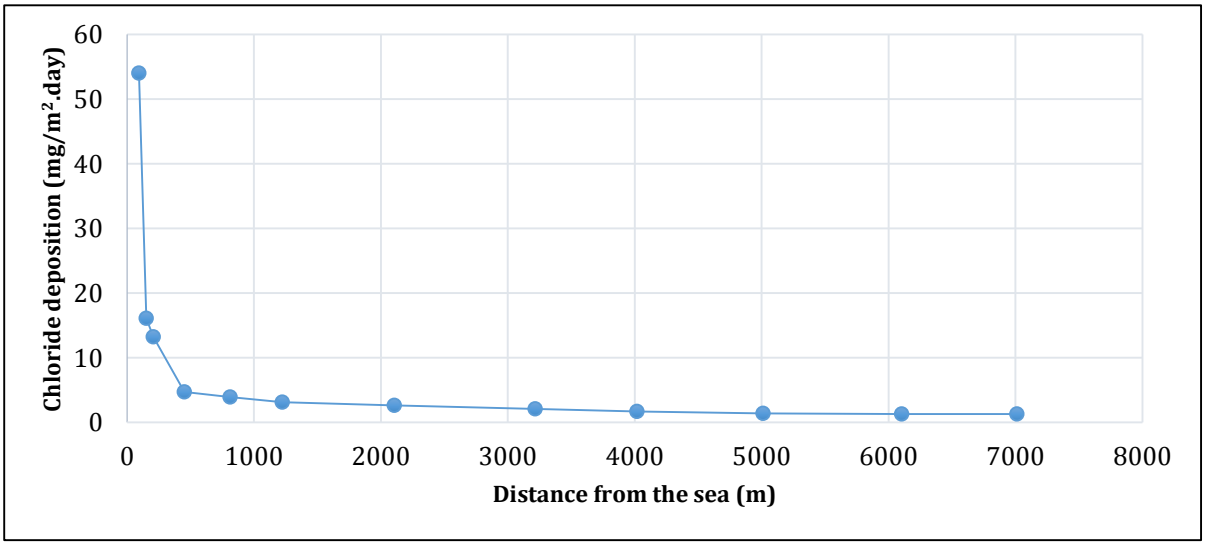

Figure 2.22: Chloride deposition on the wet candle device at varying distances in Chittagong, Bangladesh (data sourced from Hossain & Easa, 2011)

Hossain et al., (2009) and Meira et al., (2010) also indicated in their analysis that airborne chloride concentration carried by the wind was consistent for about 0 – 200 m (452 m for Hossain et. al) from the coast and then experienced a drastic decrease (*Figure 2.22*). However, most of the research conducted has been in specific locations

with differing weather conditions, thus making conclusions more empirical and difficult to adapt in different environments. Hence, to accurately estimate the rate of airborne chloride deposition in any environment, it is essential to measure the atmospheric chloride concentration and its corresponding weather conditions. The period of exposure of the wet candle device in Chittagong, Bangladesh was 6 months. It should be also noted that the plot in Figure 2.22 are a total representative for the period of exposure without particular regard given to the influence of seasons.

2.7.4.2 **Corrosion exposure simulation using salt spray chamber**

Another method that can be used to model the response of concrete structures to the deposition of airborne chlorides and also monitor the ingress pattern of the chloride ions into respective specimens is a salt spray chamber.

The SANS 9227 is a standardized salt spray test method for testing corrosion rates of metals (SANS 9227:2007). But if the airborne chloride concentration and deposition rate of a location is known it can be incorporated in the salt spray chamber test for concrete specimens with or without reinforcing steel. It is essential that salt loading of the environment to be simulated should been known when using the accelerated test. If this is not done results cannot be used in any way to make real life predictions.

The standard however stipulates a sodium chloride solution is prepared with a concentration of 50 g/l ± 5 g/l. The pH of the sodium chloride solution should be regulated to range from 6.5 – 7.2, while the chamber's temperature is regulated at 25 ± 2 ^{0}C. The cabinet used must have a shape that homogeneity of loading can be simulated. The spraying device must be able to atomize solution into a colloid suspension of fine liquid droplets appropriately with controlled pressure and humidity. Compressed air used must be filtered to remove impurities before it is used to atomize. The pressure will be a function of the salt loading estimated from the environment.

Typical pressure range for the standard is between 70-170 kPa. Collectors to receive the settling mist of salt should be inert so that it cannot react with the salt solution. For metals, mass loss is used to calculate rate of corrosion. If concrete cylinders are been tested, chloride ion rate of penetration into concrete will be the end result. A measure of corrosion rate would be expected for concrete with embedded reinforcing steel (Castro *et al*., 1997). See Figure 2.23 for a schematic diagram of a typical salt spray chamber.

In a case study, Castro et al., (1997) tested different concrete cylinders with one embedded reinforcing bar and differing w/b ratios. The specimens were cured for periods of 1-7 days and then exposed to the artificial salt spray cabinet as discussed above. In addition, the concrete cylinders from the same batches were also concurrently exposed to a marine atmosphere for 24 months at a location 50 m from the shoreline in order to correlate the two different tests. The chloride content, corrosion rate and corrosion potential close to the steel reinforcement were monitored for the different exposures.

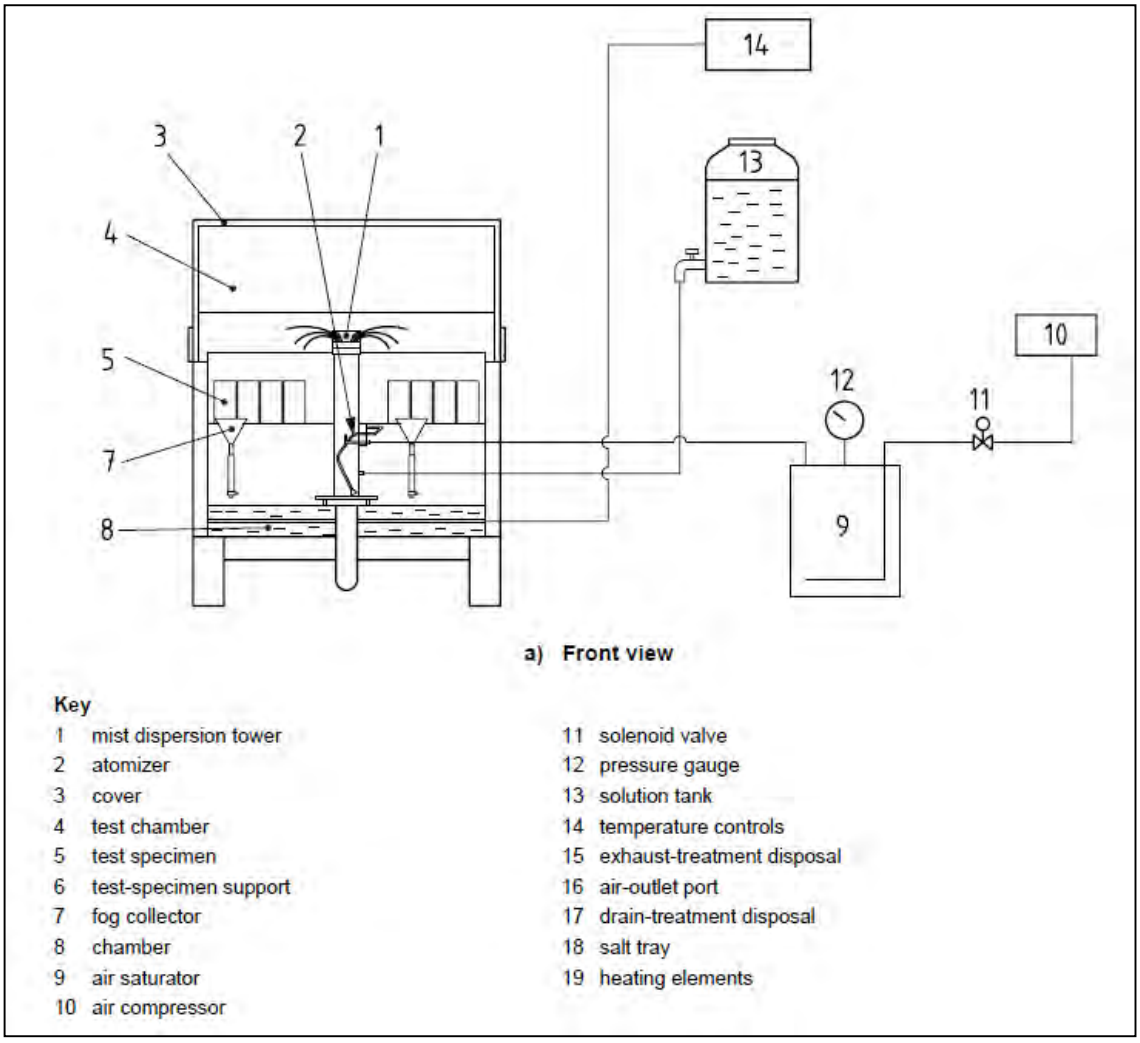

Figure 2.23: Typical design for salt spray chamber (SANS 9227:2007)

Castro et al., (1997) found that the results indicated that the salt spray chamber test had an effect of lengthening the time to corrosion initiation in concretes specimens with curing times below 7 days (i.e. 1-3 days cured concrete). The hypothesis was that unhydrated cement particles where hydrated and bound the chloride ions to form stable compounds of chloroaluminates, before the accumulation of free chlorides that initiate corrosion. However this was found not to be the case in concrete exposed to the atmosphere as it underwent a slower ingress of chlorides. This infers that the salt spray test might help in simulating corrosion rates better in metals and performance tests of concrete mix designs, but it might not replicate accurately the field exposure in the case of reinforced concrete structures.

In a more recent research, Ye et al. (2013) also explored the effects of cracks on chloride diffusivity using an artificial simulation chamber as illustrated in Figure 2.24. This environment was used to simulate varying artificial temperature, rainfall and RH using an artificial fog sprayer in an enclosed environment. The method is similar to the salt spray chamber but it is more efficient as the system is monitored and controlled using a computer. The implication of these discussed methods is that a more controlled and

effective study in a monitored environment can be carried out in simulating the response of different mixes to differing exposure conditions.

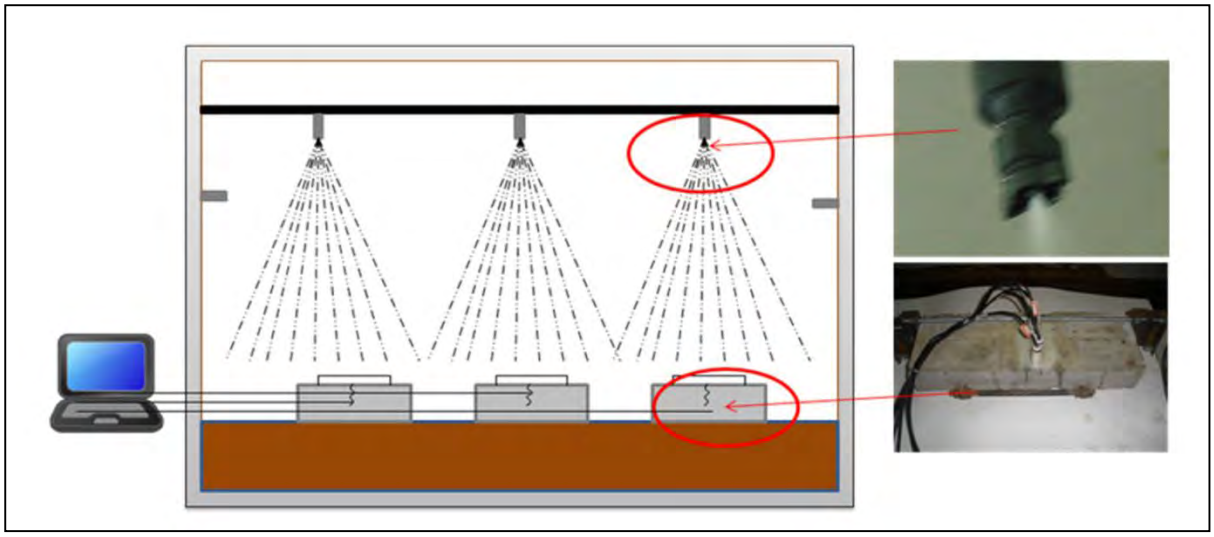

Figure 2.24: Artificial simulation chamber (Ye *et al.*, 2013)

2.7.5 Chloride concentration in the atmosphere from PM10

The term PM10 refers to particulate matter less than and equal to 10 µm in size. Usually PM10 is measured in atmospheric aerosols. Recent research interest in studying atmospheric aerosol, most importantly PM10, is attributed to anthropogenic emissions which have negative effects on human health and the environment (Pey *et al.,* 2009). Particles with size equal to 10 µm and less can be inhaled by humans easily. Besides, studies indicate that aerosols can impact the climate of a location directly by affecting radiation absorption and reflection or indirectly through prevention or favouring formation of clouds (Niyogi *et al.*, 2004; IPCC, 2007).

A study was completed in Palma de Mallorca city, the Mallorca Isle, in the Mediterranean Basin by Pey et al., (2009), where the chemical composition of PM10 was analysed. The components that were measured to establish the composition of PM10 included sulphates (SO_4^{2-}), nitrates (NO_3^-), ammonium (NH_4^+), mineral matter, marine aerosols and elemental carbon and organic matter (EC+OM).

Palma de Mallorca is a coastal city, and it experiences a Mediterranean-type climate and has a mean annual PM10 level of 29 µg/m^3 (Pey *et al.*, 2009). The marine aerosol had a major composition of sea spray aerosols. Figure 2.25 shows that sea spray aerosols make up 11 % of PM10.

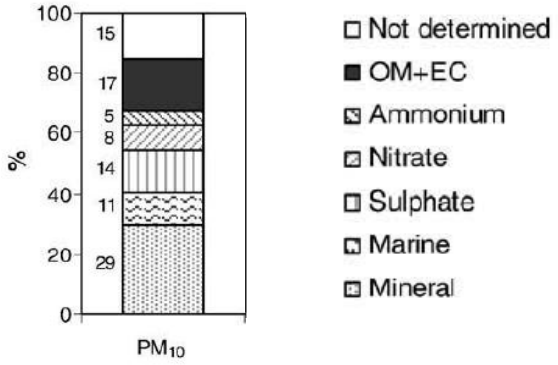

Figure 2.25: Case study percentage composition of PM10 in Mallorca city (Pey *et al.,* 2009)

Another study was completed by Pey et al., (2010) in the same city where the aim of this study was to determine the chemical composition of PM10 of any given area (Pey *et al*., 2010). Sample collection was carried out over a period of 24 hours and twice per week using pre-treated and weighed Teflon filters. The concentrations of particulate matter (PM) were measured using a difference in filter weight. The composition of PM10 included the same components as the previous study. The marine aerosol measurement included chloride and sodium ions, but in the study it was assumed that the sodium ion content was negligible by its weight component (Pey *et al*., 2010) (*Figure 2.26)*. The study was used therefore to estimate airborne chloride content in Palma. However, the use of 10% as marine aerosol content in PM10 can only be used at this location and cannot be used at another region with differing prevailing climate.

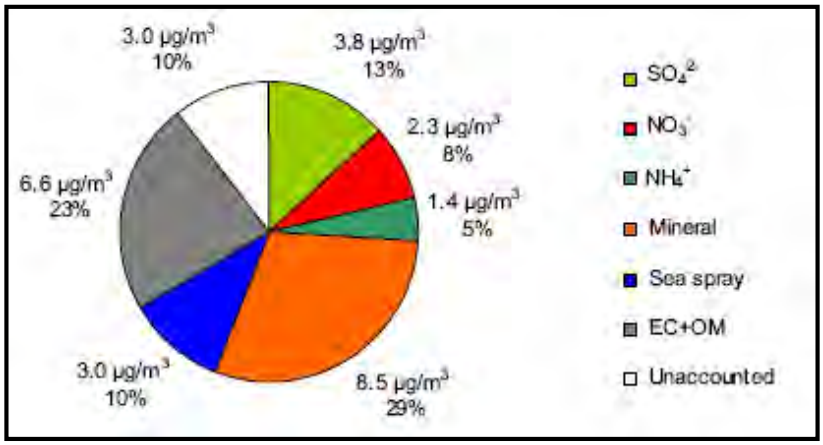

Figure 2.26: Pie chart depicting the composition of PM10 of Palma de Mallorca city (Pey *et al.,* 2010).

2.7.6 **PM10 concentration in the Cape Peninsula**

The plot in Figure 2.27 depicts the average minimum and maximum PM10 concentrations measured from 1995 – 2009 in the Cape Peninsula area. From data retrieved from air quality monitoring stations spread around the Cape Peninsula, it was found that the winter period had a higher concentration of PM10 measured

(Ralfe, 2013). Measured PM10 concentrations in the Cape Peninsula are similar to that in Palma de Mallorca. The locations examined are limited to Table View, Cape Town City Bowl, Northern Suburbs and the Cape Flats, while the Southern Suburbs, Westerly and Easterly Peninsula and Cape Point are excluded. This is because only the afore-mentioned locations have been monitored for their PM10 concentrations by the Provincial Government of the Western Cape.

The concentration of the PM10 in the Cape Flats zone is the highest at 50 µg/m^3 and lowest in the Table View area at 19 µg/m^3, but it cannot be inferred that, estimated chloride content of 10 % quantified in the Palma de Mallorca study of Pey et al., (2009) holds for the Cape Peninsula. The high PM10 concentration in the Cape flats can be as a result of the location being highly industrialized compared to Table View and the Cape Town City Bowl area. Therefore, more air pollutants are available in the atmosphere. Currently, monitoring authorities do not have any information on the chemical composition of the PM10 measured in the Cape Peninsula. This could provide essential information on atmospheric chloride concentration levels experienced in the Cape Peninsula.

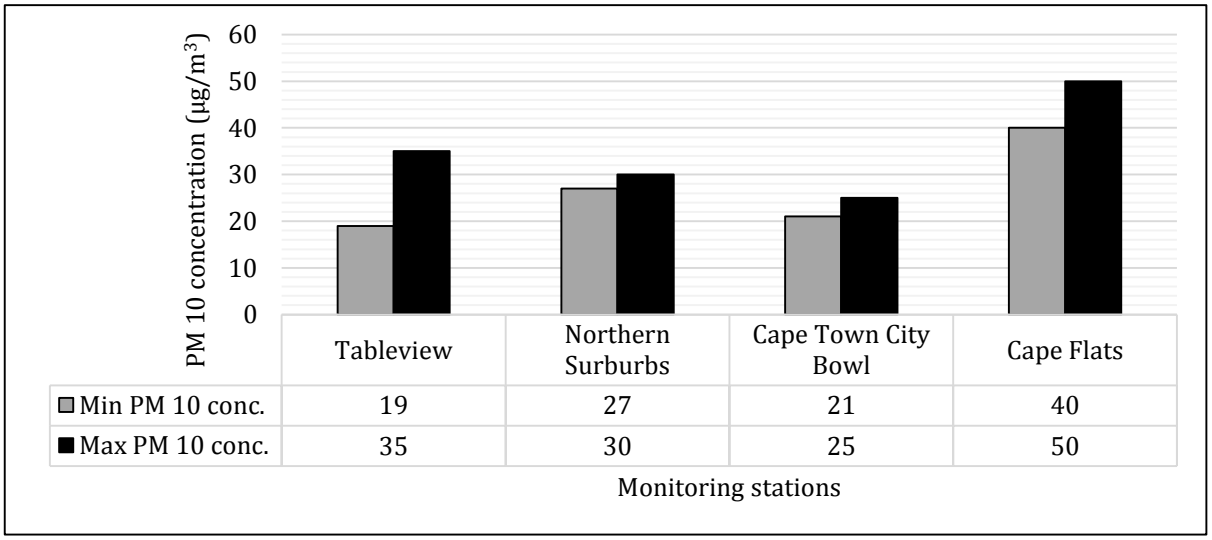

Figure 2.27: Minimum and Maximum PM10 concentrations of locations in the Cape Peninsula from 1995 – 2009 (Ralfe, 2013)

2.7.7 Modelling airborne chloride concentration using environmental parameters

The production of airborne chloride in the open ocean may either occur by bursting of bubbles generated from whitecaps and/or breaking off of spume drops from crests of whitecaps by winds. Ocean production is also dependent on water depth (sea bed depth) and fetch. Fetch is the uninterrupted distance a wave can travel across the water before being deposited. Monahan et al., (1986) demonstrated that the production from the former is given by Equation 2-9:

$$\frac{dF_o}{dr} = W\tau - 1\frac{dE}{dr} \quad (2\text{-}9)$$

Where $\frac{dF_o}{dr}$ is airborne chloride production (m^{-2} s^{-1} μm^{-1}), r is aerosol radius (mm), W is instantaneous fraction of the sea surface covered by whitecaps, τ is the time constant characterizing the exponential whitecap decay (measured in seconds), and $\frac{dE}{dr}$ is the differential whitecap aerosol productivity, i.e. the number of droplets per increment droplet radius produced by the decay of a unit area of whitecap. However, equation (2-9) could be approximated by the Equation 2-10, where B = (0.380 – log r)/0.650.

$$\frac{dF_o}{dr} = 1.373V^{3.41}r^{-3} \times 10^{1.19exp-\mathrm{B}^2} \quad (2\text{-}10)$$

For spume drops production which is relatively dependent on higher wind speeds of between 7-11 ms^{-1}, Monahan et al., (1986) approximated by Equation 2-11;

$$\frac{dF_1}{dr} = 6.45 \text{ x } 10^{-4}\exp(2.08V)r^{-3}\exp(-D^2) \quad (2\text{-}11)$$

Where D = 2.18(1.88 – log r) and V is wind speed at an elevation of 10 m. Therefore, total airborne chloride production from ocean whitecap activity is given by

$$\frac{DF}{dr} = \frac{dF_o}{dr} + \frac{dF_1}{dr} \quad (2\text{-}12)$$

Further research by Cole *et al*., (2003b) in South Australia, using Monahan et al., (1986) airborne chloride generation models and with the aid of the CFD models predicted that airborne salinity varied with increasing distance inland according to the following expression:

$$[\mathrm{A(d)}] = (A_i) * [(0.9 * e^{-d/(0.1)}) + (0.1 * e^{-d}) \quad (2\text{-}13)$$

Where, A_i is the surf-produced concentration at the beach line which is also $\frac{dF_o}{dr}$, A(d) is the concentration at a distance d (in kilometres) from the beach line. The model also predicts the concentration of ocean produced aerosol would vary with distance, as shown by

$$[\mathrm{OA(d)}] = (OA_i)exp^{-d/x} \quad (2\text{-}14)$$

Where, OA_i is the concentration of ocean-produced aerosol at the shoreline, OA(d) is the concentration of ocean-produced aerosol at a distance d (in kilometres) respectively, and x is the decay constant derived from the CFD study and has a value of 50. The limitation to the models postulated are that they cannot be used to evaluate airborne chloride concentration of a location accurately without GIS and climate data. They have also been derived from data retrieved from specific locations.

2.8 CORROSION SEVERITY MAP BASED ON EXPOSED ZINC

Data on atmospheric corrosivity gathered from research carried out by the Council for Scientific and Industrial Research (CSIR) illustrated in the map in Figure 2.28 shows the classification of South Africa into different exposure zones based on different air quality monitoring the corrosion rates and severity of exposure of zinc plates. However, they do not explicitly measure airborne chloride concentration.

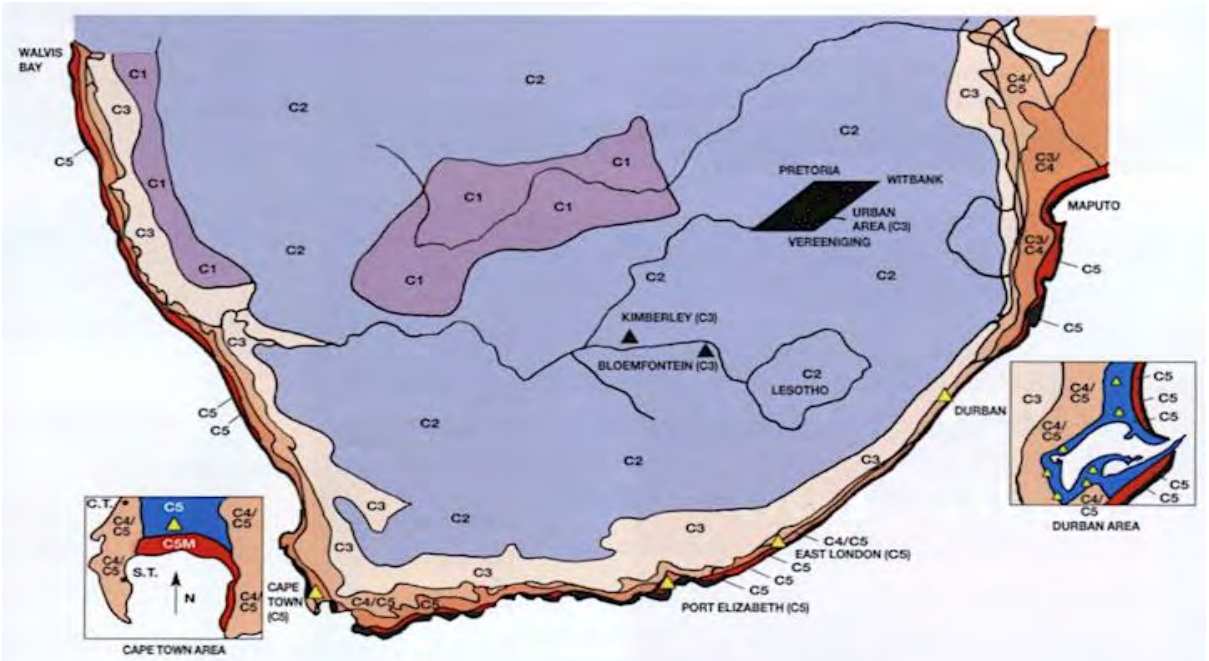

CATEGORY	DESCRIPTION	LEGEND	SEVERITY OF CORROSION	CORROSION RATE OF UNCOATED MILD STEEL	ZINC COATING LOSS
C5+	USUALLY LESS THAN 50 m from H.W.M		SEVERE MARINE	>300µm/YEAR	>30 µm/YEAR
C5	USUALLY 50m TO 1km FROM H.W.M		MARINE	200 - 300 µm/YEAR	15 - 30 µm/YEAR
C4/C5	40km TO 100km FROM SEA		AVERAGE MARINE	20 - 200 µm/YEAR	2 - 15 µm/YEAR
C3	1km TO 40km FROM SEA		MILDLY MARINE	10 - 20 µm/YEAR	1 - 2 µm/YEAR
C2	INLAND		RURAL	LESS THAN 10 µm/YEAR	<0.8 µm/YEAR
C1	INLAND		DESERT	LESS THAN 5 µm/YEAR	<0.5 µm/YEAR
C3	URBAN INLAND		INDUSTRIAL	10 - 30 µm/YEAR	1 - 3 µm/YEAR
C5	URBAN COASTAL		MARINE INDUSTRIAL	50 - 150 µm/YEAR	5 - 15 µm/YEAR
H.W.M – HIGH WATER MARK					

Figure 2.28: Map of risk of corrosion of mild steel and zinc of South Africa (HDGASA, 2005)

The map illustrates the risk of corrosion of exposed galvanised steel and zinc but the severity is not be expected to be similar to chloride-induced corrosion severity for reinforcement embedded in concrete.

Also, from the classification map in Figure 2-28, it is seen that locations closer to the coastline (classified as $C5^{+}$) which are less than 50 m from the high water mark (H.W.M) are more susceptible to the risk of corrosion and hence metal structures in this area are classified to be under severe marine conditions. C5 and C4 also represent locations with high corrosion rates of 2 – 30 µm/year. Specifically, the enlarged Cape Town area image in the figure also indicates that the exposure conditions in the location ranges from C5 – C4 which is "Average marine" to "Severe marine".

Noticeably all locations with high corrosion rates are close to the coastal zone. This validates that the marine environment is the most aggressive environment for susceptibility of metals to corrosion. This severity of corrosion however decreases at locations that are inland such as C3, C2 and C1 with corrosion rates between 0.5 – 2 µm/year.

2.9 CLOSURE

The Cape Peninsula is divided into zones according to where weather monitoring stations are located. Assessing the data from the monitoring stations located around the Cape Peninsula, it was found that the Cape Peninsula experiences a low RH (64 %) during the warmer seasons, spring and summer, and a high RH (78 %) during the cooler seasons, autumn and winter. The average precipitation that occurs on the Cape Peninsula is low during spring and summer and high during winter, and the number of rain days during winter is more than that of summer. The wind speed experienced around the Cape Peninsula is relatively high due to the exposure to winds blowing off the Atlantic Ocean with occasional gale-force winds in summer referred to as the "Cape Doctor". These winds transport sea spray across the Cape Peninsula and cause higher concentrations of chlorides in the atmospheres of the exposure zones that are bordered by the sea. During the warmer period, a south easterly wind is experienced and during the cooler period, a north westerly wind is experienced.

The Cape Peninsula climate is windy, relatively humid and cold in winter and warmer and less humid in summer. In spite of all these factors been supposedly corrosion prospering, the severity of exposure in temperate regions are usually noted to be lower compared to countries in tropical and equatorial latitudes (Corvo *et al.*, 2008; Castro *et al.*, 2001; HDGASA, 2005; Maldonado *et al.*, 2006; Bertolini *et al.*, 2013). This can be attributed to the generation and distribution of airborne chlorides being assumed to be lower from the sea to the mainland. This hypothesis would be examined in this study. In the assessment of the severity of RC structures exposure to airborne chlorides, the prevailing climate of a location plays a definitive role. Therefore, understanding the influence of climatic conditions on airborne chloride production and

transportation in the Cape Peninsula would be a useful tool for adequate design of RC structures for durability.

The models discussed in 2.7.7 are only useful when the generated chloride aerosol and their transference inlands are estimated in each micro-location using GIS data (Cole *et al.*, 2004). These models may be incorporated in the Cape Peninsula to estimate aerosol generation and transportation as it shares a similar Mediterranean climate like South Australia where the model was generated. However, the process involves the use of CFD and GIS data representative of the Cape Peninsula into the model. These reviewed modelling methods are beyond the scope of this study.

CHAPTER 3

3 Experimental methodology

3.1 INTRODUCTION

This chapter discusses the methods used to carry out the investigations in this study. It also discusses the selection of the monitored locations in the Cape Peninsula. Furthermore, it was imperative that an investigation on the effects of weather conditions on deposition rate be carried out, hence the weather data for locations where the wet candle device was exposed were also obtained. In addition, the laboratory test method used in determining the chloride contents of the wet candles and concrete cores collected from existing RC structures around the Cape Town area is described. Figure 3.1 summarises the aim and expected outcome of the methodology.

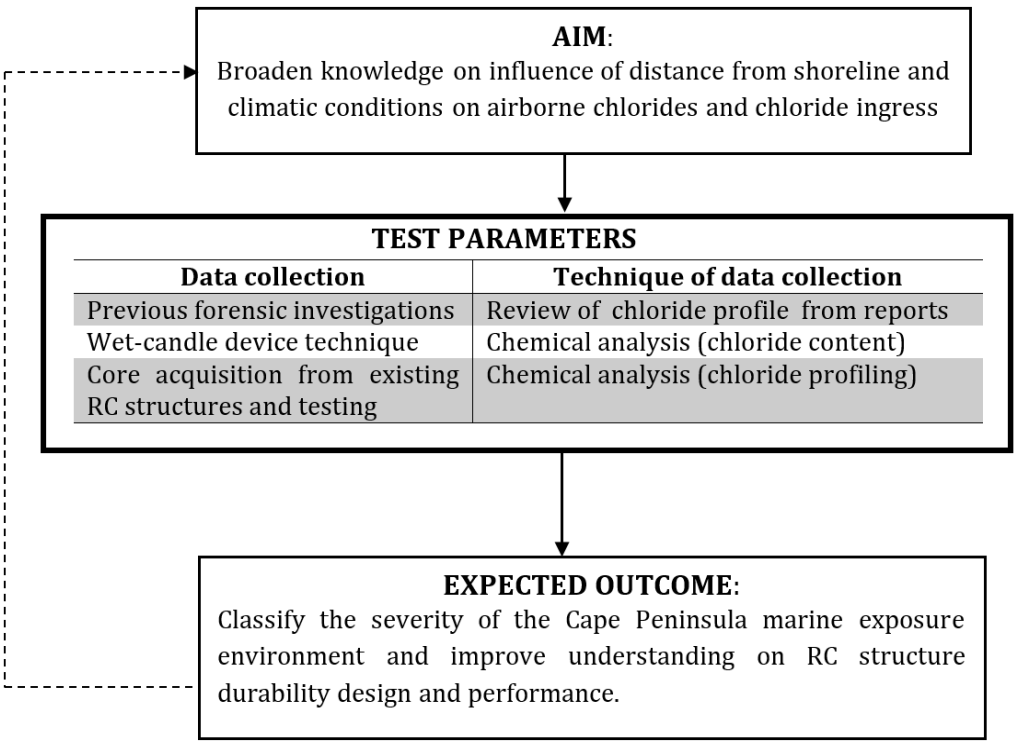

Figure 3.1: Methodology of data collection and expected outcome

Lastly, in order to determine the quality, determine outliers in the data and aid in the interpretation of data collected, the methods of statistical analyses carried out on the datasets are also discussed.

3.2 WET CANDLE DEVICE

The wet candle method provides data on the salinity of the atmosphere rather than the effects of the salinity on RC structures. The method measures the total amount of atmospheric chlorides arriving at a vertical surface, and thus gives an indication of chloride deposition rate.

The wet candle device was used to inform a classification of the severity of exposure of RC structures to airborne chloride deposition in the Cape Peninsula. When the severity of exposure for a specific location is known, a more informed design can be implemented for a structure. The wet candle was used to quantify the concentration of airborne chlorides for a particular location at varying distances from the shore. The aerosols (airborne chlorides) were captured on the surface of the wick and drawn into the flask through capillary forces. The deposition rate of the wet candle device is defined in milligrams of chloride deposited per exposed area of wick per day ($mgCl/m^2.day$).

Samples from the monitoring stations were collected twice a month and the candles were then replaced with new candles. The monthly airborne chloride concentration for a particular location was the sum two weekly measurements. The only exceptions to this sequence were for the months of May, September, October and November where the candle was exposed for a full month undisturbed.

3.2.1 Fabrication of the wet candle device

The materials used in fabricating the device were polyvinyl chloride (PVC) sheets, galvanized steel pipes for the support and coated steel plates for the base. The dimensions and design were carried out according to the ASTM G-140 (ASTM G-140-02: 2008). The only modification to the design was with regards to the number of legs for the supports. Only one (1) was used as opposed to two (2) in the ASTM method; but this provided adequate structural stability and the device also withstood wind pressures. Figure 3.2(a) is an example of an installed wet candle device with Figure 3.2b indicating its dimensions. Five (5) no. devices were fabricated for monitoring the locations discussed in Section 3.2.2.

The sides of the wet candle apparatus were closed in order to simulate a unidirectional capture of airborne chlorides and provide adequate stiffness for the structure. It also aided in securing the wet candle apparatus from wash-off effect of rainfall.

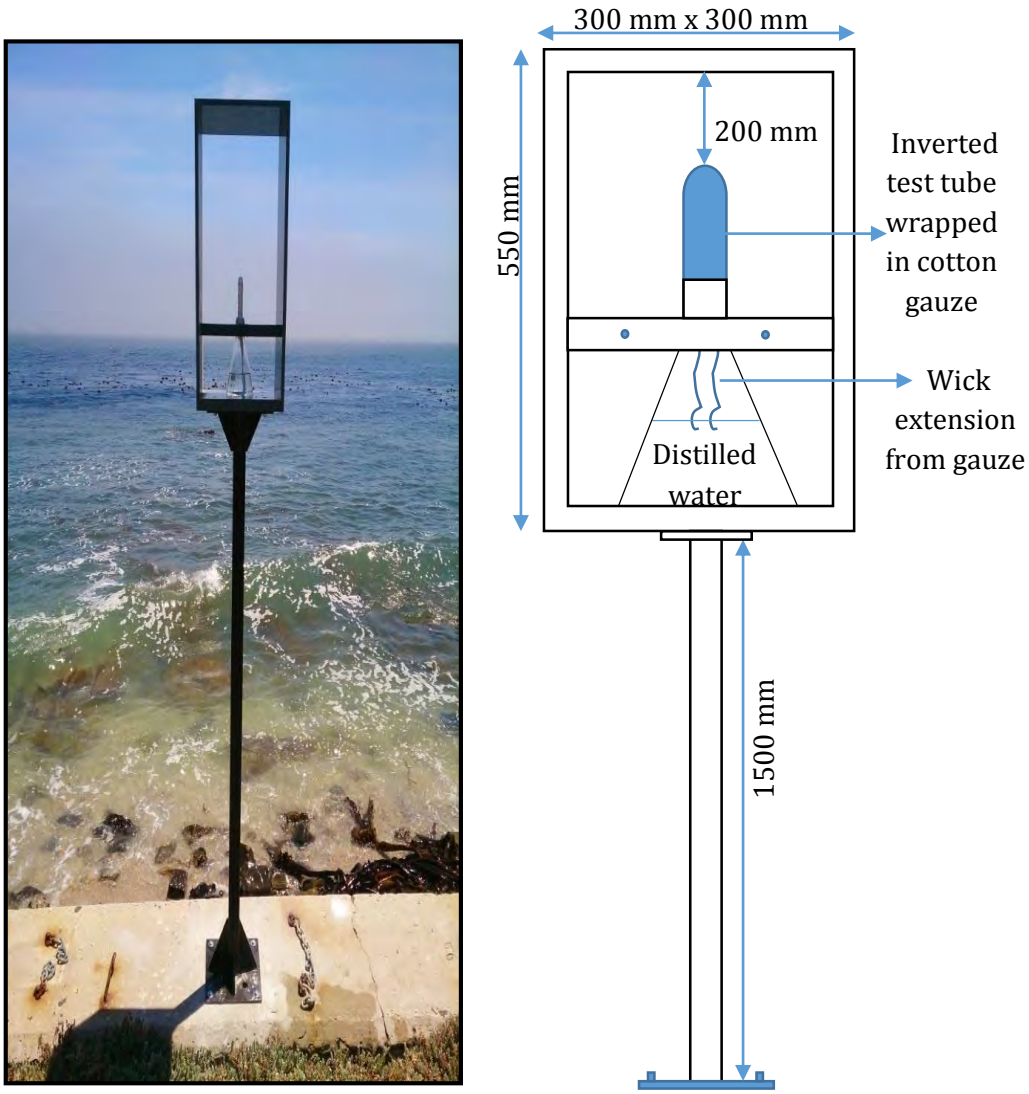

Figure 3.2: a) Wet candle device setup at Granger Bay, b) Dimensions

3.2.2 **Selected locations for wet candle device monitoring**

The SANS 10100-2 states that the airborne chloride exposure class for a RC structure within a range of 1–30 km from the sea is "very severe" (SANS 10100-2:2009). Therefore, in order to evaluate the main objective of investigating the effect of distance from the sea on airborne chloride concentration, four (4) of the monitored locations were aligned approximately in a straight line to the prevailing wind direction. Only one of the locations was out of alignment, this was in order to evaluate the changes in seasonal wind direction.

Distance measurements of the select locations were accomplished using Google Earth. The distance measured to the device was taken from the nearest coastline to the monitoring location. Figure 3.3 shows the monitored locations on a map of the Cape Town area and Table 3-1 provides more information on distance, global coordinates, average wind speeds and directions. The devices were installed so as to face the

coastline direction. In areas where this was not easily detectable, the devices were installed in the direction of the seasonal wind.

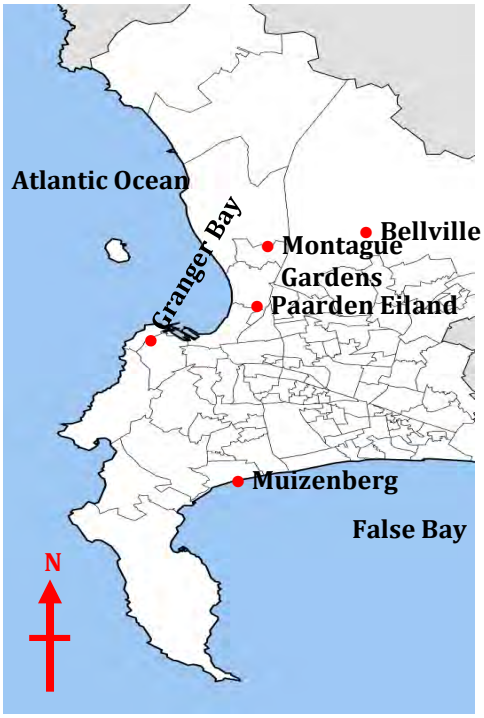

Figure 3.3: Locations monitored using wet candle device

Table 3.1: Monitoring location information

Location name	**Concentration of infrastructure**	**Latitude and Longitude** (degrees)#	**Nearest distance to coastline** (m) #	**Wind direction and average daily speed**
Granger Bay (GB)	Urban	-33.901855, 18.415755	50	Summer, Spring & Autumn – SE – 21 km/h Winter – NW – 17 km/h
Muizenberg (M)	Urban	-34.107324, 18.470468	150	Summer, Spring – SE – 27 km/h Autumn – SW – 20 km/h Winter – NW – 18 km/h
Paarden Eiland (PE)	Urban/ industrial	-33.906065, 18.476213	250	Summer, Spring, Autumn – SE – 29 km/h* Winter – NW – 20 km/h*
Montague Gardens (MG)	Industrial	-33.871029, 18.520473	2700	Summer, Spring, Autumn – SE – 29 km/h* Winter – NW – 20 km/h*
Bellville (B)	Industrial	-33.909804, 18.625291	13550	

* Average wind speed from Weather Underground (www.wundeground.com), # Accuracy to the nearest 3 m

For further investigations on the influence of seasonal changes on airborne chloride deposition rate, the locations were selected in such a way as to simulate exposure to

both seasonal wind directions of south-easterly (SE) in summer and north-westerly (NW) in winter. Only Muizenberg has a different prevailing south-westerly (SW) wind direction in autumn as shown previously in Figure 2.3b in Chapter 2 and in Table 3.1. The seasonal variations in wind directions and speeds for each location play an important role in the distance travelled by the airborne chlorides and their residence time.

In order to have optimum exposure to capture airborne chlorides, the devices were set-up in locations with low concentration of immediately surrounding infrastructure. This would ensure that the effect of surface roughness (vegetation and infrastructure) in interfering with airborne chloride deposition was reduced. However, apart from the devices at Granger Bay and Muizenberg (*Appendix D*), the wet candle device at the other locations were still relatively inland (distance > 2 km) such that there were still infrastructure in their vicinity.

Finally, the choice of the location of each sampling station depended on the availability of an open, safe and secured area, free of interference from walls, trees or other obstructions, thus permitting wind circulation. The farthest location, Bellville, was at a distance of 13.5 km from the coastline. The selection of this maximum distance from the coastline for monitoring was motivated from previous studies by researchers using the wet candle device (Hossain et al., 2009; Meira et al., 2010).

3.2.1 Chloride content of exposed wet candle devices

The wet candles from the sampling stations were collected every two weeks for each month of exposure. This ensured the flasks did not dry out due to evaporation as this would hinder the capillary process which aided in airborne chloride capture. The wick and wick solution in the conical flasks were retrieved from the wet candle device. The wick and the solution were soaked in a 500 ml flask containing distilled water. After collection from site, the setup was allowed to stand for 24 hours in the laboratory at a temperature of 23˚C and RH of 50 %.

The flasks were sealed to ensure that there was no contamination from the environment. The chloride content of the solution was then tested using the same method as the powdered concrete samples (ASTM C-1152). The ASTM C-1152 method is discussed in section 3.3.2. Three (3) samples from each solution were tested after 7 days which was a precautionary measure to ensure full dissolution of captured dry salt. The average concentration of the 3 samples was used to characterize the concentration of a solution.

3.2.2 Weather conditions during period of exposure

Weather data for each sampling station during the period of monitoring was acquired from the South African Weather Service (SAWS). SAWS have several air quality, weather

and greenhouse gas monitoring stations around the Cape Peninsula. Average wind speed, average precipitation, relative humidity and temperature data collected covered the period of exposure of the wet candle device. The measured weather conditions will be related to the chloride deposition within the exposure period.

3.3 CHLORIDE PROFILING OF EXISTING RC STRUCTURES IN THE CAPE PENINSULA

The methodology of concrete core collection from the selected existing RC structures in the Cape Peninsula is discussed in this section. The major objectives are sample collection and chloride profiling in order to examine for each RC structure the chloride ingress patterns. Importance of this cannot be over-emphasized as it aids in proper comparison between measured chlorides in the marine environments and chlorides that actually deposit. It can also be used to deduce the rate at which these deposited chlorides penetrate into varying concrete structures in marine exposure environments.

3.3.1 Study locations and rationale for selection

In compiling the collated data, the RC structures were categorised into groups according to their distances from the sea and concrete material characteristics (such as binder content, compressive strength and cover depth). This was to aid in the comparison of the structures and allow for accurate interpretation of results obtained. However, in situations where binder content or w/b for a RC structure information could not be retrieved from the authority, an estimated binder content was inferred using typical contents in erstwhile specifications.

Public infrastructure in the Cape Peninsula are under the jurisdiction of either the City of Cape Town or the Provincial Government of the Western Cape (PGWC). With their permission, access to obtain core samples from the bridges for chloride content profiling was achieved. Chloride profiling was carried out on 8 bridges and 1 retaining wall. The components of the bridges from which cores samples were collected included guard railings, piers and abutments. Due consideration was given to cored sample orientation to the coast and predominant wind direction. Table 3.2 and Figure 3.4 show the locations of the RC structures with their corresponding distances from the nearest coastline. The measured distance to the structure was measured from the nearest coastline, assuming that this would impact the RC structure more with regard to airborne chloride generation and transportation.

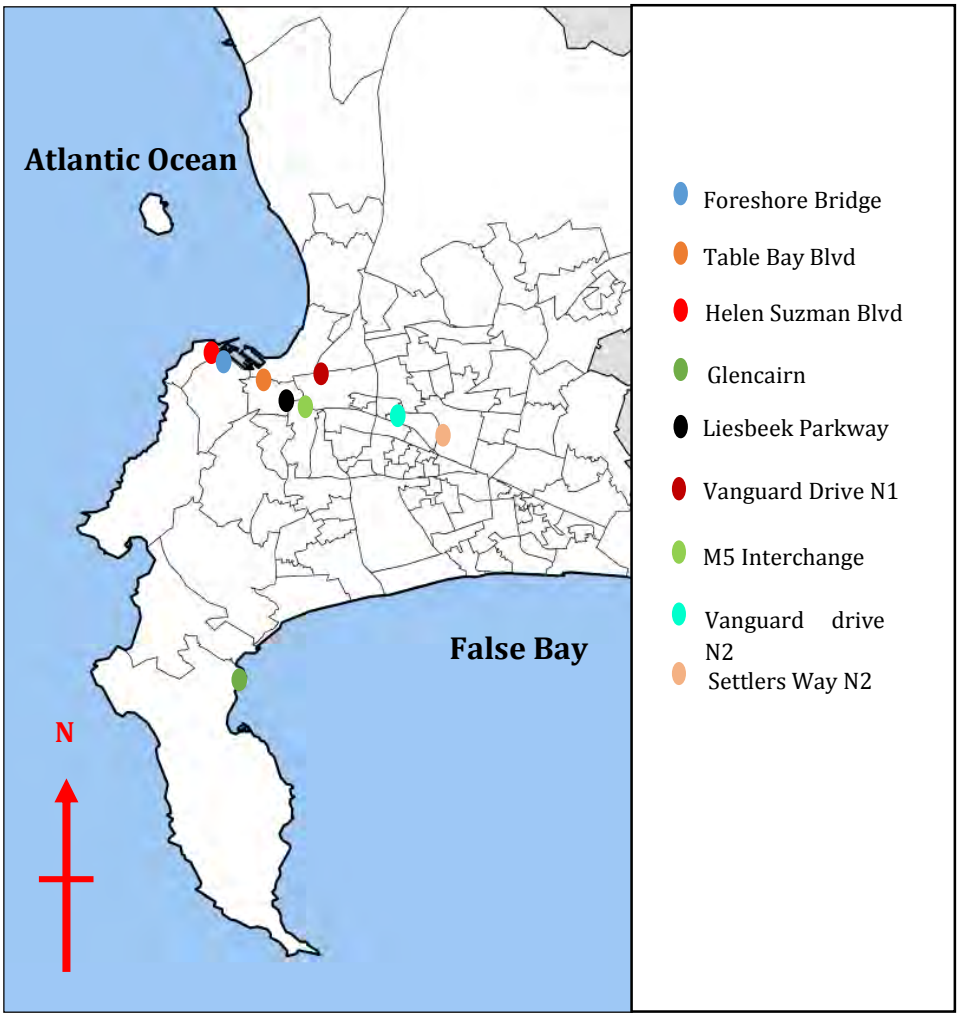

Figure 3.4: Locations in the Cape Peninsula where concrete cores were collected

Table 3.2: Information on existing RC structures tested

Location of structure and coordinates#	**Owner/ Authority**	**Type of Structure**	**Distance from sea** (m)
Foreshore bridge (-33.919712, 18.434659)	City of Cape Town	**Bridge**	250 - 300
Table Bay Blvd Interchange to Lower Church Street (-33.921602, 18.448954)	City of Cape Town	**Bridge**	300 - 350
Helen Suzman Blvd (-33.912598, 18.419848)	City of Cape Town	**Bridge**	700 - 800
Glencairn, Simons Town (-34.168433, 18.430646)	City of Cape Town	**Retaining Wall**	30 - 50
Liesbeek Parkway Interchange on Settlers Way (N2) (-33.944039, 18.476456)	PGWC	**Bridge**	3600 - 4000

Table 3.2: continued

Location of structure and coordinates#	**Owner/ Authority**	**Type of Structure**	**Distance from sea** (m)
Vanguard Drive Interchange on the N1 (-33.885244, 18.531198)	PGWC	**Bridge**	4000 - 4200
M5 Interchange on Settlers Way(N2) (-33.943521, 18.483593)	PGWC	**Bridge**	4000 - 4200
Vanguard Drive Interchange on the Settlers Way(N2) (-33.955174, 18.540914)	PGWC	**Bridge**	8500 - 9000
Settlers Way N2 by Airport Approach (-33.966016, 18.572125)	PGWC	**Bridge**	11200 - 11500

Accuracy to the nearest 3 m

Figure 3.5 and Figure 3.6 presents images of some of the RC structures where concrete core samples were collected for chloride content profiling.

Figure 3.5: a) Helen Suzman guardrail (GR) b) Core collection from Helen Suzman
c) Underside of deck Table Bay d) Core collection on Table Bay pier

Figure 3.6: a) Foreshore bridge guardrail b) Glencairn retaining wall
c) M5 barrier railing d) Liesbeek Parkway pier

3.3.2 **Chloride content testing of concrete cores from existing RC structures**

3.3.2.1 **Sampling and testing procedure**

Chloride profiling was carried out according to the ASTM C-1152 which is a test method for acid-soluble chloride content in concrete (ASTM C-1152:2012). The concrete cores which were collected from the RC structures were sliced into 10 mm thick discs. The length of each core was dependent on the depth of the concrete cover to the steel in the structure. The sliced discs were powdered using a pulveriser. Analysing chloride content at the 10 mm interval informs on the amount of chlorides by mass of cement at the varying depth. The limitation for 10 mm interval arose from ensuring human safety. As a result, the maximum depth of 10 mm for each core sample was not be exceeded during the slicing process.

The ASTM C-1152 provides information on the total chloride content which includes both 'bound' and 'free' chlorides in the concrete matrix and pore solution. Bound chloride ions within the cement matrix are not extractable using the water dissolution of the powder sample from concrete when tested according to ASTM C-1218 or C-1524. The only applicable method in this case is using acid digestion to release the "bound" chlorides ions according to ASTM C-1152 (Grace, 2006). This is important as the focus of this study is to analyse the exposure of the RC structures to airborne chloride deposition rather than the consequent dynamics involved in reinforcement corrosion.

The materials were powdered using a pulveriser and titrated with an automatic titrator (Mettler Toledo – Rondolino DL 50) device using a potentiometric titration method (*Figure 3.7*). The powdered sample was initially dissolved using distilled water and then digested with nitric acid (HNO_3) for a minimum of thirty (30) minutes. After which a buffer solution of sodium acetate ($C_2H_3NaO_2$) was added to ensure the pH of the sample was maintained at zero. The samples were topped up to the 60 ml mark using distilled water, to allow for dispersion of chlorides in the solution. They are then placed in the automatic titrator and the titrant silver nitrate (0.1M $AgNO_3$) solution is injected into the sample.

Figure 3.7: Titration stand and automatic titration device

The reaction paths for the chemical processes involved in this procedure are listed below:

- Acid – 1.0M HNO_3 is added to the diluted powder (with distilled water) and it digests the sample and forms a weak acid bond of hydrochloric acid (HCl). Thus the Cl^- can easily go into solution and dissociate from the hydrogen ion (H^+)
- The buffer solution sodium acetate ($C_2H_3NaO_2$) maintains the pH (at 0), that ensures the chloride ions can easily be dissociated from the acid bond.
- The titrant - 0.1M of $AgNO_3$ consumes the chloride ions and forming silver chloride (AgCl).
- At the endpoint of the reaction, silver chloride (AgCl) is formed which precipitates as a low solubility white substance.

$$AgNO_3\,(aq) + HCl\,(aq) \longrightarrow AgCl\,(s) + HNO_3\,(aq)$$

3.3.2.2 **Chloride content and apparent diffusion coefficient analysis**

The chloride profile for a core was taken as the chloride content of each 10 mm slice as shown in a sample plot in Figure 3.8. Most studies utilize a curve fitting method for the determination of the C_s as illustrated in Figure 3.8 by dotted red lines.

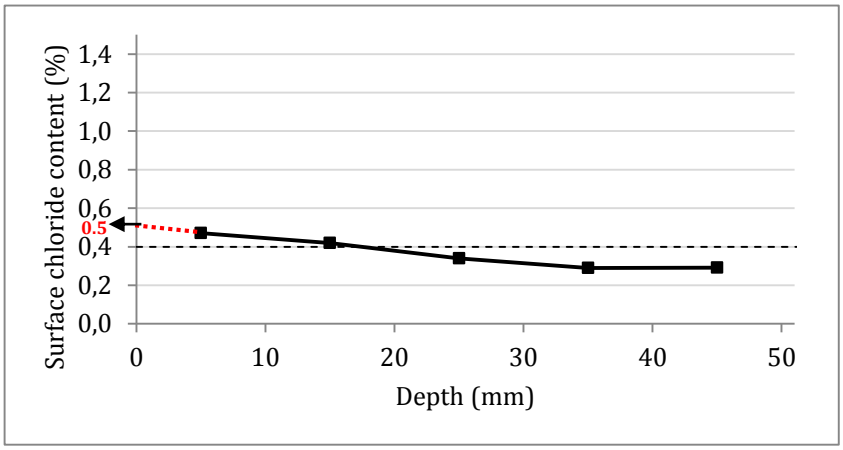

Figure 3.8: Sample chloride profile

However, the shortcoming of curve fitting is that in some cases it tends to overestimate the C_s. Therefore, in order to eliminate this error, an assumption was made that the chloride content of the sample from a depth of 0-10 mm was a representative of the C_s. This assumption is an oversimplification of the real situation but it aided in an assessment of RC structure exposure severity to airborne chlorides. With the C_s deduced, the apparent diffusion coefficient D_{ac} for the structures, was determined using Crank's error function solution of Fick's 2nd law of diffusion as defined in section 2.5.2, and is shown in Equation 3-1, it is derived from equation 2-6 in Chapter 2.

$$D_{ac} = \left[\frac{X(erf.C_s)}{2(C_{x,t}-C_s)}\right]^2 \qquad (3\text{-}1)$$

Typically, in order to be able to carry out a comparison of D_{ac} of structures with different ages, there is need to normalize the effects of their age differences. This is most important in structures below 10 years old as the effects of chloride binding by the cement paste is still dominant. But for structures above 20 years, the cement paste's capacity to bind chlorides is most probably depleted and therefore D_{ac} is steadier and is comparable. All the RC structures examined in this study were above 30 years old.

3.4 CASE STUDIES FROM PREVIOUS FORENSIC INVESTIGATIONS

An analysis was carried out on data collated from previous condition assessment investigations carried out by the Concrete Materials and Structural Integrity Research Unit (CoMSIRU) of the University of Cape Town on 38 different RC structures in the Cape Town area. A sample size of about 110 chloride content datasets was retrieved for

the total number of structures. The representative data for each structure was deduced from either single observations or through averaging of about 5-15 datasets.

The RC structures assessed included buildings, wastewater treatment structures and water reservoirs. These structures are located in Cape Town, South Africa or the Namib Desert, Namibia and they are all exposed to airborne chloride attack. The structures in Namibia are examined independently in this study because they represent a rare case of airborne chloride exposure as discussed further below.

In order to characterize the quality of concrete and the severity of the environment, an investigation of the interrelationship between the ages of structures, cement contents, compressive strengths, surface chloride contents and apparent diffusion coefficients was carried out.

The objective of the assessment was to categorise the RC structures according to their locations from the coastline and quality of concrete. The quality of the concrete was benchmarked on the basis of concrete compressive strength and apparent chloride diffusion coefficients of these structures. There were many uncertainties in the data and the interpretation was therefore difficult, but it nevertheless provided a basis for comparison. The reason why an extrapolation of surface chloride concentrations (C_s) from the fitted curve was not used in the case study section, was because some of the structures did not have enough data points for extrapolation to be carried out. Therefore, the C_s was deduced from the 0-10 mm depth of the concrete core sample.

3.4.1 **RC structures by location**

3.4.1.1 **Cape Town**

Various structures in the Cape Peninsula (Cape Town area) had previously been assessed by the Concrete Materials and Structural Integrity Research Unit (CoMSIRU) of the University of Cape Town. Twenty Nine (29) No. of these structures were selected for investigation in this study. The date of assessment of these structures ranged from 1996–2013. The ages of the RC structures examined generally ranged between 34 – 40 years, with only one structure estimated to be 70 years old. Their distances from the coast varied from 50 m to 15 km from the nearest coastline (*see Appendix A for detailed information*).

3.4.1.2 **Namibia**

A forensic assessment of concrete structures (water reservoirs) was carried out on the in 2010/2011. Nine (9) No. water reservoir structures underwent condition assessment and the findings are discussed in this research. These reservoirs are located in the Namib Desert which borders the Atlantic Ocean. The age of the reservoirs ranged from 30–40 years old and their distances from the nearest coastline varied from 5 km to 70 km. See Appendix A for detailed information.

3.4.2 Compressive strength and binder content

For the RC structures examined in this study it was difficult to gather information on the cement content, but estimated values ranging from 280-420 kg/m^3 were derived from some of the reports provided (*See Appendix A*). These values were estimated on the basis that all the structures were above the age of 34 years, therefore an assumption that the binder type was pure Portland cement was made. With the aforementioned and the measured compressive strength of cores taken from the structures, the binder content could be estimated for some of the structures.

3.5 STATISTICAL ANALYSIS

This section discusses the statistical methods used in this study to find correlations or variations between the data collated. It also aids in providing clarity on the presence of relationships or the lack of it between the variables. The methods used are the multiple regression analysis and the Kruskal-Wallis test for sensitivity analysis. The level of statistical significance in this study has been defined at 0.05 (5 %).

3.5.1 Multiple regression analysis

Multiple regression analysis is a method in which the observed data (dependent variable) are modelled using a combination of independent variables simultaneously (Cohen *et al*., 2003). It is also useful when the relationships are nonlinear as it utilizes polynomial or logarithmic models to establish statistically significant relationships. In order to model a linear regression relationship between a dependent variable (Y) and a set of 'k' independent variables (X_1, X_2, X_3,..., X_k), the general multiple regression equation is expressed in Equation 3-2:

$$Y' = A + \beta'_1 X_1 + \beta'_2 X_2 + \beta'_3 X_3 + \ldots\ldots + \beta_k X'_k \qquad (3\text{-}2)$$

Where Y'_j is the predicted value of dependent variable (Y) which is resolved from multiplying the estimated coefficients (β') with the independent variable (X_j) and a constant A value is added to the sum. The coefficient (β) is a numeric weighting which is dependent on the influence of X_j on Y. Equation 3-2 is also called a fitted regression equation. Since Y' is estimated for Y, it is important to calculate the values of the residuals (e_j) as shown in Equation 3-3. A plot of the residuals is an indicator that the regression equation adequately predicts/estimates the dependent variable.

$$e_j = Y_j - Y'_j \qquad (3\text{-}3)$$

Multiple regression analyses were carried out to determine the correlation coefficient for the relationship between distance of RC structure, age, climate and the average surface chloride content (C_s). This method of analysis was used as it was able to take into consideration factors including the age of the structure the prevailing climate and the distance from sea. In this study, the distance from sea, age of structure and

prevailing climate are the independent variables and C_s is the dependent variable. All the independent variables have been assumed in this study to have an influence on a structures C_s. Equation 3-4 was used in this study to predict the influence of age of the structure (X_1) and distance from the sea (X_2) on the C_s (Y):

$$Y' = A + \beta_1 X_1 + \beta_2 X_2 \quad (3\text{-}4)$$

Coefficient of determination (R^2) is the percentage of variation or the "measure of scatter" of the dependent variable explained by the independent variable (Peter, 2008). Table 3.3 shows a typical multiple regression analysis table predicted by the multiple regression analytical model. It has been observed that with increasing number of variables the "R^2" value also increases. Therefore, the "adjusted R^2" value accounted for this by taking into consideration the individual relationships of the independent variables to the C_s. The adjusted R^2 value simply quantifies the ability of the independent variables to predict the dependent variable. A higher adjusted R^2 indicates a better fit of the model to the data.

Table 3.3: Interpretation of regression analysis results with hypothetical values

Components	Values	Explanation
R Square	0.80	R^2
Adjusted R Square	0.61	Adjusted R^2 used if more than one x variable
Standard Error	0.44	This is the sample estimate of the standard deviation of the error
Observations	5	Number of observations used in the regression analysis

Typically, the adjusted R^2 value provides a value equal to the R^2 value if all the independent variables influence the dependent variable, or a lesser value if some of them do not influence the dependent variable.

Tests of significance for R^2

After the regression analysis was completed, it is important to determine whether the multiple regression coefficient was statistically significant. This is because in most cases R^2 value calculated from observed data are always positive. Especially in cases that have large datasets, the observed R^2 value between the variables can be close to +1, even when all correlations in the data are actually zero (Cohen *et al*., 2003). The multiple regression procedure capitalizes on chance by assigning higher weights to variables which have the most statistically significant relationships with the dependent variables.

The lack of statistical significance of the data indicates that the observed sample multiple regression value could well be due to chance. Equation 3-5 is an F-test expression may be used to test the null hypothesis (H_0) which states that there is no

correlation between the variables, based on a set of degrees of freedom (k) from N sample size (Cohen *et al.*, 2003):

$$F = \frac{R^2/k}{(1-R^2)/(N-k-1)}, dof = k, N-k-1 \quad (3\text{-}5)$$

When carrying out the test for significance, values of $F > F_{critical}$ at a level of significance of $\alpha = 0.05$ (5 %), indicate that the null hypothesis H_0 is rejected. For example, if a dataset satisfies the H_0 criterion, then it is implies that there is no direct relationship between the variables been tested. Table 3.4 and Table 3.5 show definitions of the terms used for inference of statistical significance.

Table 3.4: Statement of hypothesis

Hypothesis	Statement	Inference
Null hypothesis, H_0	H_0: $F < F_{critical}$ at $\alpha = 0.05$ (5 %)	All Independent variables have zero contributions to the dependent variable **(statistically insignificant)**
Alternative hypothesis, H_1	H_1: $F > F_{critical}$ at $\alpha = 0.05$ (5 %)	At least one of the independent variables does not equal zero **(statistically significant)**

Table 3.5: F-test table (with hypothetical values)

	df	SS	MS	F	Significance F
Regression	2	1.605	0.8025	4.0635	0.1975
Residual	2	0.395	0.1975		
Total	4	2			

Where, df is the degrees of freedom, SS is the total sum of residual and regression squares, MS is the mean of the total sum of squares, F and significance of F indicates F-test values for rejection or acceptance of the H_0 correspondingly.

3.5.2 **Kruskal-Wallis test**

In addition to the significance test for R^2, the Kruskal-Wallis test; a non-parametric test (non-normal distributions and non-equal variance) that was identified suitable for sensitivity analysis of the dataset collated in this study was carried out.

A histogram plot of the sampled data (*Appendix E)* indicated that the data was left skewed and decreased towards the right for surface chloride concentration C_s. While it was right skewed and increased from left to right for the independent variable data (distance and age). This means the distributions of all the variables data were all non-parametric (non-normal). The sensitivity analysis was conducted to provide information on which independent variable had a larger influence on the dependent variable.

For, the Kruskal-Wallis test, when the p value (also α) is greater than 0.05, instead of rejecting the null hypothesis H_0, it is accepted. The H_0 statement as shown in Table 3.6 implies that the variables are identical and therefore the independent variables have an influence on the dependent variable (whether directly or inversely).

Table 3.6: Statement of hypothesis

Hypothesis	Statement	Inference
Null hypothesis, H_0	H_0: $p > 0.05$	Dependent variable and independent variable are identical **(direct or inversely related)**
Alternative hypothesis, H_1	H_1: $p < 0.05$	Dependent variable and independent variable are non-identical **(no relationship)**

3.5.3 Mixed effects models

The intuition for introducing mixed model effect was based on data collected for the wet candle device at varying locations. The term mixed model refers to the use of both fixed and random effects in the same analysis (Seltman, 2014). The influence of the fixed and random effects in a dataset arise either from taking repeated measurements over time or space, or due to multiple related outcome measures at a point in time.

Mixed effects models typically provides a flexible approach in these situations, because it allows a wide variety of correlation patterns to be explicitly modelled. The fixed effects usually have levels of primary interest that are not expected to change if the measurements are repeated. In this study, the weather data obtained such as wind speed, RH and temperature are defined as the fixed effects. While the random effects which is the variable specific to this study is the '*chloride deposition rate*' repeatedly measured over the 12-month period. Table 3.7 shows a reduced sample of data analysed to indicate how repeated measurements are tabulated.

Table 3.7: Mixed model table with reduced sample data

		Random effects	**Fixed effects**			**Repeated measurements**
Variables	ID	Deposition rate ($mg.Cl/m^2.day$)	Ave. monthly wind speed (km/h)	Ave. monthly RH (%)	Ave. monthly temp (°C)	Time variance (months)
Granger Bay	1	2,13	23	71	22	1 (Dec/Jan)
Granger Bay	1	6,24	20	75	23	2 (Feb)
Granger Bay	1	5,11	18	76	20	3 (Mar)
Granger Bay	1	4,01	14	70	19	4 (Apr)
Granger Bay	1	54,67	16	78	15	5 (May)
Muizenberg	2	1,95	16	60	21	1 (Dec/Jan)
Muizenberg	2	5,5	19	59	23	2 (Feb)
Muizenberg	2	3,73	15	64	19	3 (Mar)

Table 3.7 continued

		Random effects	**Fixed effects**			**Repeated measurements**
Variables	ID	Deposition rate ($mg.Cl/m^2.day$)	Ave. monthly wind speed (km/h)	Ave. monthly RH (%)	Ave. monthly temp (°C)	Time variance (months)
Muizenberg	2	4,62	13	61	14	4 (Apr)
Muizenberg	2	4,34	13	69	11	5 (May)

The mathematical theorems used in the mixed effect model are out of the scope of this study, but for further information see Seltman (2014) and Winter (2013). A statistical software "R" was used to carry out the analysis. The interpretation of the results are based on the p or α value. If the p value is greater than 0.05 (5 %) then there is no significant relationship between the dependent variable and the independent variable. However, if the p value is less than 0.05 then there exists a significant relationship.

CHAPTER 4

4 Results and discussion

4.1 INTRODUCTION

In this chapter, an analysis of the data from the exposed wet candle devices and the corresponding prevailing weather conditions during their exposure are examined. Also discussed in-depth is the analysis of the results of the tests carried out on different components of the RC structures outlined in Section 3.3.1. The chloride content data collated from the previous forensic investigations are also analysed and discussed. Finally, an attempt was made to holistically analyse and interpret the total data that was collected so as to improve understanding and find synergies.

4.2 WEATHER CONDITIONS DURING INVESTIGATION

In order to characterize the effects of weather variations on airborne chloride deposition rate, the weather conditions during the exposure were monitored. The weather data collated include average wind speed, wind direction, precipitation, temperature and RH. The daily weather data were averaged over a 1 month period. The period of monitoring was December 2013 – November 2014 (12 months). All representative weather data was retrieved from the South African Weather Service (SAWS), with the exception of the temperature and wind speed data retrieved from additional stations at Sea Point, Paarden Eiland and Muizenberg provided by Weather Underground (Weather Underground Ltd., 2014). The impact of the microclimates of each location on their airborne chloride exposure severity are discussed in Section 4.3.2.

4.3 AIRBORNE CHLORIDE CONCENTRATION MEASUREMENTS

The period of monitoring ensured that a study on effects of seasonal changes and the influence of RC structures distance from the sea on the severity of their exposure to airborne chlorides could be examined. The monthly chloride content of the wet candle

device for each location as well as the method of calculation of their respective deposition rates are presented in Appendix B.

4.3.1 Influence of distance from sea on deposition rate

The total measured airborne chloride deposition rates in the Cape Peninsula area for the exposure period of 12 months are presented in Table 4.2 and plotted in Figure 4.1. The monitored locations are marked with the following abbreviations Granger Bay (GB), Muizenberg (M), Paarden Eiland (PE), Montague Gardens (MG) and Bellville (B).

Table 4.1: Chloride deposition rate per monitored location

LOCATIONS	GB	M	PE	MG	B
Distance from sea (m)	50	150	250	2700	13550
Total chloride deposition rate ($mgCl/m^2.day$)	138.1	30.7	34.1	12.5	11.8

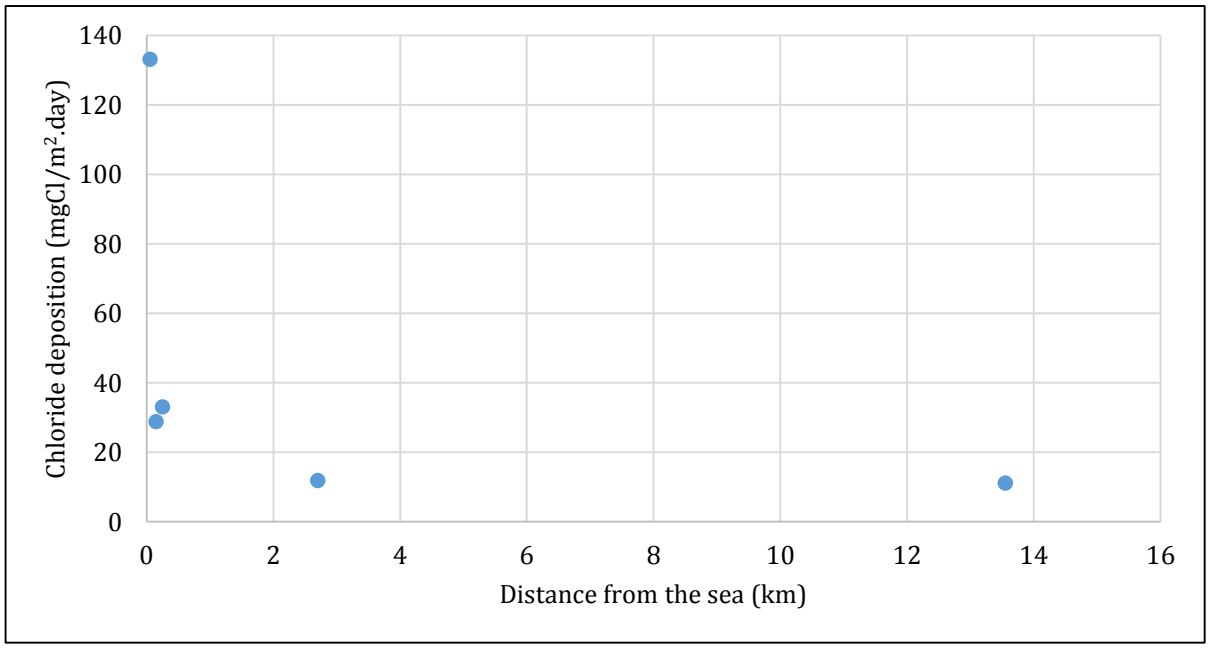

Figure 4.1: Chloride deposition on the wet candle device at varying distances from the sea in Cape Town, South Africa

Previous similar investigations in the coastal environments of Bangladesh and Brazil by Hossain & Easa (2011) and Meira *et al.*, (2010) respectively indicated that as the distance of the wet candle device from the sea increased, the concentration of airborne chloride ions captured by the device decreased.

The visible trend from Figure 4.1 validates the findings from these previous investigations and showed that there was a substantial decrease in airborne salinity as the distance of the device from the coastline increased. A comparative analysis of the

plot in Figure 4.1, with the plots in Figures 2.23 and 2.24 also indicated that the Cape Peninsula had airborne chloride deposition rates that were 50–86 % higher than the measured deposition rates in Chittagong, Bangladesh at the distance of 0–200 m from the coastline. But, the airborne chloride deposition rates measured at Joao Pessoa, Brazil were noted to be about 3-4 times greater than the deposition rates in the Cape Peninsula area.

Table 4.2: Total measured chloride deposition in Chittagong, Bangladesh (Hossain & Easa, 2011)

Distance from sea (m)	93	152	207	452	811	1222	2105	3216	4019	5013	6105	7012
Chloride deposition ($mgCl/m^2.day$)	54	16.1	13.22	4.71	3.93	3.11	2.62	2.10	1.71	1.42	1.31	1.32

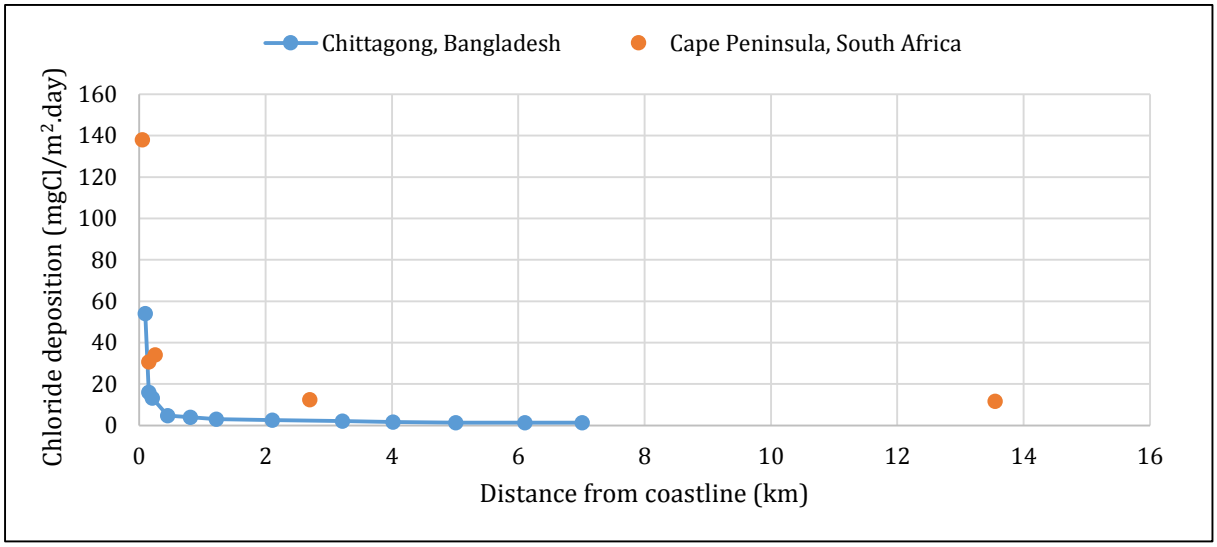

Figure 4.2: Comparison of deposition rates in the Chittagong, Bangladesh and the Cape Peninsula, South Africa.

Furthermore, a comparison of the total deposition rate at Chittagong, Bangladesh with the Cape Peninsula deposition rate as shown in Figure 4.2 indicated that higher deposition rates were measured at inland locations in the Cape Peninsula. For example, Location B (13.5 km) was found to have a chloride deposition rate about 10 times more than that measured at a distance of 7.0 km from the Chittagong coast. The reason for the higher deposition rates were attributed to the higher wind speed experienced in the Cape Peninsula (20–30 km/h) compared to Chittagong (5–16 km/h) (Weather2 Ltd., 2014).

In order to classify the airborne chloride exposure zones, the ISO 9223 was adopted. The ISO 9223 (ISO 9223:1992) aids in classifying the severity of an exposure environment according to the annual average airborne chloride concentration measured using the wet candle technique as presented in Table 4.3. Chloride deposition rate in the S_0 category is usually regarded to be insignificant from the corrosion point of

view for exposed metals. The airborne salinity in the monitored locations are between the S_1 and S_2 categories. From the measured deposition rates in the Cape Peninsula, it was found that the airborne chloride exposure severity ranges between 'moderate' and 'severe' between the distances of 0–13.5 km. A classification scheme for the Cape Peninsula exposure to airborne chlorides using the ISO 9223 will be proposed in Chapter 5.

Table 4.3: Classification of airborne chloride concentration (ISO 9223:1992)

Deposition rate of chlorides ($mgCl/m^2.day$)	**Category**
$S \leq 3$	S_0
$3 \leq S \leq 60$	S_1
$60 \leq S \leq 300$	S_2
$300 \leq S \geq 1500$	S_3

4.3.2 **Influence of seasonal changes on deposition rate**

4.3.2.1 **Season**

During the period of monitoring, the wet candle devices were protected from the washing effects of rainfall; therefore it presented the worst case of exposure to airborne chloride deposition. However, the role of rainfall in the washing of the exposed surfaces of the RC structures can be beneficial if there is high precipitation over a period of time. But in periods when concrete is saturated with moisture as a result of precipitation, it can inherently aid in the ingress of chlorides into the RC structure.

The influence of individual weather elements on the deposition rate are also examined in sections that follow. But the scope in this study is limited to wind direction, wind speed and relative humidity (RH), this is because as suggested by literature a linked relationship can be deduced from these weather elements with regards to airborne salinity (Lovett, 1978; Monahan *et al.*, 1986; McKay, 1994). The output of this analysis may be used in modelling the influence of wind and RH on airborne chloride deposition rates over a longer seasonal regime (climate) in the Cape Peninsula.

The averages of the weather data were used as independent variables to analyse the monthly airborne chloride deposition rates. Table 4.4 presents a breakdown of monthly chloride deposition rates with the daily weather data averaged over a monthly period. The table also contains data on extreme weather exposure conditions, specifically maximum and minimum weather conditions. Though, the use of averages in most instances conceals the presence of extreme weather conditions. It must be understood that extreme weather conditions as a matter of fact contribute to the airborne chloride deposition severity that is experienced by a location. But because extreme weather conditions usually have a short duration, this implies that their use in modelling or explaining the dependent variable might result in inaccurate prediction models.

Table 4.4: Monthly chloride deposition rates with corresponding weather data

Months	**Dec - Jan**	**Feb**	**Mar**	**Apr**	**May**	**Jun**	**Jul**	**Aug**	**Sep**	**Oct**	**Nov**
Granger Bay (GB)											
Deposition rate ($mgCl/m^2.day$)	**2.1**	**6.2**	**5.1**	**4.0**	**54.7**	**35.9**	**18.7**	**4.0**	**2.6**	**2.2**	**2.6**
Ave. daily wind speed (km/h)	23 (55*)	20 (48*)	18 (52*)	14 (48*)	16 (58*)	15 (48*)	13 (52*)	14 (47*)	15 (40*)	17 (45*)	15 (37*)
Ave. daily RH (%)	71 (94*)	75 (94*)	76 (94*)	70 (94*)	78 (100*)	77 (100*)	78 (100*)	75 (100*)	75 (94*)	72 (94*)	68 (94*)
Ave. daily temp (℃)	22 (11#)	23 (13#)	20 (7#)	19 (5#)	15 (4#)	13 (2#)	12 (1#)	14 (3#)	15 (4#)	18 (6#)	18 (9#)
Muizenberg (M)											
Deposition rate ($mgCl/m^2.day$)	**2.0**	**5.5**	**3.7**	**4.6**	**4.3**	**3.6**	**3.5**	**0.7**	**0.9**	**0.9**	**0.9**
Ave. daily wind speed (km/h)	16 (54*)	19 (59*)	15 (50*)	13 (46*)	13 (48*)	11 (41*)	11 (43*)	12 (45*)	11 (42*)	10 (41*)	11 (52*)
Ave. daily RH (%)	60 (71*)	59 (69*)	64 (72*)	61 (69*)	69 (74*)	68 (74*)	70 (77*)	70 (57*)	71 (56*)	74 (65*)	74 (65*)
Ave. daily temp (℃)	21 (13#)	23 (13#)	19 (13#)	14 (10#)	11 (10#)	12 (6#)	13 (4#)	16 (8#)	16 (9#)	18 (10#)	18 (10#)
Paarden Eiland (PE)											
Deposition rate ($mgCl/m^2.day$)	**1.6**	**4.4**	**3.5**	**3.2**	**6.4**	**6.0**	**5.7**	**1.4**	**0.8**	**0.4**	**0.5**
Ave. daily wind speed (km/h)	25 (77*)	21 (76*)	17 (69*)	14 (64*)	15 (63*)	13 (80*)	14 (79*)	17 (69*)	15 (58*)	21 (74*)	21 (74*)
Ave. daily RH (%)	70 (97*)	74 (97*)	78 (98*)	69 (97*)	72 (96*)	73 (59*)	71 (58*)	75 (57*)	77 (56*)	78 (65*)	69 (67*)
Ave. daily temp (℃)	21 (13#)	22 (13#)	19 (13#)	19 (10#)	15 (10#)	14 (6#)	14 (4#)	16 (8#)	16 (9#)	18 (10#)	18 (10#)
Montague Gardens (MG)											
Deposition rate ($mgCl/m^2.day$)	**0.09**	**0.0**	**1.6**	**1.4**	**3.3**	**3.1**	**1.9**	**0.4**	**0.3**	**0.3**	**0.4**
Ave. daily wind speed (km/h)	**Paarden Eiland weather station data used**										
Ave. daily RH (%)											
Ave. daily temp (℃)											
Bellville (B)											
Deposition rate ($mgCl/m^2.day$)	**0.03**	**0.0**	**1.6**	**1.5**	**3.0**	**2.8**	**1.5**	**0.4**	**0.3**	**0.3**	**0.3**
Ave. daily wind speed (km/h)	**Paarden Eiland weather station data used**										
Ave. daily RH (%)											
Ave. daily temp (℃)											

*maximum wind speed and RH measured daily # minimum temperature measured daily

Figure 4.3: Monthly airborne chloride deposition rates in the Cape Peninsula area

* May, June and July data for Granger Bay (54.67, 35.85 and 18.68 mgCl/m².day respectively) which are extremes are omitted to allow for comparison

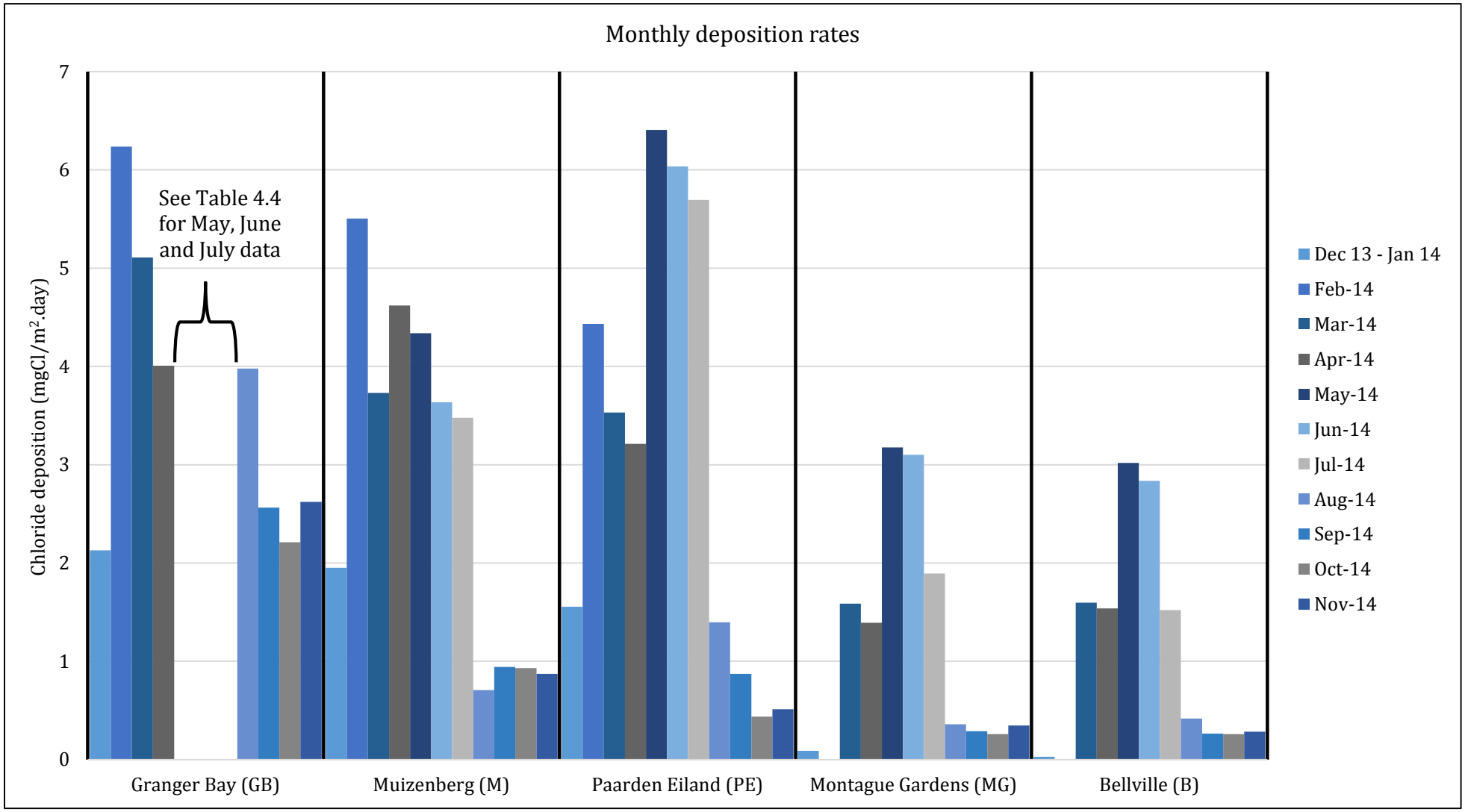

Figure 4.4: Airborne chloride deposition rates per location in the Cape Peninsula

* May, June and July data for Granger Bay (54.67, 35.85 and 18.68 mgCl/m².day respectively) which are extremes are omitted to allow for comparison

4.3.2.2 **Influence of wind on deposition rate in the Cape Peninsula**

The wind direction in summer for the Cape Peninsula is south-easterly and north-westerly in the winter period as indicated in Figure 4.5 and previously discussed.

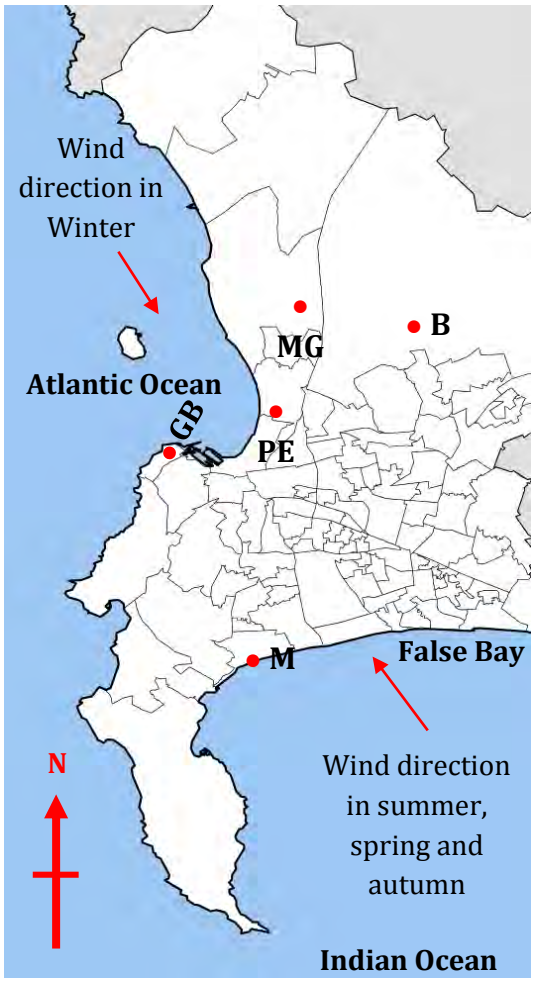

Figure 4.5: Locations monitored using wet candle device

Figure 4.6 illustrates the variations of monthly chloride deposition rates measured with corresponding average daily wind speed per location. The general trend in Figures 4.5a, c, d and e indicate that with increased average monthly wind speed there was less deposition. Therefore, the influence of the change in seasonal wind direction has been attributed to be more significant than the wind speed. But in Figure 4.5b, the trend indicates that with higher wind speed, there is a higher chloride deposition on the wet candle. The factors that influenced these findings are discussed in the sub-sections that follow.

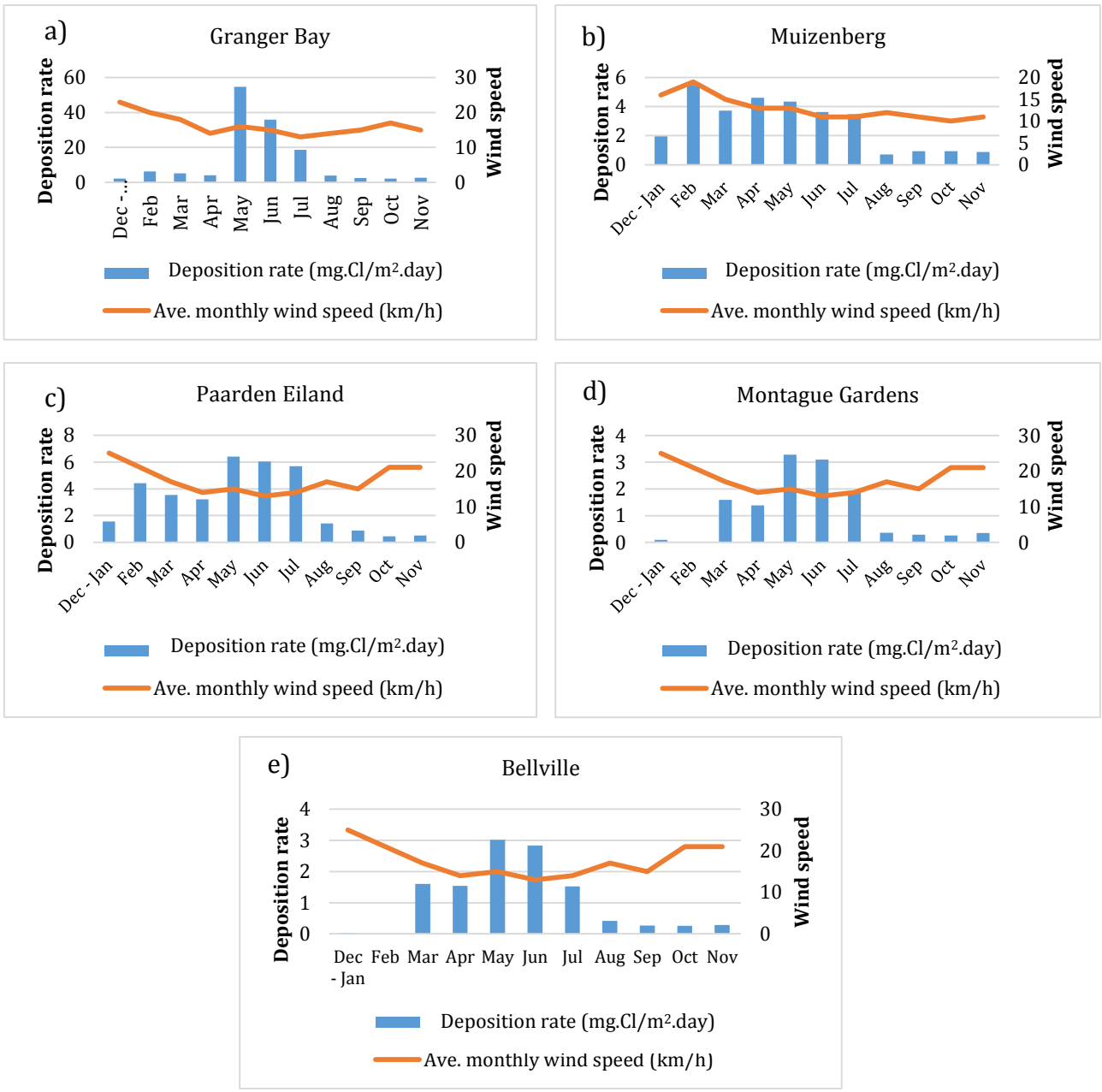

Figure 4.6: Influence of wind speed on the deposition rates in the monitored locations

Granger Bay (GB)

From Figure 4.4 and Figure 4.6a, it can be noted that the deposition rates in Granger Bay had a substantial increase (about 13 times more) in May than in the month of April from 4 mgCl/m².day to 54.7 mgCl/m².day when the prevailing wind direction changed. This is because in winter the prevailing wind direction towards GB comes from the direction of the sea. This implied that the most severe exposure season to airborne chloride deposition for the GB location was the winter period.

For the summer period, the most severe exposure month was the month of February. The month of May had the highest deposition rate for the monitored months in autumn. The increase in the autumn deposition rate can be attributed to the change in season.

The transition into the winter season commenced and consequently there was a change in prevailing wind direction as illustrated in Figure 4.5.

With consideration of the average daily wind speed variations averaging from 15-23 km/h during the monitoring period, it was observed that the influence was not very distinct in the seasons except in winter. After the significant increment in deposition rate in April, decreases in wind speed were accompanied by corresponding decrease in deposition rate.

It was also noted that the transition from winter to spring drastically reduced the deposition rate measured at GB by about 79 % in August (from 18.7 mgCl/m^2.day to 4 mgCl/m^2.day). In addition, there were no significant changes to deposition rates from September to November to the deposition rate in August. This ultimately indicated the change in prevailing wind direction played a vital role in the monthly airborne chloride deposition rate.

Muizenberg (M)

The Muizenberg location which is exposed more to the south-easterly prevailing wind direction experienced a drop in its chloride deposition rate of about 6 %, 21 %, and 25 % from May-July respectively from the month of April (4.6 mgCl/m^2.day). The highest exposure month at location M was the month of February with a deposition rate of 5.50 mg.Cl/m^2.day.

However, this does not imply the summer period had a significantly higher deposition rate compared with the other seasons. But the seasonal change in wind direction definitely had a reducing effect on the deposition rate. From Figure 4.6b indicates that there was also a halving of the deposition rates during the transitions between seasons as average monthly speed decreased from 11-16 km/h. The measured deposition rates from September to November were the same at 0.9 mgCl/m^2.day.

It must be noted that the monitoring station at the Muizenberg location was at an elevation of about 3 m on the roof of a building, as this provided the only secure and open location for monitoring. Hence, the reduction in chloride deposition rate measured at Muizenberg compared to the rates at Granger Bay could be attributed to the higher elevation of the device. This phenomenon, which is the influence of the surface orientation and the elevation of a RC structure's components to the source of chlorides on its exposure severity will be examined in Section 4.4.2.

Paarden Eiland (PE)

The proximity of PE (sample station 3), to the Atlantic Ocean implied that it was also exposed to the north-westerly wind in winter. This can be noted from the increased deposition rates of about 77-99 % in May, June and July (between 5.7-6.4 mgCl/m^2.day) from the measured deposition rate in the month of April (3.2 mgCl/m^2.day). The implication of the location of PE, is that it also experienced a higher airborne chloride

deposition rate in the winter period. But wind speed variations were not noted to impact the airborne salinity directly.

A decrease of 75 % in airborne salinity concentration was observed in August (1.4 mgCl/m^2.day) compared to July. This reduction suggested a revert of the prevailing wind direction from north-westerly to south-easterly as was the case. This observation also applied to Montague Gardens and Bellville both experiencing 81 % and 72 % decreases in airborne chloride deposition rates respectively in the month of August.

Montague Gardens (MG) and Bellville (B)

During monitoring, the deposition rates at both MG and B were quite similar and therefore the discussions of their findings are grouped together. MG and B were the farthest monitored locations, and in the summer months, their deposition rates where either insignificant or zero. However, as the monitoring progressed, it was continuously increasing and peaked during the winter period. These locations are closer to the Atlantic Ocean coastline than the Indian Ocean, hence, their exposure to chloride deposition noticeably increased in the period when the north-westerly winter wind was prevalent.

Location MG experienced an increase in deposition rate of between 36-128 %, with the most severe exposure month to airborne chlorides in May. It was discovered that changes in monthly wind speed did not directly influence the chloride deposition rates. In fact, the months (April–July) with the highest deposition rates (1.4 and 3.3 mgCl/m^2.day) had the lowest average wind speeds (13-15 km/h).

Bellville was under the least influence of airborne chloride deposition. The weather data used to classify the exposure environment at Bellville was situated at PE and similar conclusions could be drawn on the influence of wind speed on deposition rate. The most severe exposure period also fell in the month of May with a deposition rate of 3.02 mgCl/m^2.day. There was also a significant decrease in the measured deposition rates from August to September. The month with the lowest exposure was October with a deposition rate of 0.26 mgCl/m^2.day. It is important to note that in January and February, no chlorides were captured on the wet candle at the Bellville location.

4.3.2.3 **Influence of relative humidity on deposition rate in the Cape Peninsula**

The RH describes the moisture content in the atmosphere of an environment. With higher RH, airborne chloride particles experience a proportionate increase in atmospheric residence time. The analysis in the section would be carried out based on average monthly RH recorded. Figure 4.7 is a plot of average monthly RH vs monthly chloride deposition rates. The deposition rate is plotted on the left vertical axis and the RH is plotted on the right vertical axis.

Figure 4.7(a-e) illustrates the influence on RH on the airborne chloride concentrations in the monitored locations. During the winter season, where the average RH was between 73-78 % compared to summer (59-74 %) in all locations, there was a

significant doubling in the measured deposition rates at Granger Bay. While the other locations experienced increases with regards to airborne salinity during periods of low RH. There was no visible trend at the Muizenberg location with respect to the influence of RH on the deposition rates.

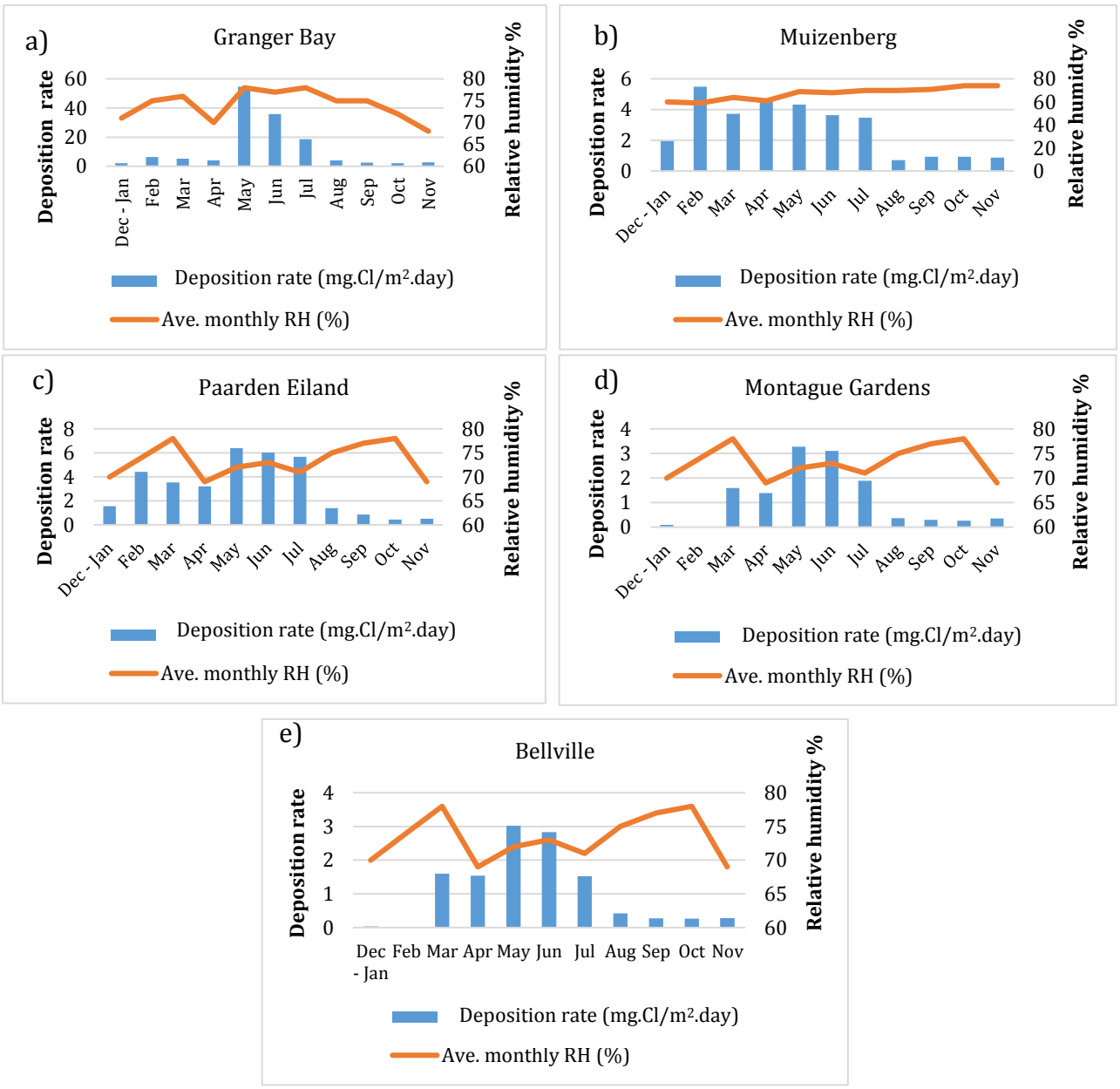

Figure 4.7: Influence of RH on the deposition rates in the monitored locations

The reduction in airborne chloride concentration at Granger Bay was considered not to be significant because on the ISO 9223 scale the deposition rates for May, June and July (54.7, 35.8 and 18.7 mgCl/m².day) still fell in the S_1 category. This was majorly influenced by the moisture content in the environment which served as a carrier of airborne chloride ions dissolved in it and transported them inland.

From the analysis of wind speed, wind direction and RH it was observed that the weather conditions would influence the residence time of airborne chlorides in the atmosphere and their deposition onto surfaces. It was also noted that climatic factors that promote increased moisture content in the atmosphere such as high RH, low temperature, increased precipitation are important in the transportation of ocean generated airborne chloride particles.

4.3.3 Mixed model effect analysis of deposition rates

In order to understand the synergistic effect of the environment on the airborne chloride deposition rates, the mixed effect model method was employed. The mixed model method is described in Section 3.5.3. Table 4.5 presents the results from the mixed model effect analysis.

Table 4.5: Mixed model analysis on the monthly deposition rates

Fixed effects: Deposition rate ~ wind speed + RH + temp + time				
	Value	**Standard Error**	**Degree of freedom** (*df*)	**p-value**
Intercept	- 4.48	30.96	35	0.890
Wind speed	0.70	0.52	35	0.190
RH	0.61	0.38	35	0.120
Temperature	-2.34	0.76	35	0.004
Time	-1.25	0.48	35	0.014
Number of observations	43			
Number of groups	4			

From Table 4.5, it can be noted that the p values for wind speed and RH are greater than 0.05 (0.19 and 0.12 respectively). This implies that both wind speed and RH do not play significant roles in the deposition rates. This supports earlier deductions, because from previous analysis it was found that the wind direction played a more vital role than both wind speed and RH. However, temperature and time were found to be significant with p values of 0.004 and 0.014 respectively. Temperature changes influence moisture presence in the atmosphere and therefore increases the residence time of airborne chlorides in the atmosphere.

4.4 CHLORIDE PROFILES FROM EXISTING RC STRUCTURES

Nine RC structures as outlined in Table 3.3, were cored for samples in order to carry out chloride profiling testing. The influence of the distance of the RC structure from the coastline and its surface orientation (facing the coastal wind direction or otherwise) of the structure's components (such as the piers and barrier railings) on the airborne chloride deposition rates were analysed and ingress patterns were inferred from the findings.

To extract useful parameters from chloride profiles, a curve fitting technique is normally used. However, in this study the surface chloride concentrations C_s were inferred from chloride contents at depths of 0-10 mm from the surface of each structure as opposed to extrapolation of the C_s from the fitted curve. This is because the use of extrapolation can sometimes be misleading or misrepresentative of the true situation. In addition, the structure's true surface chloride contents was not easily attainable due to the sample collection method. Samples were collected using the wet coring method which may have washed away surface depositions. Another limitation arose from the slicing of the cores into thinner discs. For reasons of safety, a disc thickness of less than10 mm for each 40 mm diameter core was not practical.

The new data on the Cs of existing structures was analysed individual of the data from previous forensic investigations. This was because of the objective of analysing the influence of orientation of structural components to coastline on their severity of exposure. A combined analysis is carried out subsequently.

4.4.1 Influence of distance on surface chloride deposition onto RC structures

A summary of RC structures examined for the purpose of this study are presented in Table 4.6. It provides information on the ages of the structures, the components were cores were collected, and their respective orientations to the coastline and the measured surface chloride concentrations C_s.

Table 4.6: Summary of information on RC structures sampled and analysed in this study

Location of structure	**Structural component cored**	**Distance from sea** (m)	**Estimated age of structure** (years)	**Average surface chloride content C_s** (% by mass of binder)	**Orientation and other comments**
Glencairn, Simons Town	Retaining Wall	50	50	2.51	Sea facing
Glencairn, Simons Town	Retaining wall	50	50	2.64	Sea facing
Glencairn, Simons Town	Retaining wall	30	50	3.48	Sea facing

Location of structure	**Structural component cored**	**Distance from sea** (m)	**Estimated age of structure** (years)	**Average surface chloride content C_s** (% by mass of binder)	**Orientation and other comments**
Glencairn, Simons Town	Retaining wall	50	50	4.5	Sea facing
Foreshore Freeway (Section M)	Barrier railing 1	300	40	0.44	Sea facing
Foreshore Freeway (Section M)	Barrier railing 2	250	40	0.48	Non-sea facing
Lower Church Street (over Table Bay Boulevard)	Pier	300	51	0.39	Sea facing
Lower Church Street (over Table Bay Boulevard)	Barrier railing 1	300	51	0.47	Sea facing
Lower Church Street (over Table Bay Boulevard)	Barrier railing 2	350	51	0.37	Non-sea facing
Helen Suzman Blvd	Pier 1	700	40	0.49	Non-sea facing
Helen Suzman Blvd	Pier 2	800	40	0.36	Sea facing
Helen Suzman Blvd	Barrier railing 1	800	40	0.47	Non sea facing
Helen Suzman Blvd	Barrier railing 2	700	40	0.61	Sea facing
Helen Suzman Blvd	Barrier railing 2	700	40	0.31	Non sea facing
Helen Suzman Blvd	Barrier railing 2	700	40	0.52	Sea facing
Settlers Way (over Liesbeek Parkway)(N2)	Barrier railing	4000	N/A	0.62	Sea facing
Settlers Way (over Liesbeek Parkway)(N2)	Pier	4000	N/A	0.78	Sea facing
Vanguard drive Interchange on the N1 - M7 Northbound (over N1)	Pier	4200	N/A	1.15	Sea facing
Vanguard drive Interchange on the N1 - M7 Northbound (over N1)	Barrier railing	4200	N/A	1.2	Sea facing
M5 Interchange on Settlers Way(N2) - Black River Parkway (over Settlers Way)	Barrier railing	4200	N/A	0.94	Non-sea facing
Vanguard drive Interchange on the Settlers Way(N2)	Pier 1	9000	N/A	0.87	Sea facing
Vanguard drive Interchange on the Settlers Way(N2)	Pier 1	9000	N/A	1.32	Non-sea facing
Settlers Way N2 by Airport Approach	Pier	11500	N/A	0.77	Sea facing

Table 4.6: continued

Location of structure	Structural component cored	Distance from sea (m)	Estimated age of structure (years)	Average surface chloride content C_s (% by mass of binder)	Orientation and other comments
Settlers Way N2 by Airport Approach	Pier	11500	N/A	0.7	Non-sea facing
Settlers Way N2 by Airport Approach	Barrier railing	11500	N/A	0.74	Non-sea facing

N/A – not available, see Appendix E for plot of C_s vs age and distance

The orientation of the structures was determined by their exposure to the direction of the coastline rather than the prevailing wind direction which was not an easy phenomenon to determine per location. In order to characterize the influence of distance on deposition of chlorides on RC structures the graph in Figure 4.8 was plotted (*see Appendix C for full data and statistics of variables*). The justification for direct comparison of C_s values is presented in Chapter 3 on chloride content analysis.

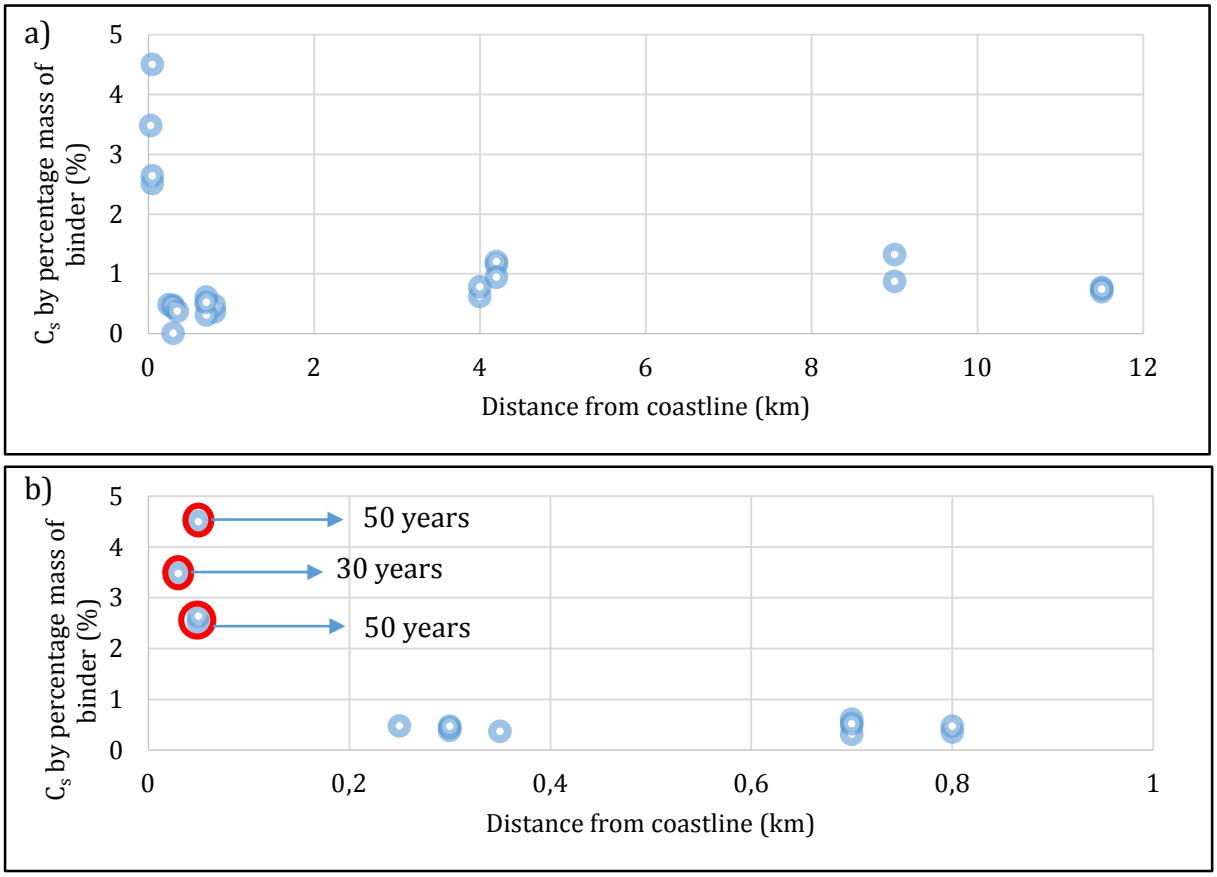

Figure 4.8: a) C_s vs distance for existing RC structures in the Cape Peninsula (0-12 km) and b) C_s vs distance of RC structures from sea (0-1 km)

The RC structures from a distance of 0-1 km from the coastline fall within similar age categories and therefore have similar concrete mix design parameters. However the general trend indicates that the C_s decreases considerably as the structure's distance from the coastline increases. The only exceptional cases where C_s of 1.37 % and 0.87 % (Vanguard Drive) were measured at a distance of 9 km in Figure 4.8a were attributed to

the surface roughness of surrounding locations (Figure 3.4). It was noted that there were few buildings and vegetation around these structures which could have obstructed deposition onto the structures. Based on visual observation of Figure 4.8b, the age of the RC structures that are closer to the sea is not significant. This will be analysed using the Kruskal-Wallis test.

For a proper understanding of the relationship between distance of the structure and its surface chloride concentration in relation to the age of exposure, a multiple regression analysis was also carried out. Due to the limitations in retrieving the age of some structures, data from Settler's Way (Airport and Liesbeek Parkway), Vanguard Drive (over N1 and N2) and M5 Interchange were excluded from the analysis. Table 4.7 shows the results of the analysis.

Table 4.7: Multiple regression analysis and ANOVA of age, distance and C_s of existing RC structures

Regression Statistics	
R^2	0.51
Adjusted R Square	0.43
Standard Error	1.03
Observations	15

ANOVA

	df	*SS*	*MS*	*F*	*Significance F*
Regression	2	13.38	6.69	6.26	0.014
Residual	12	12.82	1.07		
Total	14	26.20			

It can be deduced from the multiple regression analysis of C_s (dependent variable) with regard to RC structures "age" and "distance" that the R^2 is 0.51. In addition the F-test value of 6.26, has a significance value of 0.014 which has a p or α that is less than 5 %, implying that the correlation is statistically significant. It can also be deduced that distance and the exposure time (years) to airborne chlorides are determinant factors in surface chloride concentration increase or decrease.

Based on the coefficients of distance, age of structure and the intercept, the equation for the regression line is expressed by:

$$C_s = 2.51 - 0.0033(d) + 0.00039(y) \quad (4\text{-}1)$$

Where d is distance from coastline (m) and y is the age of structure (years). Equation 4-1 provides a good model for predicting exposure to airborne chlorides in the Cape Peninsula but its accuracy in predicting severity of exposure might be influenced by limited dataset used in the analysis.

The residuals plot for the predicted C_s values using the linear regression model in Equation 4-1 is presented in Figure 4.9. The plot indicates that the model equation

provides a good prediction for the influence of age and distance of RC structure on its C_s. This is because it is evident that the residual plot satisfies the condition of a normal distribution (homoscedastic – constant variance).

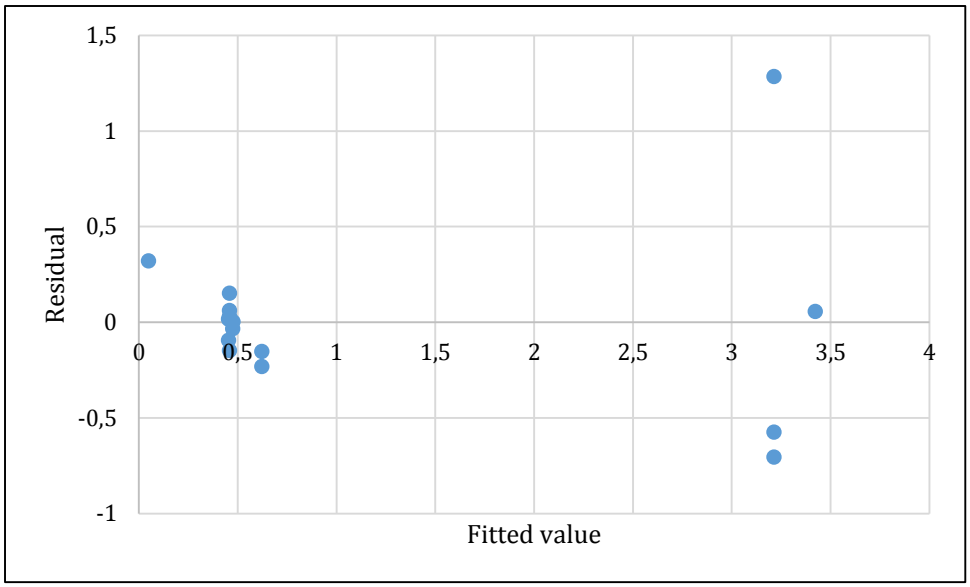

Figure 4.9: Residual plot of predicted C_s values

The Kruskal-Wallis test was carried out to deduce to which variable the reducing C_s was most sensitive. The results of the analysis are presented in Table 4.8.

Table 4.8: Kruskal-Wallis test on dataset for existing structures in the Cape Town area

Kruskal-Wallis rank sum test	C_s by distance from coastline (m)	C_s by age of structure (years)
Chi-squared	9.96	8.73
df	14	14
p-value	0.13	0.013

From Table 4.8, it can be deduced that the p values for distance and age are 0.13 and 0.013 respectively. This implies that with regard to distance the p value is greater than 0.05 and therefore H_0 holds, where H_0 is interpreted as the C_s of a RC structure in a location being sensitive to its distance from the sea but not to the time of exposure of the structure. Therefore, the availability of airborne chlorides in the atmosphere in an environment is most important in characterising its severity of exposure of an RC structure rather than its age.

4.4.2 Influence of surface orientation on chloride ingress

One of the objectives of this study, was to examine the effects of a structure's orientation to the sea (shoreline) on its airborne chloride deposition. Maio et al. (2004) suggested that chloride content of RC structures varied with height and orientation as illustrated in Figure 4.10. But Maio et al. (2004) indicated that this statement was only

valid for locations where the wind blew directly from the sea to the structures without the interference of obstacles (such as vegetation and other structures).

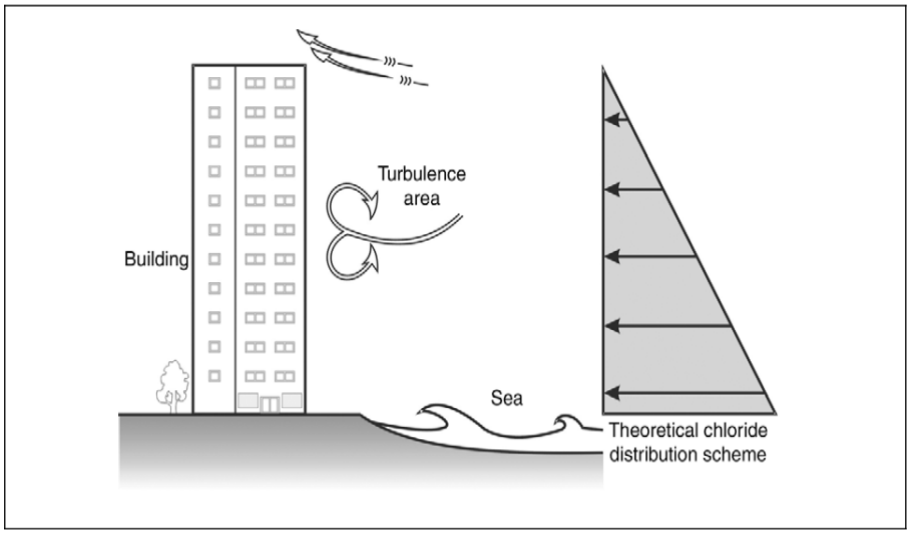

Figure 4.10: Influence of RC structure height on chloride deposition (Maio et al. 2004)

Two RC structures were examined to validate the effects of height or position of structural components on deposition rate. Figure 4.11 and Figure 4.12 illustrate the plot of surface chloride contents of bridge components with respect to their orientation. Information for other structures can be seen in Table 4.4 in the orientation column. It was not possible to evaluate the effects of height by varying the heights of core collection on the same bridge component due to time constraints. The terminologies 'sea facing' and 'non-sea facing' inferred the frontal direction of the component where core collection occurred with regard to the sea.

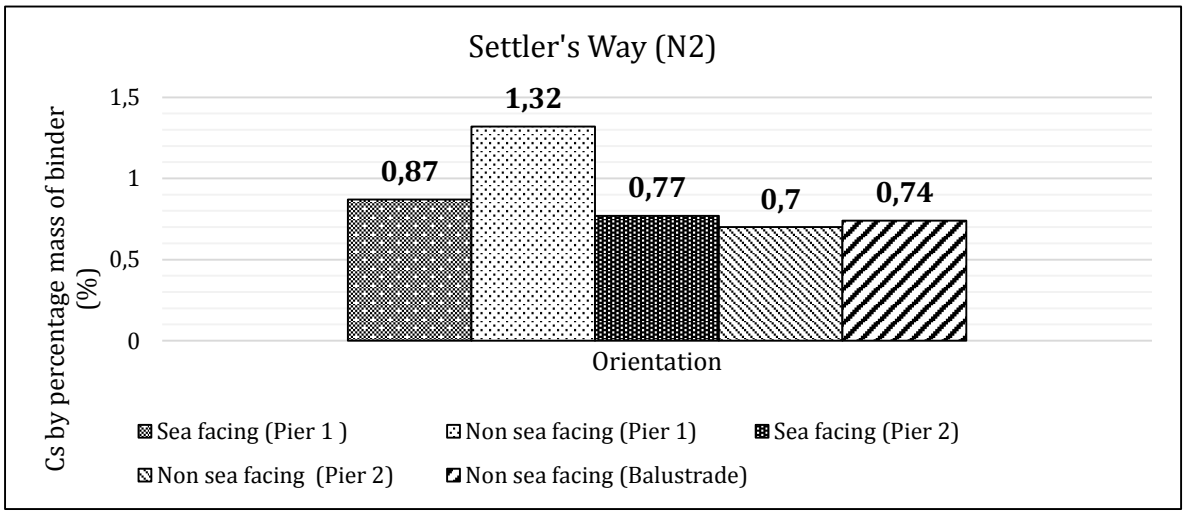

Figure 4.11: Comparison of C_s for components on Settler's Way (N2)

From Figure 4.11, a comparison of the influence of orientation to direction of the sea in Pier 1, indicated that the non-sea facing face of the pier had a higher C_s. However, this was unexpected, as the hypothesis was that the components with most severe exposure to airborne chloride deposition would be the components directly facing the sea. But

this result was found to be similar to research carried out by Medeiros *et al.*, 2013, where they observed that orientation did not have any effect on severity of exposure. It was notable that the differences in surface chloride concentrations were minimal except for the C_s value of 1.32 measured in the non-sea facing Pier.

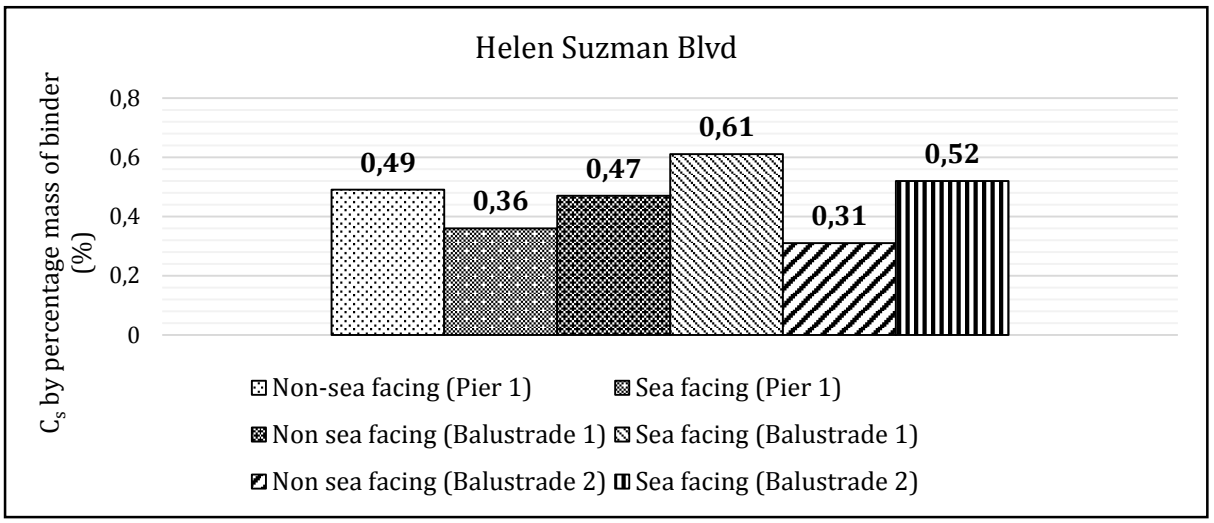

Figure 4.12: Comparison of C_s for components on Helen Suzman Boulevard

In Figure 4.12, the same scatter in data with regard to components and orientation to sea is noted. It is noteworthy that the balustrade components on the Helen Suzman Boulevard seemed to be consistent with the hypothesis. However, the overall data suggests that with RC structures closer to the coastline, the influence of orientation is negligible with respect to exposure to airborne chloride attack compared to other influences such as distance from sea, exposure to wind, precipitation and concrete quality. But to fully understand this phenomenon, further investigations are required.

4.5 CASE STUDIES FROM PREVIOUS FORENSIC INVESTIGATIONS

4.5.1 Introduction

During recent years, chloride profiling of a number of existing concrete structures exposed to airborne chloride attack have been recorded by researchers in the Concrete Materials and Structural Integrity Research Unit at UCT.

4.5.2 Influence of RC distance from sea on chloride deposition rate

The farther the distance of a RC structure from the source of airborne chlorides, the lower the expected chloride deposition rate on its surface and subsequent ingress into the structure. This is as a result of the airborne particles having certain residence time in the atmosphere which is determined by the prevailing weather conditions such as wind, temperature and RH as discussed earlier. Table 4.9 and Table 4.10 both show the ages of the structures examined, their distances from the nearest coastline and their

respective surface chloride contents for the Cape Peninsula and Namib Desert, Namibia respectively.

Table 4.9: Summary of information on RC structures previously investigated in the Cape Town area

Location of structures	**Age of structures** (years)	**Distance from coastline** (m)	**Average surface chloride content C_s** (% by mass of binder)
Miramar, 40A Victoria Road, Bantry Bay	40	50	1.57
Koeberg Power Station	34	150	0.78
Koeberg Pump Structure	34	160	1.26
Twin Towers North Block, Seapoint	40	180	0.53
Cinnabar Building, Muizenberg	40	200	3.05
Plein Street	40	1200	1.02
4 Dorp Street	40	1800	0.07
9 Dorp Street	40	1800	0.62
37 Roeland Street, Cape Town	40	1900	0.19
169 Blaauwberg Road	40	1910	1.30
Rex Trueform, 263 Victoria Road, Salt River	70	2500	0.54
27 Wale Street	40	3000	0.62
Wingfield Bridge 2 Deck Centre Span	35	4200	0.14
Wingfield Bridge 1 Deck Centre Span	35	4300	0.19
Vasco Boulevard Road over Rail SW Wingwall	35	6300	0.05
Vasco Boulevard Road over Rail S Abutment	35	6300	0.06
UCT Sports centre	44	8200	0.46
Parow West Underpass SW Wingwall	35	9000	0.04
Parow West Underpass S Abutment	35	9000	0.05
Parow North Interchange Piers	35	9100	0.16
Durban Heights WTW - New	41	11500	0.32
Karl Bremmer Intersection SW Wingwall	35	11800	0.08
Karl Bremmer Intersection NW Westwall	35	11800	0.09
Durban Heights WTW - Old	47	12000	0.35
Tygervalley Road Bridge W Abutment - Old	35	13800	0.08
Bill Bezuidenhout Underpass Side of Deck	35	14900	0.04

Table 4.10: Summary of information on RC structures previously investigated in the Namib Desert of Namibia

Location of structures	**Age of structures** (years)	**Distance from coastline** (m)	**Average Surface Chloride Content C_s** (% by mass of binder)
Namwater - Swakopmund Reservoir	40	5000	1.06
Namwater - Mile 7 Reservoir	30	14000	1.32
Namwater - High Dune Reservoir	40	15000	0.56
Namwater Reservoir Collector 1 - Rooibank	40	20000	0.54
Namwater - Schwarze Kuppe Reservoir	40	20000	0.75
Namwater Reservoir Collector 2- Rooibank	40	20300	0.60
Namwater - Rooibank Reservoir	40	25000	0.60
Namwater - Rossing 3 Reservoir	30	70000	0.31
Namwater - Rossing 1 Reservoir	40	70000	0.54
Namwater - Rossing 2 Reservoir	40	70000	0.70

From the data collated, the plot of the average surface chloride content (C_s) by percentage mass of binder to distance from coast are depicted in Figures 4.13 and 4.14. From Figure 4.13, the Cape Town area indicates that there is a significant drop in average surface chloride content C_s of the structures as distance increases from 2-14 km (2000 to 14000 m). The presence of low airborne chloride concentrations at such distances indicates that the design codes would probably have over-designed for the durability performance (against chloride-induced corrosion) for such RC structures.

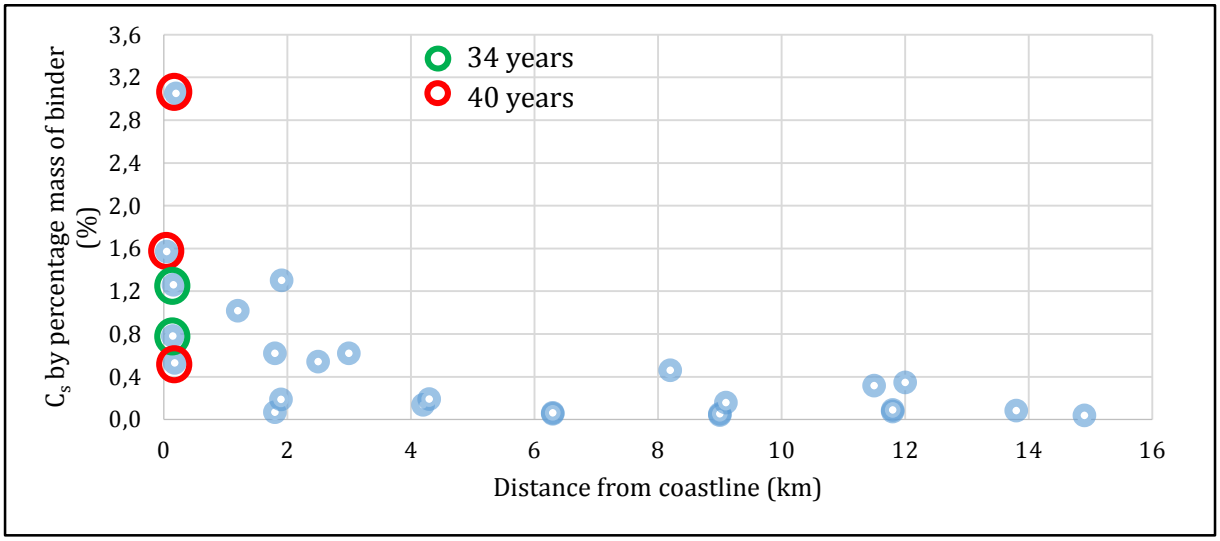

Figure 4.13: Average surface chloride content vs distance of the RC structure from the coastline in the Cape Town area

In Figure 4.14 (Namibian structures), even though the C_s decreases, it should be noted that there is still a high concentration of C_s at distances over 65 km. Du ring the survey of the structures, it was observed that fog generated at the sea was transported inland to the RC structures. Hence, it was concluded that irrespective of the RC structures distance from sea, airborne chlorides may still be transported inland through the movement of fog which is generated at the sea. Coastal fogs are credited to be frequent carriers of fine droplets of seawater generated from spray action (Mehta, 1991).

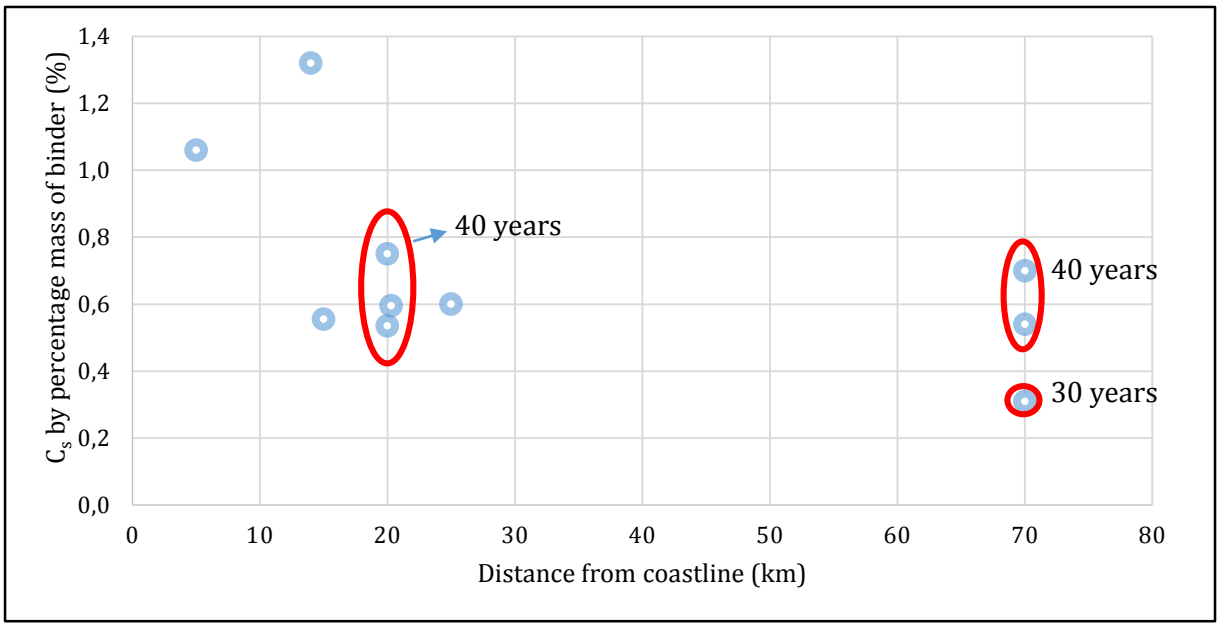

Figure 4.14: Average surface chloride content vs distance of Namib Desert RC structures from the Namibian coastline

The plot in Figure 4.14 also indicated that two RC structures at a distance of 70 km from the Namibian coast still had C_s as high as 0.3 % and 0.7 %. Also, it should be noted that when corrosion measurements were carried out using half-cell potential, the measurements indicated that there was active corrosion of the reinforcing steel in these structures. The scatter and corresponding increase in C_s observed at a distance of 70 km in the Namibian plot can be attributed to the movement of fog from the Namibian coast to the inland locations. However, it is noted from the Figures 4.13 and 4.14 that the age of the RC structures might not play an active role in the exposure severity to airborne chlorides.

4.5.3 **Regression analysis**

Similar to the methodology used in the analysis of the RC structures sampled and analysed, a multivariate analysis was carried out on the collated data. The variables considered were age of the structure and its distance from coastline in relation to its surface chloride concentration (see Table 4.11 & Table 4.12 for the statistics of the variables).

Table 4.11: Summary of statistics of variables for Cape Peninsula RC structures

	Age (years)	Distance (m)	Surface chloride concentration, C_s (%)
Minimum value	34	50	0,039
1st Quartile	35	1800	0,0795
Median	40	4300	0,32
Mean	39,07	5631	0,5451
3rd Quartile	40	9050	0,7
Maximum value	70	14900	3,05

Table 4.12: Summary of statistics of variables for Namib Desert RC structures

	Age (years)	Distance (m)	Surface chloride concentration, C_s (%)
Minimum value	30	14000	0,31
1st Quartile	40	20000	0,54
Median	40	20300	0,6
Mean	37,78	36033	0,6578
3rd Quartile	40	70000	0,7
Maximum value	40	70000	1,32

The results for the multiple regression analysis are also presented in Table 4.13 and Table 4.14.

Table 4.13: Multiple regression analysis and ANOVA of age, distance and C_s of RC structures in the Cape Peninsula

Regression Statistics					
R^2	0.34				
Adjusted R Square	0.28				
Standard Error	0.57				
Observations	26				
ANOVA					
	df	*SS*	*MS*	*F*	*Significance F*
Regression	2	3.88	1.94	5.90	0.0086
Residual	23	7.57	0.33		
Total	25	11.45			

From Table 4.13, it can be observed that the C_s is explained by age of structure and its distance from the coastline to about 34 % (0.34). However, the F-test indicates that the correlation is statistically significant since it satisfies $F > F_{critical\ (2,\ 25,\ 0.05)}$ (5.90>3.39). This implies that both of the independent variables (age or distance) have significant (non-zero) contributions to C_s.

Table 4.14: Multiple regression analysis and ANOVA of age, distance and C_s of RC structures in Namib Desert, Namibia

Regression Statistics	
R^2	0.38
Adjusted R Square	0.20
Standard Error	0.26
Observations	10

ANOVA

	df	*SS*	*MS*	*F*	*Significance F*
Regression	2	0.29	0.14	2.11	0.1920
Residual	7	0.48	0.07		
Total	9	0.76			

From Table 4.14, the coefficient of determination (R^2) for the C_s vs age and distance relationship is 0.38 for the Namib Desert water reservoir structures and an adjusted R^2 value of 0.20. It also has an F-value (2.11) which is less than the $F_{critical\ (2,\ 9,\ 0.05)}$ (4.26). This indicates that the relationship is not statistically significant and thus H_0 (both of the independent variables (age and distance) have no contributions to the C_s) is accepted. This inference supports the aforementioned suggestion that related the measured surface chloride concentrations to the influence of fog movement inland from the sea.

4.5.4 **Sensitivity analysis**

The Kruskal-Wallis test described in Chapter 3 was carried out on the variables: surface chloride content (C_s), age of RC structure and its distance from the coastline. This was to determine which of the independent variables had the most influence on the C_s. Table 4.15 presents the results of the analysis.

Table 4.15: Kruskal-Wallis test on previous Cape Town area investigations dataset

Kruskal-Wallis rank sum test	C_s by distance from coastline (m)	C_s by age of structure (years)
Chi-squared	32.2	22.8
df	28	28
p-value	0.27	0.0019

The p-values for distance from sea and age are 0.27 and 0.0019 (Table 4.15). This implies that with regard to distance the p-value is greater than 0.05 and therefore H_0 holds. This means that C_s of a RC in a location is influenced or more sensitive to its distance from the sea compared to its age. Specifically in this study, it must be noted that the relationship is inverse, as distance of RC from the coastline increases, the surface chloride concentration decreases.

The p-value for age of structure is found to be lower than 0.05, the alternative hypothesis holds. Therefore, the C_s is not particularly influenced by its age of exposure of the structure. This is expected as only when airborne chloride particles are transported inland or are present in the environment can they be deposited on structures.

4.5.5 Influence of concrete compressive strength on diffusion

This section intends to examine the influence of concrete compressive strengths measured from cores taken from the structures in relation to their resistance to permeation of chlorides. In the past, compressive strength was used not only as a basis for structural design but also incorporated as an indicator for durability (Hilsdorf, 1995). But evaluations carried out to validiate and/or verify the limitations of this approach have indicated that this method infact has a lot of shortcomings (Mehta & Burrows, 2001; Narasimhan & Chew, 2009). Therefore, an examination of available data was carried out for further understanding of concrete's compressive strength on its permeability.

Figure 4.15 indicates that there is apparently no correlation between concrete compressive strength and its corresponding permeability (apparent diffusion).

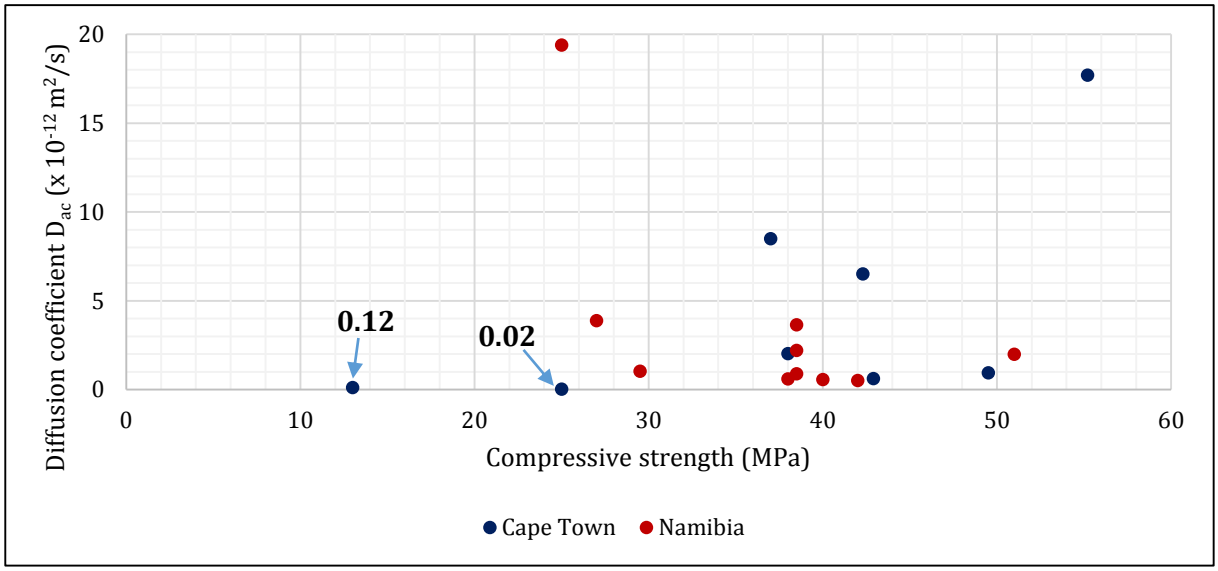

Figure 4.15: Apparent diffusion of RC structures against measured compressive strength

The apparent diffusion coefficients D_{ac} were derived from the age of the concrete structures, their surface chloride contents and chloride contents at a known depth. The compressive strength of the structures was derived from concrete cores collected and tested in the laboratory. The scatter in the plot of apparent diffusion coefficients D_{ac} with compressive strengths is an indicator.

The locations of the RC structures were illustrated using different colour schemes in the plot. Noticeably, concrete structures where relatively lower compressive strengths were

measured still showed a low D_{ac}. Hence, it is suggested that concrete material designers should deviate from the assumption that prescribing higher concrete compressive strength for RC structures exposed to ingress of deleterious species will reduce permeability and make them more durable.

The durable performance of the lower strength concretes (< 30 MPa) seen in Figure 4.15 may be attributed to the chloride binding capacity of the binder used. This implies that emphasis should be placed on binder type as opposed to compressive strength.

4.5.6 Summary of findings from previous forensic investigations

The influence of concrete strength was examined by plotting the structures apparent diffusion coefficient to its corresponding measured compressive strength. The scatter from the plot inferred that the strength of a concrete structure has no direct influence on its chloride diffusion. However, this does not mean that it is impossible to propose a relationship, nonetheless it is a complicated relationship, and hence should not be a basis for durable concrete design.

From the analysis of results carried out on the case studies, it can be deduced that airborne chlorides in the Cape Town area travel further distance inland than most reviewed literatures suggests (~ 200 m - 2 km) (Hossain & Easa, 2011; Meira *et al.*, 2010). The results of the analysis suggested that RC exposure to airborne chloride attack in the Cape marine environment might be limited to a distance of about 16 km from the coast, not up to 30 km as is generally indicated by the SANS 10100-2. RC structures beyond this distance can be classified as experiencing moderate marine exposure or no effects of marine exposure at all. This inference is however specific to the weather conditions of the Cape Town marine environment.

In Namibia, a different scenario is noted; this is attributed to the airborne chloride particles travelling inland as far as 70-75 km as a result of fog movement. This portrays the importance of location specific studies to determine severity of RC exposure.

4.6 CHAPTER SUMMARY

Wet candle: The collection and analysis of the chloride deposition rate using the wet candle technique aided in characterizing the severity of exposure in the Cape Peninsula. It was deduced that location B at a distance of 13.5 km from the nearest coastline had a relatively lower deposition rate compared to Granger Bay.

The influence of weather conditions on the transportation of airborne chlorides was also established. It was noted that during the season change which was accompanied with a change in prevailing wind direction, the deposition rate in the 5 monitored locations was either reduced or exponentially increased. For locations GB, PE, MG and B the most severe exposure season were in winter, and more specifically the month of

May. However, for Location M which is exposed to the south-easterly wind direction, a lower deposition rate was measured in winter, with the highest rate measured in the summer periods in February.

It was also discovered that with the transition from winter to autumn, the measured deposition rate decreased within the range of 72 – 80 % for all locations exposed to the north-westerly winter wind. However, location M also experienced the same decrease but the reason for the reduction is not known.

Case studies: For the RC structures examined in this study for the purposes of finding the influences of distance from coastline and orientation on airborne chloride attack. It was found that distance plays a major role in airborne chloride exposure. At distances exceeding 14 km, the influence of airborne chlorides on RC structures in the Cape Town marine environment will be minimal. In the case of effects of structural orientation on airborne chloride attack, it was found not be significant.

CHAPTER 5

5 Conclusion and recommendations

5.1 GENERAL CONCLUSIONS

The main objective of this study was to assess the severity of RC exposure to airborne chloride attack in the Cape Peninsula marine environment. Therefore, from the key research questions, the data analysed and discussed in the preceding sections, the following conclusions can be drawn:

a) The wet candle technique has been effective in providing a basis for characterization for concrete structures exposure to deposition of atmospheric chlorides in the Cape Peninsula.

b) The winter season posed the most threat in terms of airborne chloride transportation from the sea compared to other seasons. This was particularly noticeable at locations GB, PE, MG and B which were exposed to the north-westerly wind direction in winter. These locations experienced deposition rates that doubled or tripled during the winter season. However, location M which was exposed more to the south-easterly summer wind had the summer season as the most severe season of exposure to airborne chlorides. But the differences in deposition rates in summer compared to winter at M was insignificant, therefore it was concluded that the severity of exposure at M during both seasons are similar.

c) Analysis of the influence of the individual weather conditions (wind speed/direction and RH) indicated that there was no significant trend in most cases. While wind speed variations indicated lower deposition rates at GB, PE, MG and B, at location M there was increased deposition rates during seasons with higher wind speed. With regards to RH, locations GB, PE, MG and B indicated higher deposition rates at lower RH and at location M there was no visible influence of RH on the deposition rate. This motivated the use of the mixed model method of statistical analysis to simulate the combined influence of all the weather conditions on the deposition rates measured by the wet candle device.

d) Using the mixed model analysis, it was found wind speed and RH do not play significant roles in deposition rates of a locality. This was found to diverge from previous research studies but the influence of these weather conditions in the case of the Cape Peninsula with regards to airborne chlorides validated the finding. However, temperature and time were found to influence the deposition rate.

e) The examination of the susceptibility of existing RC structures in Cape Town to airborne chloride attack indicated that their distance from sea and their age of exposure played vital roles in the severity the structures experienced. At a distance of 11 km from the coastline, the measured surface chloride concentration (C_s) had considerably decreased by 82 % (from 4.5 % to 0.7 % by mass of binder) compared to the retaining wall structure that was 30 m from the sea.

f) With respect to the RC structures assessed in Namibia, it was noted that in exceptional cases, weather factors such as fog and dew could aid in the transfer of chlorides inlands to distances as far as 70 km from the coastline

g) Extensive testing to assess the effects of orientation on RC structures was not carried out. However, it was found that a RC structure's components orientation to the direction of the prevailing wind had no significant effect on the measured surface chloride concentration.

h) In addition, in this study an analysis of the influence of compressive strength on the resistance to the permeation of chlorides (apparent diffusion) into RC structures was carried out. It was found that there is no correlation between both parameters. This is because with the aid of new technologies, concrete compressive strength can be improved without corresponding improvement to the permeability resistance. Therefore it is suggested that for durability design, the use of high compressive strength as the singular criteria to define improved concrete resistance to deleterious species ingress is not acceptable.

i) From the analysis of data from previous forensic investigations, it was found that there was a significant drop in the C_s as the RC structure's distance increased from 2-14 km. This is clearly seen by the measured C_s at 14 km being 0.04 % by mass of binder while the C_s at 50 m was 1.57 % by mass of binder.

Finally, the evaluation of the Cape Peninsula marine environment using the wet candle device indicated that there is a limit to the extent of RC exposure to airborne chloride attack. Likewise, the combined analysis of data from existing structures and previous forensic investigations indicated that RC structures at the distance of 14 km from the coastline had a C_s that was 97 % less than at 50 m from the coastline (0.04 % and 1.57 % by mass of binder respectively). The reasons for the varying severity were found to be

significantly influenced by prevailing weather conditions of a location culminating as the prevailing microclimate.

5.2 PROPOSED MARINE CLASSIFICATION SCHEME FOR THE CAPE PENINSULA

It is the objective of this study to provide a refinement of the current classification scheme for RC structures exposed to airborne chlorides. Therefore, based on wet candle device investigations and the analysis of C_s data for the RC structures the Cape Peninsula location, Table 5.1 has been proposed.

Table 5.1: Classification for RC structures exposed to airborne chloride attack in the Cape Peninsula using ISO 9223

Deposition rate of chlorides ($mgCl/m^2.day$)	**Category** (ISO 9223)	**Airborne chloride exposure zones** (ISO 9223)	**Distance of RC to nearest coastline** (km)
$60 \leq S \leq 300$	**S_2**	Severe	0 – 3
$3 \leq S \leq 60$	**S_1**	Moderate	3 – 14
$S \leq 3$	**S_0**	Insignificant	> 14

The severity of the exposure zones based on the measured airborne chloride deposition rates was adapted from the ISO 9223 in Table 4.3. In this proposed classification scheme, 'very severe' exposure has not been used in categorizing any exposure zone as it has been reserved to refer to RC structures which are in direct contact with seawater only.

The derivations of the distance classes limits were based on the analysis of data on the C_s of RC structures. The distance limits were derived from Equation 4-1 in the preceding chapter. The chloride threshold level limit of 0.4 % for reinforcement corrosion was selected and based on the calculations, the ranges were selected.

5.3 RECOMMENDATIONS

Several methods exist in estimating the airborne chloride concentration and deposition rate. In this study the wet candle device, the salt spray chamber (Section 2.7.4.2) and the use of PM 10 (Section 2.7.5) concentration were discussed and reviewed. For future research, it is recommended that a study that can encompass the combined use of these methods would provide a better simulation on the effects of airborne chloride availability and consequent ingress into concrete. The wet candle device and PM10 both provide an estimation of the airborne salinity of a location. The salt spray chamber can

then be used to simulate the response or performance of concrete structures to the measured airborne salinity.

Finally, it is recommended that a continuous monitoring of a location is carried out on a long-term basis (at least 2-3 years). This is in order to ascertain the accuracy of airborne chloride measurements in the Cape Peninsula over the annual period of 1 year (December 2013 – November 2014) carried out in this study.

CHAPTER 6

6 References

Alexander, M. & Beushausen, H., 2009. Deformation and volume change of hardened concrete. In G. Owens, ed. *Fulton's Concrete Technology*. Midrand, South Africa: Cement and Concrete Institute, pp. 111 – 154.

Alhozaimy, A. et al., 2012. Coupled effect of ambient high relative humidity and varying temperature marine environment on corrosion of reinforced concrete. *Construction and Building Materials*, 28(1), pp.670–679.

Angst, U., 2011. *Chloride induced reinforcement corrosion in concrete - Concept of critical chloride content – methods and mechanisms*. Norwegian University of Science and Technology.

American Society for Testing and Materials. ASTM G-140: Standard test method for determining atmospheric chloride deposition rate by wet candle method. *Annual book of ASTM standards*. Philadelphia (USA): ASTM; 2008

American Society for Testing and Materials. ASTM C-1152: *Standard test method for Acid-Soluble Chloride in Mortar and Concrete*. *Annual book of ASTM standards*. Philadelphia (USA): ASTM; 2012

Anguelova, M.D. & Webster, F., 2006. Whitecap coverage from satellite measurements: A first step toward modelling the variability of oceanic whitecaps. *Journal of Geophysical Research: Oceans*, 111.

Ann, K.Y. & Song, H.-W., 2007. Chloride threshold level for corrosion of steel in concrete. *Corrosion Science*, 49(11), pp.4113–4133.

Anwar Hossain, K.M., Easa, S.M. & Lachemi, M., 2009. Evaluation of the effect of marine salts on urban built infrastructure. *Building and Environment*, 44(4), pp.713–722.

Arito, P., 2012. *Discrete Sacrificial External Anodes and Their Use in Service Life Extension of Chloride Contaminated Reinforced Concrete Structures*. University of Cape Town.

Ballim, Y., Alexander, M. & Beushausen, H., 2009. Durability of concrete. In G. Owens, ed. *Fulton's Concrete Technology*. Midrand, South Africa: Cement and Concrete Institute, pp. 201–236.

Bamforth, P.B., Price, W.F. & Emerson, M., 1997. *An international review of chloride ingress into structural concrete*, Riccarton, Edinburgh: Transport and Road Research Laboratory.

Banville, M.H., 2008. Assessment and repair of concrete structures. *Interface*, July(Floors and Water Vapor Invasion), pp.26–34. Available at: www.rci-online.org [Accessed June 9, 2014].

Baroghel-Bouny, V. et al., 2011. Easy assessment of durability indicators for service life prediction or quality control of concretes with high volumes of supplementary cementitious materials. *Cement and Concrete Composites*, 33(8), pp.832–847.

Basheer, P.A.M., 2001. 16 - Permeation Analysis. In V. S. Ramachandran & J. J. B. T.-H. of A. T. in C. S. and T. Beaudoin, eds. *Handbook of Analytical Techniques in Concrete Science and Technology Principles, Techniques, and Applications*. Norwich, NY: William Andrew Publishing, pp. 658–737.

Bertolini, L., Elsener, B. & Pedeferri, P., 2013. *Corrosion of steel in concrete: prevention, diagnosis, repair* 2nd ed., Weinheim: Wiley-VCH.

Brown, J., 1991. Carbonation. The effect of exposure and concrete quality: field survey results from some 400 structures J. M. Baker et al., eds. *Durability of Building Materials and Components*.

BSI, 2002. *BS 8500-1: Concrete – complementary British Standard to BS EN 206-1. Part 1: Method of specifying and guidance for the specifier*, London, UK.

Cascudo, O. & Helene, P., 2000. Influence of the steel type on the reinforcement corrosion in concrete. *Sustainable Construction into the Next Millennium: Environmentally Friendly and Innovative Cement Based Materials*, pp.635–647.

Castro, P., De Rincon, O.. & Pazini, E.., 2001. Interpretation of chloride profiles from concrete exposed to tropical marine environments. *Cement and Concrete Research*, 31(4), pp.529–537.

Castro, P., Veleva, L. & Balancan, M., 1997. Corrosion of reinforced concrete in a tropical marine environment and in accelerated tests. *Construction and Building Materials*, 11(2), pp.75–81.

CCAA, 2009. *Chloride Resistance of Concrete*, Sydney,Australia. Available at: http://www.concrete.net.au/publications/pdf/ChlorideResistance.pdf.

CCANZ, 2005. *Information bulletin : IB 83 Chloride Content of Fresh Concrete*, Wellington, New Zealand. Available at: www.cca.org.nz.

CEN, 2002. BS EN 1990:2002 - Eurocode - Basis of structural design. *Eurocode*, 1990(2002).

Chang, C.-F. & Chen, J.-W., 2006. The experimental investigation of concrete carbonation depth. *Cement and Concrete Research*, 36(9), pp.1760–1767.

Climatemps.com, 2008. *Analysis of South Africa Climate, Average Weather, Temperatures, Precipitation/ Rainfall, Sunshine hours, Daylight hours, Cloudy hours, Relative humidity, Wind speed and Frost.* [Online]

Cohen, J., Cohen, P., West, S. G., & Aiken, L. S. (2003). *Applied multiple regression/correlation analysis for the behavioural sciences, 3rd Ed*. Mahwah, NJ: Lawrence Erlbaum Associates.

Cole, I.S. et al., 2004. Holistic model for atmospheric corrosion Part 4 – Geographic information system for predicting airborne salinity. *Corrosion Engineering, Science and Technology*, 39(1), pp.89–96.

Cole, I.S. et al., 2003. Holistic model for atmospheric corrosion: Part 2 - Experimental measurement of deposition of marine salts in a number of long range studies. *Corrosion Engineering, Science and Technology*, 38(4), pp.259–266.

Cole, I.S., Lau, D. & Paterson, D. a., 2004. Holistic model for atmospheric corrosion Part 6 – From wet aerosol to salt deposit. *Corrosion Engineering, Science and Technology*, 39(3), pp.209–218.

Cole, I.S., Paterson, D.A. & Ganther, W.D., 2003. Holistic model for atmospheric corrosion Part 1 – Theoretical framework for production , transportation and deposition of marine salts. *Corrosion Engineering, Science and Technology*, 38(2), pp.129–134.

Corvo, F. et al., 2008. Outdoor–indoor corrosion of metals in tropical coastal atmospheres. *Corrosion Science*, 50(1), pp.220–230.

Costa, A. & Appleton, J., 2002. Case studies of concrete deterioration in a marine environment in Portugal. *Cement and Concrete Composites*, 24, pp.169–179.

Costa, A. & Appleton, J., 1999. Chloride penetration into concrete in marine environment—Part I: Main parameters affecting chloride penetration. *Materials and Structures*, 32(May), pp.252–259. Available at: http://link.springer.com/article/10.1007/BF02479594 [Accessed November 11, 2013].

Cowling, R., Macdonald, I. & Simmons, M., 1996. The Cape Peninsula, South Africa: physiographical, biological and historical background to an extraordinary hot-spot of biodiversity. *Biodiversity and Conservation,* Volume 5, pp. 527-550.

Crank, J. & Nicholson, P., 1947. A practical method for numerical evaluation of solutions of partial differential equations of the heat-conduction type. In Proceedings of the Cambridge Philosophical Society. 43, pp. 50–67.

Daigle, L., Lounis, Z., Cusson, D., (2004), Numerical prediction of early-age cracking and corrosion in high performance concrete bridges – Case study; *Proceedings of Annual conference of the Transportation Association of Canada Innovations in Bridge Engineering*, Québec city, Québec

Deacon, H., 2004. The Cape doctor in the nineteenth century. In H. Deacon, H. Phillips, & E. Van Heyningen, eds. *The Cape doctor in the nineteenth century: A social history*. Amsterdam - New York, NY: Rodopi, pp. 17–42.

Dhir, R.K. & Byars, E. a., 1993. PFA concrete: chloride diffusion rates. *Magazine of Concrete Research*, 45(162), pp.1–9.

EN206-1, 2000. *NS-EN 206-1: Concrete, Part 1: Specification, performance, production and conformity*, Brussels.

Encyclopædia Britannica Online, 2014. Cape doctor (wind system) -- Britannica Online Encyclopedia.

Fagerlund, G., 1985. Essential data for service life prediction Larrry W. Masters, ed. *Problems in Service Life Predicition of Building and Construction Materials*, Series E(No. 95), pp.113 – 138.

Fairall, C., Davidson, K. & Schacher, G., 1983. An analysis of the surface production of sea-salt aerosols. *Tellus B*, 35B(1983), pp.31–39.

Finlayson-Pitts, B.J. & Hemminger, J.C., 2000. Physical Chemistry of Airborne Sea Salt Particles and Their Components. *The Journal of Physical Chemistry A*, 104(49), pp.11463–11477.

Gao, Y., Chen, S.B. & Yu, L.E., 2007. Efflorescence relative humidity of airborne sodium chloride particles: A theoretical investigation. *Atmospheric Environment*, 41(9), pp.2019–2023.

Glass, G.K. & Buenfeld, N.R., 2000. Chloride-induced corrosion of steel. *Progress in Structural Engineering and Materials.*, 2(4), pp.448–458.

Gong, S., Barrie, L. & Blanchet, J., 1997. Modeling sea-salt aerosols in the atmosphere: 1. Model development. *Journal of Geophysical …*, 102, pp.3805–3818.

Grace, W.R., 2006. *Chloride Ion Contribution of Admixtures to Concrete*, Cambridge, Canada.

Gribble, J., 2006. Pre-Colonial Fish Traps On the South Western Cape Coast, South Africa. *Underwater Cultural Heritage ar Risk*, pp.29–31.

Grieve, G., 2009. Cementitious Materials. In G. Owens, ed. *Fulton's Concrete Technology*. Midrand, South Africa: Cement and Concrete Institute, pp. 1–14.

Gustafsson, M. & Franzén, L., 1996. Dry deposition and concentration of marine aerosols in a coastal area, SW Sweden. *Atmospheric Environment*, 30(6), pp.977–989.

Harkel, M.J.T., 1997. The effects of particle-size distribution and chloride depletion of sea-salt aerosols on estimating atmospheric deposition at a coastal site. *Atmospheric Environment*, 31(3), pp.417–427.

El Hassan, J. et al., 2010. Reliability-based assessment of the effect of climatic conditions on the corrosion of RC structures subject to chloride ingress. *Engineering Structures*, 32(10), pp.3279–3287.

HDGASA, 2005. Corrosion Resistance of Hot Dip Galvanized Coatings. In *STEEL PROTECTION BY HOT DIP GALVANIZING AND DUPLEX COATING SYSTEMS*. Bedfordview, Johannesburg: Hot Dip Galvanizers Association Southern Africa, pp. 39–45. Available at: www.hdgasa.org.za/steelProG/c/corrResistance.pdf?

Hilsdorf, H., 1995. Concrete compressive strength. transport characteristics and durability. In H. Hilsdorf & J. Kropp, eds. *Performance criteria for concrete durability*. London, UK: CRC Press, pp. 165–195.

Hossain, K.M.A. & Easa, S.M., 2011. Spatial distribution of marine salts in coastal region. *International Journal of Research and Reviews in Applied Sciences*, 7(3), pp.228–235.

Huet, B. et al., 2005. Electrochemical behavior of mild steel in concrete: Influence of pH and carbonate content of concrete pore solution. *Electrochimica Acta*, 51(1), pp.172–180.

International Organization for Standardization. 1992. *Corrosion of metals and alloys - Corrosivity of atmospheres – Classification*. (ISO 9223:1992). Geneva, Switzerland: International Organization for Standardization.

IPCC, 2007. *Climate Change 2007 : An Assessment of the Intergovernmental Panel on Climate Change*, Valencia, Spain.

Jones, A.M., Harrison, R.M. & Baker, J., 2010. The wind speed dependence of the concentrations of airborne particulate matter and NOx. *Atmospheric Environment*, 44(13), pp.1682–1690.

JSCE, 2010. *Standard specifications for concrete structures - 2007 "Design,"* Tokyo, Japan.

Justnes, H., 1998. A review of chloride binding in cementitious systems. *Nordic Concrete Research-Publications*, pp.1–16.

Kelly, D., 2007. BRE, Design life of buildings—a scoping study. *Scottish Building Standards Agency, Glasgow*, (January), p.37.

Kessy, J., Alexander, M. & Beushausen, H., 2013. *Durability specifications for structural concrete – an International Comparison*. University of Cape Town. Available at: http://uctscholar.uct.ac.za/PDF/102615_Kessy_J.pdf.

Khatri, R.. & Sirivivatnanon, V., 2004. Characteristic service life for concrete exposed to marine environments. *Cement and Concrete Research*, 34(5), pp.745–752.

König, O. & Kaufmann, J., 2012. *Weather statistics map - South Africa.* [Online] Available at: www.windfinder.com

Lee, J.-S. & Moon, H.-Y., 2006. Salinity distribution of seashore concrete structures in Korea. *Building and Environment*, 41(10), pp.1447–1453.

Lindvall, A., 2007. Chloride ingress data from field and laboratory exposure – Influence of salinity and temperature. *Cement and Concrete Composites*, 29(2), pp.88–93.

Lothenbach, B., Scrivener, K. & Hooton, R.D., 2011. Supplementary cementitious materials. *Cement and Concrete Research*, 41(12), pp.1244–1256.

Lovett, R., 1978. Quantitative measurement of airborne sea-salt in the North Atlantic. *Tellus*, 30, pp.358–364.

Mackechnie, J.R., 1995. *Prediction of Reinforced Concrete Durability in the Marine Environment*. PhD Thesis, University of Cape Town.

Maio, A. Di, Lima, L. & Traversa, L., 2004. Chloride profiles and diffusion coefficients in structures located in marine environments. *Structural concrete*, 1(5), pp 1464-1469.

Maldonado, L., Pech-Canul, M.A. & Alhassan, S., 2006. Corrosion of zinc-coated reinforcing bars in tropical humid marine environments. *Anti-Corrosion Methods …*, 53(6), pp.357–361.

Martínez, I. & Andrade, C., 2009. Examples of reinforcement corrosion monitoring by embedded sensors in concrete structures. *Cement and Concrete Composites*, 31(8), pp.545–554.

Matthew, D. et al., 2006. Relative Humidity in Concrete. *Concrete International*, 28(October), pp.51–58.

Medeiros, M.H.F. et al., 2013. Reinforced concrete in marine environment: Effect of wetting and drying cycles, height and positioning in relation to the sea shore. *Construction and Building Materials*, 44, pp.452–457.

Mehta, P.K., 1991. *Concrete in the marine environment* A. Bentur & S. Mindes, eds., Essex, England: Elsevier Science Publishers Ltd.

Meira, G.R. et al., 2014. Analysis of chloride threshold from laboratory and field experiments in marine atmosphere zone. *Construction and Building Materials*, 55, pp.289–298.

Meira, G.R. et al., 2010. Durability of concrete structures in marine atmosphere zones – The use of chloride deposition rate on the wet candle as an environmental indicator. *Cement and Concrete Composites*, 32(6), pp.427–435.

Meira, G.R., Andrade, C., Alonso, C., et al., 2007a Salinity of marine aerosols in a Brazilian coastal area—Influence of wind regime. *Atmospheric Environment*, 41(38), pp.8431–8441.

Meira, G.R., Andrade, C., Padaratz, I.J., et al., 2007b. Chloride penetration into concrete structures in the marine atmosphere zone – Relationship between deposition of chlorides on the wet candle and chlorides accumulated into concrete. *Cement and Concrete Composites*, 29(9), pp.667–676.

Meira, G.R. et al., 2003. Effect of distance from sea on chloride aggressiveness in concrete structures in brazilian coastal site. *Materiales de Construcción*, 53(271-272), pp.179 – 189.

Monahan, E.., Spiel, D.. & Davidson, K.., 1986. A model of marine aerosol generation via whitecaps and wave disruption. In E. . Monahan & G. Mac Niocaill, eds. *Oceanographic Whitecaps*. Dordrecht; Boston; Hingham, MA, U.S.A.: D. Reidel Pub. Co. ; Sold and distributed in the U.S.A. and Canada by Kluwer Academic Publishers, pp. 167–174.

Morcillo, M. et al., 2000. Salinity in marine atmospheric corrosion: its dependence on the wind regime existing in the site. *Corrosion Science*, 42(1), pp.91–104

Moreda-Piñeiro, J. et al., 2014. Influence of marine, terrestrial and anthropogenic sources on ionic and metallic composition of rainwater at a suburban site (northwest coast of Spain). *Atmospheric Environment*, 88, pp.30–38.

Morinaga, S., 1990. Prediction of service life of reinforced concrete buildings based on the corrosion rate of reinforcing steel. In J. M. Baker et al., eds. *Durability of Building Materials and Components: Proceedings of the Fifth International Conference*. Brighton, UK: Spon Press, pp. 5–17.

Muster, T.H. & Cole, I.S., 2005. Attachment Efficiencies of Salt Aerosols onto Infrastructure and Implications for Atmospheric Corrosion. *Journal of The Electrochemical Society*, 152(3), p.B125.

Mustafa, M.A. & Yusof, K.M., 1994. Atmospheric chloride penetration into concrete in semitropical marine environment. *Cement and Concrete Research*, 24(4), pp.661–670.

Muthulingam, S. & Rao, B.N., 2014. Non-uniform time-to-corrosion initiation in steel reinforced concrete under chloride environment. *Corrosion Science*, 82, pp.304–315.

Naik, T., 2008. Sustainability of Concrete Construction. *Practice Periodical on Structural Design and Construction*, 13(2), pp.98–103.

Narasimhan, H. & Chew, M.Y.L., 2009. Integration of durability with structural design: An optimal life cycle cost based design procedure for reinforced concrete structures. *Construction and Building Materials*, 23(2), pp.918–929.

Nganga, G., Alexander, M. & Beushausen, H., 2013. Practical implementation of the durability index performance-based design approach. Construction and Building Materials, 45, pp.251–261

Niyogi, D. et al., 2004. Direct observations of the effects of aerosol loading on net ecosystem CO2 exchanges over different landscapes. *Geophysical Research Letters*, 31(20), p.5.

Otieno, M., 2008. *Corrosion Propagation in Cracked and Uncracked Concrete*. University of Cape Town.

Otieno, M., Beushausen, H. & Alexander, M., 2014. Effect of chemical composition of slag on chloride penetration resistance of concrete. *Cement and Concrete Composites*, 46, pp.56–64.

Page, C.L., Short, N.R. & El Tarras, A., 1981. Diffusion of chloride ions in hardened cement pastes. *Cement and Concrete Research*, 11(3), pp.395–406.

Papadakis, V.G., Fardis, M.N. & Vayenas, C.G., 1990. Fundamental concrete carbonation model and application to durability of reinforced concrete. In J. Baker et al., eds. *Durability of Building Materials and Components: Proceedings of the Fifth International Conference*. Brighton, UK: Spon Press, pp. 27–38.

Papakonstantinou, K.G. & Shinozuka, M., 2013. Probabilistic model for steel corrosion in reinforced concrete structures of large dimensions considering crack effects. *Engineering Structures*, 57, pp.306–326.

Peter, K., 2008. Criteria for estimators. In *A guide to econometrics*. Cambridge, Massachussets: The MIT Press, pp. 10–33.

Pey, J., Querol, X. & Alastuey, A., 2009. Variations of levels and composition of PM10 and PM2.5 at an insular site in the Western Mediterranean. *Atmospheric Research*, 94(2), pp.285–299.

Pey, J. et al., 2010. A simplified approach to the indirect evaluation of the chemical composition of atmospheric aerosols from PM mass concentrations. *Atmospheric Environment,* Volume 44, pp. 5112-5121.

Pillai, S.U. & Devadas, M., 2003. Design of Beams and One-Way Slabs for Flexure. In Reinforced Concrete Design. Delhi: Tata McGraw-Hill Education, pp. 169–223.

Powers, T.C., 1958. Structure and physical properties of hardened Portland cement paste. *Journal of the American Ceramic Society*, 41(1), pp.1–6.

Ralfe, M., 2013. *Environmental Exposure Zones for the Cape Peninsula*. Undergraduuate Thesis, University of Cape Town (*unpublished*).

Reggie, 2009. Green Point Stadium. *Grains of Sand*, p.1. Available at: http://namibsands.wordpress.com/2009/07/01/green-point-stadium/ [Accessed June 27, 2014].

Roberge, P.R., 2011. Atmospheric corrosion. In W. R. Revie, ed. *Uhlig's Corrosion Handbook*. John Wiley & Sons, Ltd, pp. 299 – 326.

Ryan, P.. & Branch, G.., 2012. The November 2011 irruption of buoy barnacles Dosima fascicularis in the Western Cape, South Africa. *African Journal of Marine Science*, 34(1), pp.157–162.

Safehian, M. & Ramezanianpour, A.A., 2013. Assessment of service life models for determination of chloride penetration into silica fume concrete in the severe marine environmental condition. *Construction and Building Materials*, 48, pp.287–294.

Sandberg, P., 1999. Studies of chloride binding in concrete exposed in a marine environment. *Cement and Concrete Research*, 29, pp.473–477.

SANRAL, 2013. *The South African National Roads Agency SOC Limited - ANNUAL REPORT 2013*, Pretoria. Available at: http://sanral.ensight-cdn.com/content/Sanral_Annual_Report_13_LRES.pdf.

SANS, 2009. SANS 10100-2 : South African National Standards. 2009. *The structural use of concrete Part 2* : *Materials and execution of work*. (SANS 10100-2:2009). Pretoria, South Africa: SABS standards (*unpublished*).

Science Education Resource Centre at Carlton College (SERC). 2012. *A Primer on Stable Isotopes and Some Common Uses in Hydrology.* [Online].

Seltman, H.J., 2014. Mixed Models. In *Experimental Design and Analysis*. Pittsburgh, USA: Carnegie Mellon University, pp. 357–378. Available at: http://www.stat.cmu.edu/~hseltman/309/Book/Book.pdf [Accessed November 13, 2014].

Song, H.-W., Lee, C.-H. & Ann, K.Y., 2008. Factors influencing chloride transport in concrete structures exposed to marine environments. *Cement and Concrete Composites*, 30(2), pp.113–121.

Soshiroda, T. & Voraputhaporn, K., 1999. Recommended method for earlier inspection of concrete quality by nondestrcutive testing. In R. K. Dhir & M. J. McCarthy, eds. *Proc. Int. Conf. Concrete Durability and Repair Technology, Dundee*. Cornwall, Great Britain: Thomas Telford, pp. 259–264.

South African National Standards. 2007. *Corrosion tests in artificial atmospheres — Salt spray tests*, *Metallic and other inorganic coatings – Electroplated coatings.* (SANS 9227:2007). Pretoria, South Africa: SABS standards

Stanish, K., Hooton, R. & Thomas, M., 2000. *Testing the chloride penetration resistance of concrete: a literature review*, Toronto, Ontario, Canada.

Statistics South Africa (StatsSA), 2014. Gross Domestic Product - Third quarter 2013. Statistical release P0441, 3(February), p.75.

Strekalov, P. V & Panchenko, Y.M., 1994. The Role of Marine Aerosols in Atmospheric Corrosion of Metals. *Protection of Metals*, 30, pp.254–263.

Tanaka, Y. et al., 2006. Study on Cover Depth for Prestressed Concrete Bridges in Airborne-Chloride Environments. *PCI journal*. Available at: http://cat.inist.fr/?aModele=afficheN&cpsidt=17558520 [Accessed March 27, 2014].

Tang, Y. & Guo, B., 2011. Computational fluid dynamics simulation of aerosol transport and deposition. *Frontiers of Environmental Science & Engineering in China*, 5(3), pp.362–377.

Thomas, M.D.. & Matthews, J.., 2004. Performance of pfa concrete in a marine environment––10-year results. *Cement and Concrete Composites*, 26(1), pp.5–20.

Tinley, K.L., 1985. *Coastal dunes of South Africa*, Pretoria, South Africa: National Scientific Programmes Unit: CSIR. Available at: http://hdl.handle.net/10204/2353.

Trocónis de Rincón, O. et al., 2007. Effect of the marine environment on reinforced concrete durability in Iberoamerican countries: DURACON project/CYTED. *Corrosion Science*, 49(7), pp.2832–2843.

Tuutti, K., 1982. *Corrosion of steel in concrete*. Swedish Cement and Concrete Research Institute, Royal Institute of Technology, Stockholm.

Uysal, M., Yilmaz, K. & Ipek, M., 2012. The effect of mineral admixtures on mechanical properties, chloride ion permeability and impermeability of self-compacting concrete. *Construction and Building Materials*, 27(1), pp.263–270.

Weather2 Ltd., 2012. *Cape Town Climate History.* [Online] Available at: www.myweather2.com/City-Town/South-Africa/Cape-Town/climate-profile [Accessed 1 11 2012].

Weather2 Ltd., 2014. *Chittagong Climate History.* [Online] Available at: www.myweather2.com/City-Town/Bangladesh/Chittagong/climate-profile [Accessed 03 12 2014].

Weather Underground Ltd., 2014. *Cape Town, WESTERN CAPE [IWESTERN142].* [Online] Available at: www.wunderground.com/personal-weather-station/dashboard?ID=IWESTERN142#history/s20131020/e20141130/myear [Accessed 30 11 2014].

Wilmot, R., 2006. Corrosion protection of reinforcement for concrete structures. *The Journal of The Southern African Institute of Mining and Metallurgy*, 107(MARCH), pp.139–146.

Winter, B., 2013. *A very basic tutorial for performing linear mixed effects analyses (Tutorial 2)*, California, US. Available at: http://arxiv.org/abs/1308.5499 [Accessed July 9, 2014].

Winter, B. & Chýlek, P., 1997. Contribution of sea salt aerosol to the planetary clear-sky albedo. *Tellus, Series B: Chemical and Physical Meteorology*, 49(1), pp.72–79.

Woodcock, D.C. & Blanchard, A.H., 1980. The production, concentration, and vertical distribution of the sea-salt aerosol. *Annals of the New York Academy of Sciences*, 338, pp.330–347.

World Weather Online, 2012. *South African Weathe Averages.* [Online] Available at: http://www.worldweatheronline.com [Accessed 20 10 2012].

Ye, H. et al., 2013. Influence of cracking on chloride diffusivity and moisture influential depth in concrete subjected to simulated environmental conditions. *Construction and Building Materials*, 47, pp.66–79.

Yildirim, H., Ilica, T. & Sengul, O., 2011. Effect of cement type on the resistance of concrete against chloride penetration. *Construction and Building Materials*, 25(3), pp.1282–1288.

APPENDIX A – Data from previous forensic investigations

Table A.1: Case study data from the Cape Peninsula and Namib Desert, Namibia

Locations	**Country/ Region located**	**Estimated age of structure** (years)	**Distance from coastline** (m) **	**Concrete compressive strength** (MPa)	**Range of cover to Steel** (mm)	**Estimated cement content** (kg/m^3)	**Year of testing**	**Surface chloride content C_s** (% by mass of cement)	**Depth X for diffusion coefficient calculation** (mm)	**Chloride content at X depth** (% by mass of cement)	**Apparent diffusion coefficient D_{ac}** (mm^2/year)	**Apparent diffusion coefficient D_{ac}** (X 10^{-12} m^2/s)
Miramar, 40A Victoria Road, Bantry Bay	Cape Town, South Africa	40	50	NM	10 – 55	280	2011	1.57	40	1.28	113	3.57
Koeberg Power Station	Cape Town, South Africa	34	150	NM	NM	400	2013	0.78	45	0.58	198	6.29
Koeberg Pump Structure	Cape Town, South Africa	34	160	NM	NM	300	2006	1.26	70	0.48	51	1.61
Twin Towers North Block, Seapoint	Cape Town, South Africa	40	180	NM	NM	300	2012	0.53	35	0.44	282	8.95
Cinnabar Building, Muizenberg	Cape Town, South Africa	40	200	25	25	300	2005	3.05	25	0.73	1	0.023
Plein Street	Cape Town, South Africa	40	1200	13	NM	300	2009	1.02	15	0.50	4	0.12

Locations	**Country/ Region located**	**Estimated age of structure** (years)	**Distance from coastline** (m) **	**Concrete compressive strength** (MPa)	**Range of cover to Steel** (mm)	**Estimated cement content** (kg/m^3)	**Year of testing**	**Surface chloride content C_s** (% by mass of cement)	**Depth X for diffusion coefficient calculation** (mm)	**Chloride content at X depth** (% by mass of cement)	**Apparent diffusion coefficient D_{ac}** (mm^2/year)	**Apparent diffusion coefficient D_{ac}** (X 10^{-12} m^2/s)
4 Dorp Street	Cape Town, South Africa	40	1800	NM	30	300	2009	0.07	27.5	0.06	353	11.18
9 Dorp Street	Cape Town, South Africa	40	1800	49.5	10 – 70	300	2013	0.62	30	0.35	30	0.94
37 Roeland Street, Cape Town	Cape Town, South Africa	40	1900	NM	12 – 45	NA	2010	0.19	15	0.17	127	4.02
169 Blaauwberg Road	Cape Town, South Africa	40	1910	NM	22 – 40	300	2008	1.30	35	1.51	151	4.80
Rex Trueform, 263 Victoria Road, Salt River	Cape Town, South Africa	70	2500	NM	15 – 28	300	2012	0.54	30	0.39	44	1.40
27 Wale Street	Cape Town, South Africa	40	3000	42.9	NM	350	2013	0.62	40	0.17	19	0.61

Locations	**Country/ Region located**	**Estimated age of structure** (years)	**Distance from coastline** (m) **	**Concrete compressive strength** (MPa)	**Range of cover to Steel** (mm)	**Estimated cement content** (kg/m^3)	**Year of testing**	**Surface chloride content** C_s (% by mass of cement)	**Depth X for diffusion coefficient calculation** (mm)	**Chloride content at X depth** (% by mass of cement)	**Apparent diffusion coefficient** D_{ac} (mm^2/year)	**Apparent diffusion coefficient** D_{ac} (X 10^{-12} m^2/s)
UCT Sports centre	Cape Town, South Africa	44	8200	NM	NM	300	2012	0.46	15	0.52	83	2.64
Durban Heights WTW – New	Durban, South Africa	41	11500	42.3	50 – 80	350	2013	0.32	35	0.38	205	6.51
Durban Heights WTW – Old	Durban, South Africa	47	12000	55.2	23 – 80	350	2013	0.35	45	0.29	558	17.70
Wingfield Bridge 2 Deck Centre Span	Cape Town, South Africa	35	4200	38	NM	320	1996	0.136	60	0.039	64	2.01
Wingfield Bridge 1 Deck Centre Span	Cape Town, South Africa	35	4300	37	NM	320	1996	0.191	60	0.125	268	8.48
Vasco Boulevard Road over Rail SW Wingwall	Cape Town, South Africa	35	6300	NM	NM	NA	1996	0.052	60	0.029	167	5.30

Locations	**Country/ Region located**	**Estimated age of structure** (years)	**Distance from coastline** (m) **	**Concrete compressive strength** (MPa)	**Range of cover to Steel** (mm)	**Estimated cement content** (kg/m^3)	**Year of testing**	**Surface chloride content C_s** (% by mass of cement)	**Depth X for diffusion coefficient calculation** (mm)	**Chloride content at X depth** (% by mass of cement)	**Apparent diffusion coefficient D_{ac}** (mm^2/year)	**Apparent diffusion coefficient D_{ac}** (X 10^{-12} m^2/s)
Vasco Boulevard Road over Rail S Abutment	Cape Town, South Africa	35	6300	NM	NM	NA	1996	0.062	60	0.031	131	4.14
Parow West Underpass SW Wingwall	Cape Town, South Africa	35	9000	NM	NM	NA	1996	0.04	60	0.021	145	4.60
Parow West Underpass S Abutment	Cape Town, South Africa	35	9000	NM	NM	NA	1996	0.053	60	0.029	159	5.05
Parow North Interchange Piers	Cape Town, South Africa	35	9100	NM	NM	NA	1996	0.158	60	0.058	80	2.55
Karl Bremmer Intersection SW Wingwall	Cape Town, South Africa	35	11800	NM	NM	NA	1996	0.075	60	0.039	142	4.49
Karl Bremmer Intersection NW Westwall	Cape Town, South Africa	35	11800	NM	NM	NA	1996	0.088	60	0.039	105	3.33

Locations	**Country/ Region located**	**Estimated age of structure** (years)	**Distance from coastline** (m) **	**Concrete compressive strength** (MPa)	**Range of cover to Steel** (mm)	**Estimated cement content** (kg/m^3)	**Year of testing**	**Surface chloride content** C_s (% by mass of cement)	**Depth X for diffusion coefficient calculation** (mm)	**Chloride content at X depth** (% by mass of cement)	**Apparent diffusion coefficient** D_{ac} (mm^2/year)	**Apparent diffusion coefficient** D_{ac} ($X\ 10^{-12}$ m^2/s)
Tygervalley Road Bridge W Abutment – Old	Cape Town, South Africa	35	13800	NM	NM	NA	1996	0.084	60	0.04	119	3.76
Bill Bezuidenhout Underpass Side of Deck	Cape Town, South Africa	35	14900	NM	NM	NA	1996	0.039	60	0.028	411	13.03
Namwater – Swakopmund Reservoir	Namib Desert, Namibia	40	5000	38	31 – 91	NA	2011	1.06	15	0.82	19	0.60
Namwater – Mile 7 Reservoir	Namib Desert, Namibia	30	14000	38.5	33 – 84	NA	2011	1.32	15	1.08	28	0.89
Namwater – High Dune Reservoir	Namib Desert, Namibia	40	15000	51	23 – 53	NA	2011	0.56	15	0.47	63	1.99
Namwater Reservoir Collector 1 – Rooibank	Namib Desert, Namibia	40	20000	29.5	12 – 56	-	2011	0.54	15	0.42	32	1.02
Namwater – Schwarze Kuppe Reservoir	Namib Desert, Namibia	40	20000	38.5	43 – 81	-	2011	0.75	15	0.83	115	3.65

Locations	**Country/ Region located**	**Estimated age of structure** (years)	**Distance from coastline** (m) **	**Concrete compressive strength** (MPa)	**Range of cover to Steel** (mm)	**Estimated cement content** (kg/m^3)	**Year of testing**	**Surface chloride content** C_s (% by mass of cement)	**Depth X for diffusion coefficient calculation** (mm)	**Chloride content at X depth** (% by mass of cement)	**Apparent diffusion coefficient** D_{ac} (mm^2/year)	**Apparent diffusion coefficient** D_{ac} (X 10^{-12} m^2/s)
Namwater Reservoir Collector 2-Rooibank	Namib Desert, Namibia	40	20300	40	29 – 61	-	2011	0.60	15	0.43	18	0.56
Namwater – Rooibank Reservoir	Namib Desert, Namibia	40	25000	38.5	10 – 42	-	2011	0.60	15	0.51	70	2.21
Namwater – Rossing 3 Reservoir	Namib Desert, Namibia	30	70000	27	28 – 99	-	2011	0.31	25	0.38	122	3.87
Namwater – Rossing 1 Reservoir	Namib Desert, Namibia	40	70000	42	12 – 120	-	2011	0.54	15	0.38	16	0.51
Namwater – Rossing 2 Reservoir	Namib Desert, Namibia	40	70000	25	24 – 107	-	2011	0.70	15	0.67	612	19.39

NM – not measured
NA – not available
** Distance measured using Google Earth (2013) from RC to nearest coastline

Table A.2: Statistics of variables data

	Age (years)	Distance (m)	Surface chloride concentration, C_s (%)
Minimum value	34	50	0,039
1st Quartile	35	1800	0,0795
Median	40	4300	0,32
Mean	39,07	5631	0,5451
3rd Quartile	40	9050	0,7
Maximum value	70	14900	3,05

APPENDIX B – Wet candle device

Table B.1: Measured Chloride content on wet candle

MONTHS	**Period of sample collection**	**Granger Bay** (GB)	**Muizenberg** (M)	**Paarden Eiland** (PE)	**Montague Gardens** (MG)	**Bellville** (B)
	Chloride content ($mgCl^-/g$) – milligram per gram of solution					
Dec 2013 - Jan 2014	After 6 weeks	0.361	0.331	0.264	0.015	0.005
Feb-14	1st 2 weeks	0.634	0.504	0.494	ND	ND
	2nd 2 weeks	0.424	0.43	0.258	ND	ND
	Total - 4 weeks					
Mar-14	1st 2 weeks	0.369	0.335	0.283	ND	ND
	2nd 2 weeks	0.498	0.298	0.316	0.269	0.271
	Total - 4 weeks					
Apr-14	1st 2 weeks	0.310	0.364	0.278	ND	ND
	2nd 2 weeks	0.370	0.420	0.267	0.236	0.261
	Total - 4 weeks					
May-14	Total - 4 weeks	9.276	0.736	1.087	0.539	0.512
Jun-14	1st 2 weeks	2.905	0.205	0.489	0.351	0.299
	2nd 2 weeks	3.178	0.412	0.535	0.175	0.182
	Total - 4 weeks					
Jul-14	Total - 4 weeks	3.17	0.59	0.966	0.321	0.258
Aug-14	Total - 4 weeks	0.675	0.12	0.237	0.061	0.071
Sep-14	Total - 4 weeks	0.435	0.160	0.148	0.049	0.045
Oct-14	Total - 4 weeks	0.38	0.16	0.07	0.04	0.04
Nov-14	Total - 4 weeks	0.45	0.15	0.09	0.06	0.05

ND – no deposition

Formula for calculating deposition rate:

$$\text{Deposition rate } (mgCl/m^2.\ day) = \text{Chloride content } (mgCl^-/g)/\ 2A \times t \qquad (1)$$

Where:

t = time of exposure, days

A = exposed area of gauze, calculated as follows

$$A = \pi D\ (D + L) \qquad (2)$$

Where:

A = exposed area, m^2.

D = test tube diameter, m,

L = test tube length exposed, m.

Table B.2: Average properties of wet candle during monitoring

Height of exposed tube (m)	10.5×10^{-2}
Diameter (m)	15×10^{-3}
Area of Test Tube (m^2)	56.7×10^{-4}

Table B.3: Calculated Chloride Deposition Rate

LOCATIONS	**Granger Bay (GB)**	**Muizenberg (M)**	**Paarden Eiland (PE)**	**Montague Gardens (MG)**	**Bellville (B)**
MONTHS	**Deposition rate ($mgCl.m^{-2}.d^{-1}$)**				
Dec 13 - Jan 14	2.13	1.95	1.56	0.09	0.03
Feb-14	6.24	5.50	4.43	0.00	0.00
Mar-14	5.11	3.73	3.53	1.59	1.60
Apr-14	4.01	4.62	3.21	1.39	1.54
May-14	54.67	4.34	6.41	3.18	3.02
Jun-14	35.85	3.64	6.04	3.10	2.83
Jul-14	18.68	3.48	5.69	1.89	1.52
Aug-14	3.98	0.71	1.40	0.36	0.42
Sep-14	2.56	0.94	0.87	0.29	0.27
Oct-14	2.21	0.93	0.44	0.26	0.26
Nov-14	2.62	0.87	0.51	0.35	0.28
TOTAL	138.1	30.7	34.1	12.5	11.8

APPENDIX C – Existing RC structures sampled and analysed in this study

Table C.1: Details of RC structures examined

Location of Structures (latitude, longitude)	**Structural component cored**	** **Distance from sea** (m)	**Estimated age of structure** (years)	**Concrete compressive strength** (MPa)	**Range of cover to Steel** (mm) using covermeter	**Year of testing**	**Surface Chloride Content C_s** (% by mass of cement)	**Depth X for diffusion coefficient calculation** (mm)	**Chloride content at X depth** (%by mass of cement)	**Apparent diffusion coefficient D_{ac}** (X 10^{-12} m^2/s)
Glencairn, Simons Town (-34.168832, 18.430511)	**Retaining Wall**	50	50	NM	10 - 80	**2014**	2.51	45	2.34	11.10
Glencairn, Simons Town (-34.168832, 18.430511)	**Retaining Wall**	50	50	NM	10 - 80	**2014**	2.64	45	2.77	18.99
Glencairn, Simons Town (-34.168832, 18.430511)	**Retaining Wall**	30	50	NM	10 - 80	**2014**	3.48	65	3.58	66.97
Glencairn, Simons Town (-34.168832, 18.430511)	**Retaining Wall**	50	50	NM	10 - 80	**2014**	4.50	75	3.37	0.024
Foreshore Freeway (Section M) (-33.919712, 18.434659)	**Barrier Railing**	300	40	33	25 - 45	**2014**	0.44	65	0.20	3.16
Foreshore Freeway (Section M) (-33.919712, 18.434659)	**Barrier Railing**	250	40	33	25 - 45	**2014**	0.48	45	0.22	1.50

Location of Structures (latitude, longitude)	**Structural component cored**	** **Distance from sea** (m)	**Estimated age of structure** (years)	**Concrete compressive strength** (MPa)	**Range of cover to Steel** (mm) using covermeter	**Year of testing**	**Surface Chloride Content C_s** (% by mass of cement)	**Depth X for diffusion coefficient calculation** (mm)	**Chloride content at X depth** (%by mass of cement)	**Apparent diffusion coefficient** D_{ac} (X 10^{-12} m^2/s)
Lower Church Street (over Table Bay Boulevard) (-33.921320, 18.447890)	**Pier**	300	51	NM	50 - 85	**2014**	0.39	25	N/A	N/A
Lower Church Street (over Table Bay Boulevard) (-33.921320, 18.447890)	**Barrier Railing**	300	51	NM	50 - 85	**2014**	0.47	45	0.29	2.37
Lower Church Street (over Table Bay Boulevard) (-33.921320, 18.447890)	**Barrier Railing**	350	51	NM	50 - 85	**2014**	0.37	25	0.2	0.54
Helen Suzman Blvd (-33.912598, 18.419848)	**Pier**	700	40	33	50 - 80	**2014**	0.49	55	0.25	2.72
Helen Suzman Blvd (-33.912598, 18.419848)	**Pier**	800	40	33	50 - 80	**2014**	0.36	90	0.25	20.10

Location of Structures (latitude, longitude)	**Structural component cored**	** **Distance from sea** (m)	**Estimated age of structure** (years)	**Concrete compressive strength** (MPa)	**Range of cover to Steel** (mm) using covermeter	**Year of testing**	**Surface Chloride Content C_s** (% by mass of cement)	**Depth X for diffusion coefficient calculation** (mm)	**Chloride content at X depth** (%by mass of cement)	**Apparent diffusion coefficient D_{ac}** (X 10^{-12} m^2/s)
Helen Suzman Blvd (-33.912598, 18.419848)	**Barrier Railing**	800	40	33	50 - 80	**2014**	0.47	55	0.22	2.34
Helen Suzman Blvd (-33.912598, 18.419848)	**Barrier Railing**	700	40	33	50 - 80	**2014**	0.61	55	0.37	3.89
Helen Suzman Blvd (-33.912598, 18.419848)	**Barrier Railing**	700	40	33	50 - 80	**2014**	0.31	65	0.22	11.87
Helen Suzman Blvd (-33.912598, 18.419848)	**Barrier Railing**	700	40	33	50 - 80	**2014**	0.52	55	0.34	5.35
Settlers Way (over Liesbeek Parkway)(N2) (-33.944039, 18.476456)	**Barrier Railing**	4000	N/A	35	10 - 80	**2014**	0.62	25	1.02	N/A

Location of Structures (latitude, longitude)	**Structural component cored**	** **Distance from sea** (m)	**Estimated age of structure** (years)	**Concrete compressive strength** (MPa)	**Range of cover to Steel** (mm) using covermeter	**Year of testing**	**Surface Chloride Content C_s** (% by mass of cement)	**Depth X for diffusion coefficient calculation** (mm)	**Chloride content at X depth** (%by mass of cement)	**Apparent diffusion coefficient D_{ac}** (X 10^{-12} m^2/s)
Settlers Way (over Liesbeek Parkway)(N2) (-33.944039, 18.476456)	**Pier**	4000	N/A	20	10 - 80	**2014**	0.78	100	0.45	N/A
Vanguard drive Interchange on the N1 - M7 Northbound (over N1)(-33.885244, 18.531198)	**Pier**	4200	N/A	20	25 - 45	**2014**	1.15	65	0.44	N/A
Vanguard drive Interchange on the N1 - M7 Northbound (over N1)(-33.885244, 18.531198)	**Barrier Railing**	**4200**	N/A	35	25 - 45	**2014**	1.20	75	0.45	N/A
M5 Interchange on Settlers Way(N2) - Black River Parkway (over Settlers Way)(-33.943521, 18.483593)	**Barrier Railing**	**4200**	N/A	35	50 - 85	**2014**	0.94	45	0.46	N/A
Vanguard drive Interchange on the Settlers Way(N2) (-33.955174, 18.540914)	**Pier**	**9000**	N/A	20	50 - 80	**2014**	0.87	45	0.56	N/A

Location of Structures (latitude, longitude)	**Structural component cored**	** **Distance from sea** (m)	**Estimated age of structure** (years)	**Concrete compressive strength** (MPa)	**Range of cover to Steel** (mm) using covermeter	**Year of testing**	**Surface Chloride Content C_s** (% by mass of cement)	**Depth X for diffusion coefficient calculation** (mm)	**Chloride content at X depth** (%by mass of cement)	**Apparent diffusion coefficient D_{ac}** (X 10^{-12} m^2/s)
Vanguard drive Interchange on the Settlers Way(N2) (-33.955174, 18.540914)	**Pier**	**9000**	N/A	20	50 - 80	**2014**	1.32	25	0.67	N/A
Settlers Way N2 by Airport Approach (-33.966016, 18.572125)	**Pier**	**11500**	N/A	20	NM	**2014**	0.77	45	0.48	N/A
Settlers Way N2 by Airport Approach (-33.966016, 18.572125)	**Pier**	**11500**	N/A	20	NM	**2014**	0.7	65	0.51	N/A
Settlers Way N2 by Airport Approach (-33.966016, 18.572125)	**Barrier Railing**	**11500**	N/A	35	NM	**2014**	0.74	25	0.46	N/A

NM – not measured
N/A – not available
** Distance measured using Google Earth (2013) from RC to nearest coastline

APPENDIX D – Aerial images of wet candle device monitored locations

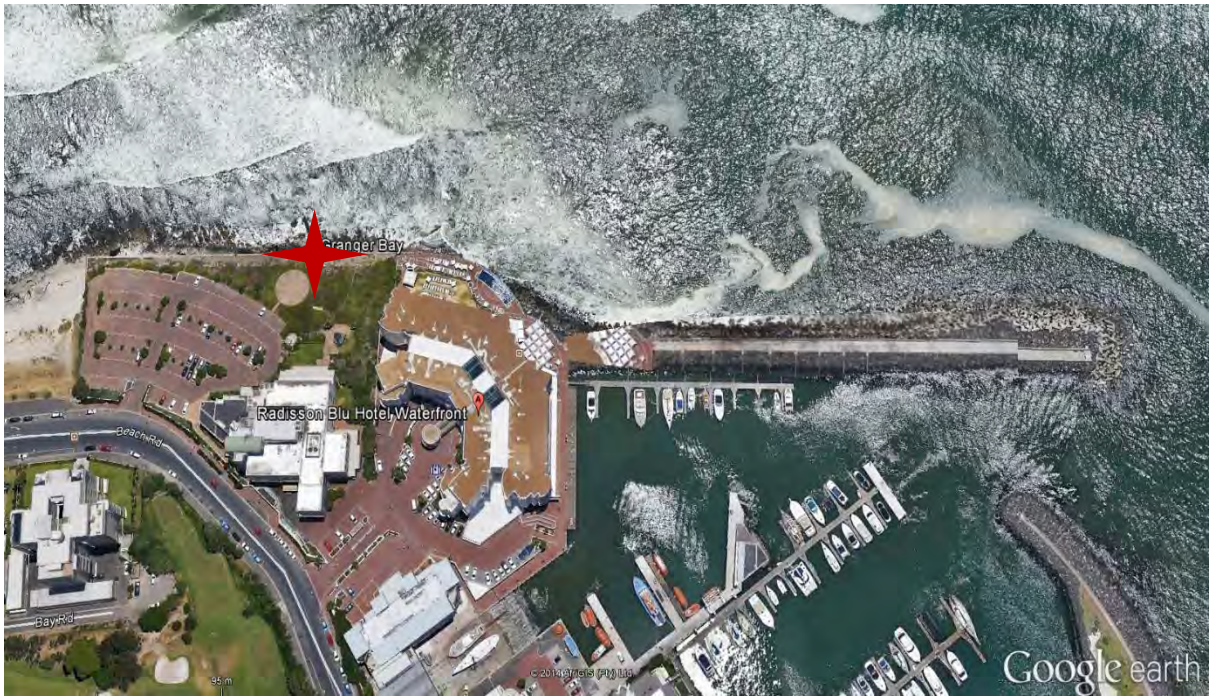

Figure D.1: Aerial view of station location at Granger Bay from Google Earth

Figure D. 2: Aerial view station location at Muizenberg

Figure D. 3: Aerial view of monitored station at Paarden Eiland station

Figure D. 4: Aerial view of monitored station at Montague Gardens

Figure D. 5: Aerial view of monitored location at Bellville

APPENDIX E – Graphs

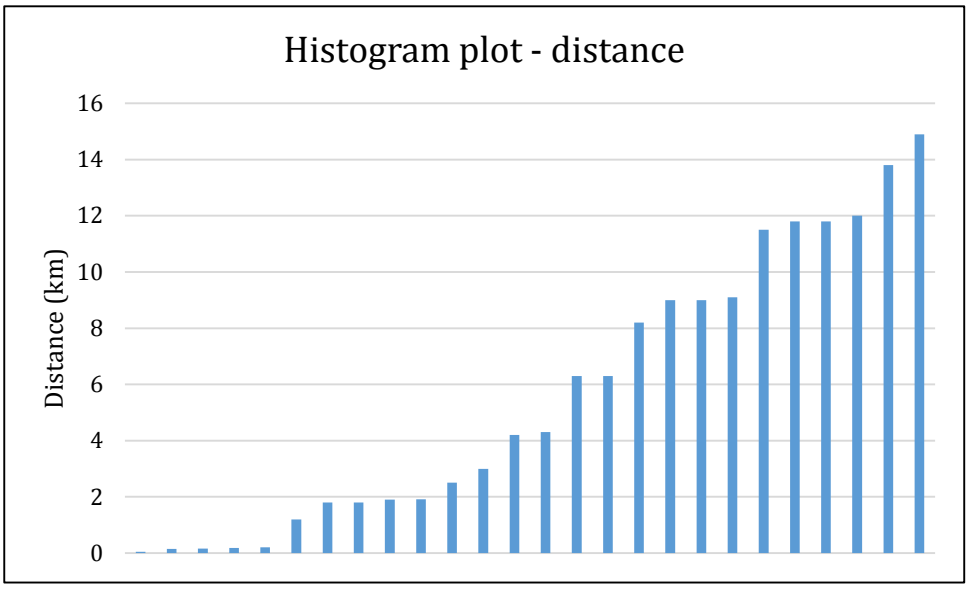

Figure E. 1: Histogram plot of RC structure's distance

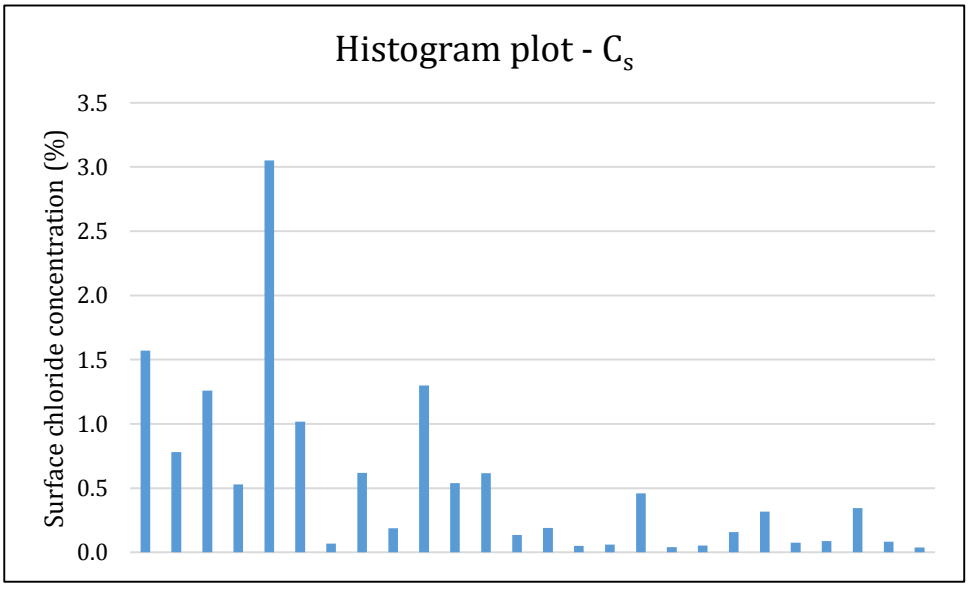

Figure E. 2: Histogram plot of RC structure's surface chloride concentrations